AJUR

American Journal of *Undergraduate Research*

Volume 21 | Issue 2 | September 2024

www.ajuronline.org

Print Edition ISSN 1536-4585
Online Edition ISSN 2375-8732

AJUR
American Journal of
Undergraduate Research

Volume 21 | Issue 2 | September 2024 | https://doi.org/10.33697/ajur.2024.114

American Journal of Undergraduate Research (AJUR) *is a national, independent, peer-reviewed, open-source, quarterly, multidisciplinary student research journal. Each manuscript of AJUR receives a DOI number. AJUR is archived by the US Library of Congress. AJUR was established in 2002, incorporated as a cheritable not-for-profit organization in 2018. AJUR is indexed internationally by EBSCO and Crossref with ISSNs of 1536-4585 (print) and 2375-8732 (web).*

Microfiber Content in Pacific Oysters (*Crassostrea gigas*) from Morro Bay, California

Julia Bures & Andrea Huvard*

Department of Biology, California Lutheran University, Thousand Oaks, CA

https://doi.org/10.33697/ajur.2024.115

Student: juliareneeb@gmail.com, jbures@callutheran.edu*
Mentor: huvard@callutheran.edu

ABSTRACT
Plastics are a major source of marine pollution. One form of plastic pollution is microfibers, which are synthetic fibers five micrometers or smaller that are shed by artificial clothing. The size of microfibers enables them to easily be ingested by a number of marine organisms, including oysters. Oysters are filter feeders and a major aquaculture asset, which presents a concern for the effects of microfiber ingestion on human health. Very few studies have been conducted quantifying microfibers using Pacific oysters (*Crassostrea gigas*) sourced from California. This study quantifies microfiber content in the Pacific oyster farmed for human consumption in Morro Bay, California. Microfibers were quantified after being isolated from oyster samples. An average of 9.12 microfibers were recovered per oyster sample. Although some of the smaller oysters contained more microfibers compared to larger oysters, this difference was not significant. There also was no significant difference between the quantities of black and blue microfibers. However, there was a significant increase in quantities of black microfibers compared to green or red microfibers. The results of this study indicate that a large amount of microfibers are present in commercial oysters, but more research needs to be conducted to determine how this will impact human health.

KEYWORDS
Marine Pollution; Microplastic; Microfiber; Trophic Transfer; Keystone Species; Aquaculture; Oyster; Human Health

INTRODUCTION

Plastics are synthetic, non-biodegradable, persistent environmental pollutants that are found in a variety of environments. Plastic pollution has been increasing dramatically in recent years, doubling from the year 2000 to 2019 from 230 million tons to 460 million tons.[1] In 2019, 1.7 million tons of plastic waste entered the ocean, which contributed to the estimation of over 30 million tons of plastic in the ocean.[1] Plastic pollution is a growing concern due to its longevity, as well as the variable forms it can take on in the environment. Persistence of both bulk and microplastic forms can exceed 20 years (on the basis of plastic bag decomposition), and even approach 600 years for fishing line.[2] This study aims to raise awareness and offer evidence of the growing problem of plastic pollution by providing additional data from the Central Coast of California, USA.

Microplastics are fragments of plastics that are five μm or less in size. Due to their small size and low density, microplastics are ubiquitous to the marine environment.[3–6] Not only does the presence of plastics and microplastics pose an environmental issue, but so do the chemicals they contain. Additive chemicals that help maintain their structural integrity, such as plasticizers, pigments, and flame retardants leach into the environment and tissues of organisms that ingest them.[7] Microfibers are a category of microplastics that are polymer-based fibers that originate from synthetic fabrics including acrylic, spandex, nylon, and polyester that get sloughed off in washing machines. A single load of laundry can release up to several thousand microfibers.[8] Due to their small size, wastewater treatment plants are unable to isolate microfibers, enabling them to enter the ocean. Another source of microfibers is the inappropriate disposal of clothing or fabrics, such as illegal dumping, which directly contributes to pollution.[9]

Once in the ocean, microplastics, including microfibers, absorb persistent organic pollutants (POPs), also known as forever chemicals, which are toxic chemicals made of organic compounds.[7] The ingestion of plastic and the chemicals they contain presents a health issue for marine species that includes blockage of the gastrointestinal (GI) tract, GI and muscle irritation, and endocrine dysfunction.[10]

In addition to microplastics and microfibers being found in various water columns due to their size,[11] they are also transferred through the ecosystem via trophic transfer.

Trophic transfer refers to smaller prey organisms ingesting microfibers and then being eaten by larger predatory organisms. Trophic transfer enables microfibers, along with the chemicals they contain (POPs), to travel through the food web and reach even the major predators at the top.[12] Fish that ingested microplastics showed signs of abnormal feeding, reproduction, and movement behaviors.[13] Additionally, microplastics were transferred from mother to offspring, and exposure in the larval state of the offspring resulted in abnormal development.[13] Not only do microfibers negatively affect fish, but they also impact bivalves. Bivalves ingest food by filtering the water around them, a process during which they also remove organic particles that nourish algae. Accumulation of microfibers in the gills of bivalves can inhibit filtration. After 39 days of exposure to microfibers, bivalve filtration has been found to decrease by 21.3%.[14] The decrease in biofiltration can have negative effects on an ecosystem by contributing to ocean eutrophication. With the decrease in filtration, organic particles remain in the water and allow algal blooms to flourish. Such algal blooms use up the oxygen in the water, resulting in the deaths of surrounding plant and animal life.

One species of bivalves that is affected by plastic pollution is oysters. Oysters are filter feeders that extract plankton or algae from the water by filtering it through their gills. They are a keystone species to the marine environment because they are an essential source of food, habitat, and biofiltration.[14–17] The close connection between the ecosystem and oysters also makes them useful as an indicator species, meaning the health of the oysters signifies the overall health of the ecosystem. Therefore, oysters can be used to indicate the amount of microfibers present in their environment. Varying amounts of microfibers have been recovered in oysters across global locations with 4–57 microplastics being quantified in Shanghai, China and 104–140 microfibers being found in Chesapeake Bay, U.S.A.[3, 6]

Oysters are a major aquaculture product. Therefore, when humans eat oysters and other seafood, they are at risk of ingesting microfibers and other microplastics. Europeans who consume shellfish may ingest up to 11,000 microplastics annually.[18] It has also been estimated that humans who eat seafood can ingest up to 54,864 microplastics in a year with mollusk consumption contributing approximately 2.65 kg of microplastics per person.[19] When ingested, microfibers can interfere with the digestive tract and leach chemicals, resulting in localized particle toxicity and irritation.[7] While little research has been conducted to evaluate the full extent of the health effects of consuming microfibers, continuous ingestion of microfibers may contribute to infections, stomach and brain damage, reproductive issues, cardiovascular issues, and cancer.[9, 20]

In this study, Pacific oysters (*Crassostrea gigas*) farmed for human consumption from Morro Bay, California were measured, weighed, and the quantity of microfibers content was recorded. The aim of this study was to contribute to evidence of microfiber pollution in the marine environment and determine if there is a correlation between oyster size and number of microfibers. The data collected was used to test the following hypotheses: 1) oysters with greater visceral wet weight would have fewer microfibers due to the allometric relationship between mass and filtration.[21] As filter feeders, oysters obtain food from the environment by siphoning water over their gills and collecting food particles that are then ingested. This filtration rate has been found to be affected by the relation between oyster size and metabolic rate.[21] Metabolic rates are allometrically scaled in relation to mass in a variety of organisms (law of allometric scaling of metabolism), including oysters.[21] Therefore as oyster mass increases, metabolic rates decrease, and filtration rates decrease. 2) Oysters with larger shell lengths will have fewer microfibers. A positive correlation has been found between shell length and weight.[22] Therefore, if oyster mass and filtration rate are allometrically related,[21] and shell length and weight are positively correlated, it is expected that shell length and filtration rate will also be allometrically related. Understanding whether size is correlated to microfiber quantity can enable consumers to predict the number of microfibers they may ingest depending on the size of the oyster they consume. Furthermore, identifying how many microfibers are being consumed can help determine the range of microfibers that needs to be ingested in order to result in aversive health effects.

METHODS AND PROCEDURES

Sample collection

Oyster samples used in the study were Pacific oysters (*Crassostrea gigas*) purchased from Grassy Bar Oyster Company based in Morro Bay, California (**Figure 1**). The oysters were purchased during the summer (July/August) and winter February/March) months with each shipment containing between 100–120 oysters. Although the details of exact harvest days are not available, oysters are frozen upon harvest, then bundled for freezing and shipment. The samples were shipped frozen and were stored in plastic bags at –20 °C until use. Before processing for microfibers, the oysters (n = 197) were measured, dissected and weighed.

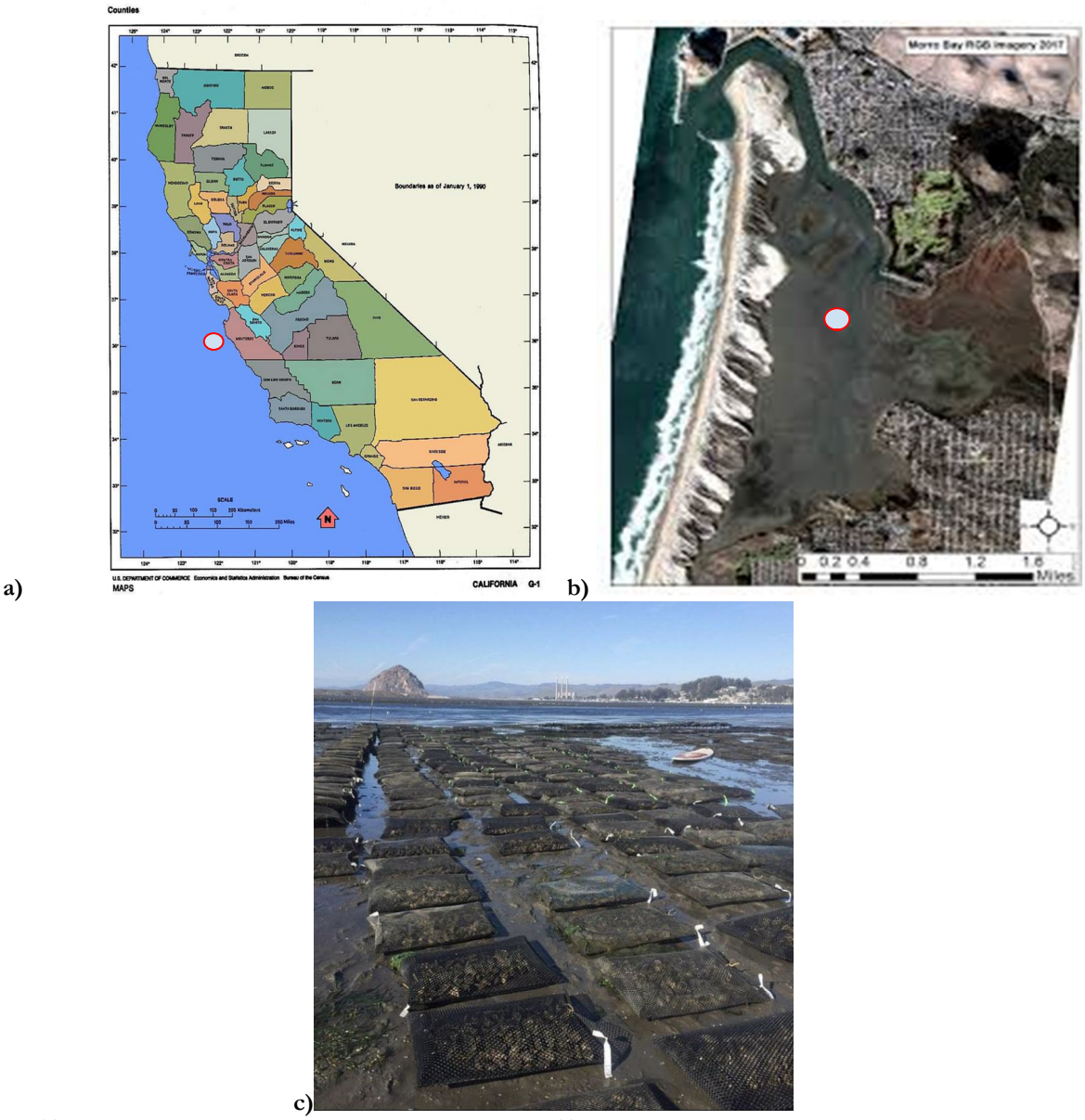

a) **b)** **c)**

Figure 1. a) The white circle indicates the location of Morro Bay, California. **b)** The white circle indicates the Grassy Bar Oyster farm. **c)** Photograph of the Grassy Bar Oyster Company harvest site obtained from the Grassy Bar Oyster Company *Instagram* account.[23]

Oyster preparation

The shell length, width, and height of each oyster were measured using a caliper, and the soft tissue, or visceral mass, was removed and weighed for wet weight. The tissue was then cut into smaller pieces using dissection scissors and ground using a mortar and pestle. The sample was added to a 500 mL beaker (beaker one) and 30 parts per thousand artificial seawater was added to bring the solution to 100 mL. All artificial seawater is made in a closed system and tested for microfiber contamination (see *Controlling for contamination* below). Due to their light weight and small size, a number of microfibers in the sample will float to the top of the beaker. To extract the floating microfibers, a wash was performed. The top layer of the sample solution was poured into a 200 mL beaker (beaker two) and more artificial sea water was added to bring both beakers to 100 mL. In order to account for as many microfibers as possible in the animal tissue, the tissue was dissolved using 30% hydrogen peroxide. For each 100 mL beaker, 100 mL of 30% hydrogen peroxide was added. Both beakers were placed on an Innova 2000 Platform Shaker set for 100 rpm for 24–48 hours. The samples were filtered using 11 µm Whatman filter paper and a Buchner funnel system with a 500 mL side arm flask.

Microfiber quantification

All microfibers on the filter paper were counted and categorized based on color as blue, black, red, or green. The filter paper containing microfibers was divided into a grid of 16 sections and examined using a Stemi 305 Stereo microscope. The microfibers were visible under the microscope when viewed at 10–40x magnification. Microfibers were identified by physical characteristics including size (< 5.0mm), color, and structure.[24] When a single oyster sample was filtered on more than one filter paper, the total number of microfibers for each filter paper was summed to obtain the total number of microfibers in that individual oyster.

Controlling for contamination

Clothing with synthetic fibers is constantly shedding microfibers, even when they are not being washed, with between 1,200 and 7,000 microfibers having been found in the air in various indoor environments.[25] In order to understand the level of contamination in the laboratory, when the samples were being prepared and processed, everyone in the lab area was required to wear a 100% cotton white lab coat. Since the lab coats were made of natural fibers, they did not shed any microfibers that could contaminate the oyster samples. In addition, all samples were covered with aluminum foil after being added to the beakers, when sitting, and when being filtered. 15 saltwater blanks were filtered to control for microfiber contamination that may occur during the preparation procedure. When observed for microfiber content, an average of 0.80 microfibers per blank saltwater sample were recovered.

Statistical analysis

Statistical analysis of microfiber quantities and oyster sizes was performed using Microsoft Excel 2008 Version 16.0. The sum and average microfiber quantity were calculated. The average oyster length and wet weight was also calculated. Linear regression was used to determine the correlation between oyster wet weight and microfiber quantity as well as shell length and microfiber quantity. A coefficient of determination (r^2) value of 0.7 was determined as indicative of a significant correlation. A one-way analysis of variance (ANOVA) was performed to compare the quantities of different colors of microfibers. Black microfibers have been found to be an abundant color of microfiber,[25] so the number of black microfibers recovered in this study were compared with blue, red, and green microfibers quantities to determine whether there were significantly more ($p < 0.05$) black microfibers than other colors.

RESULTS

The results of this study determine the quantity of microfibers in commercial oysters farmed from Morro Bay, CA. A total of 197 oysters were processed, and examined for microfibers with a total of 1,797 microfibers being positively quantified. An average of 9.12 ± 7.09 microfibers/oyster were recovered (**Figure 2**) and an average of 0.79 ± 0.90 microfibers/g wet weight (ww) was found. In order to determine if there is a correlation between oyster size and number of microfibers, both wet weight and shell length were studied. The oysters had an average visceral mass wet weight of 13.27 g (range of 5.30–24.50 g) and an average shell length of 66.46 mm (range of 50.0–85.0 mm) (**Figure 3**). The standard deviations for mean microfibers show diverse degrees of variation because the number of microfibers quantified in each sample ranged from 0–39 microfibers/sample.

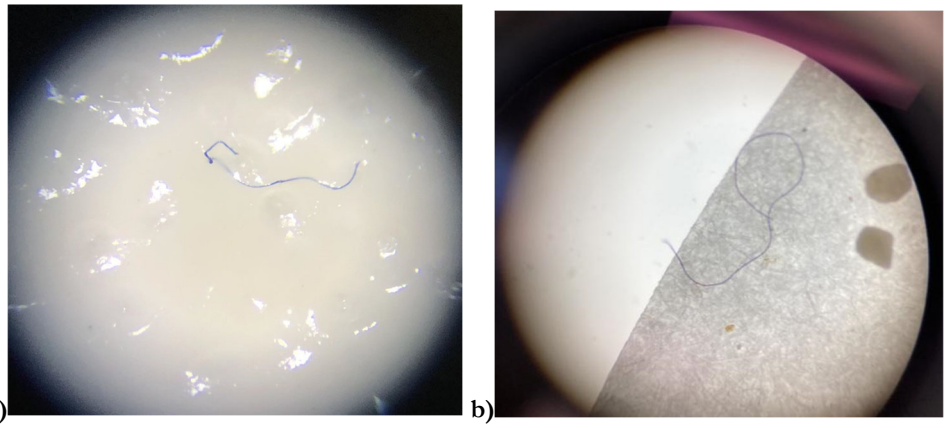

a) **b)**

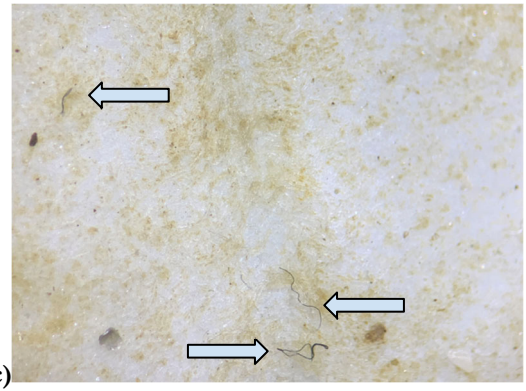

c)

Figure 2. Representative image of **a, b)** blue and **c)** black microfibers observed on filter paper.

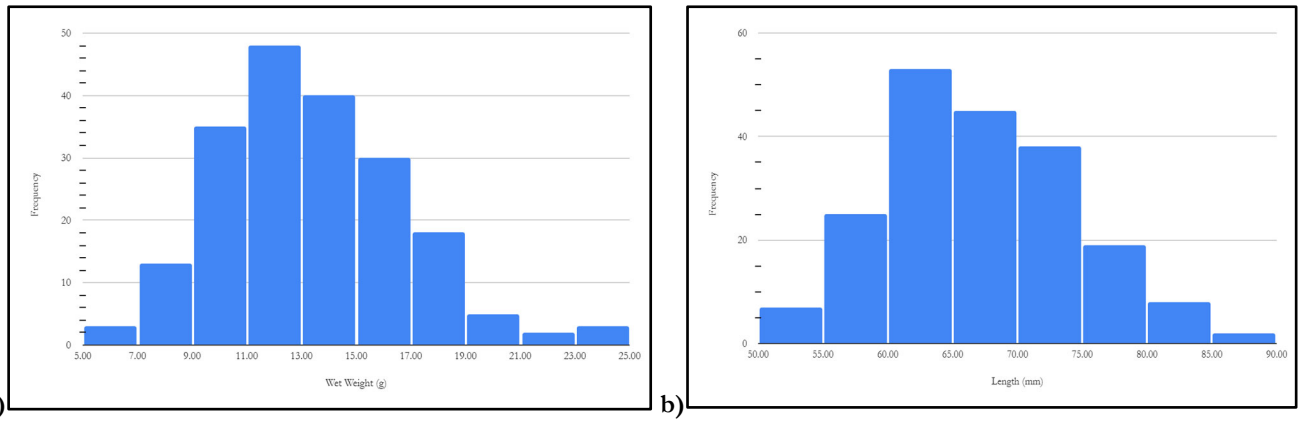

a) b)

Figure 3. Histograms summarizing the **a)** visceral wet weights and **b)** shell lengths for all oyster samples (n = 197).

Oyster wet weight varied with a difference of 19.2 g between the lowest recorded weight (5.3 g) and the highest (24.5 g). The quantity of microfibers also varied over the range in wet weight (**Figure 4**). A linear regression was performed using the number of microfibers quantified and the visceral mass wet weight of the oysters to determine if weight may be indicative of the levels of microfiber pollution (**Figure 5**). While some smaller oysters were found to contain more microfibers, the coefficient of determination indicates that this correlation is not significant ($r^2 = 0.04$). The equation obtained from the line of best fit is: Microfibers/Sample = –0.406 * (wet weight) + 14.5.

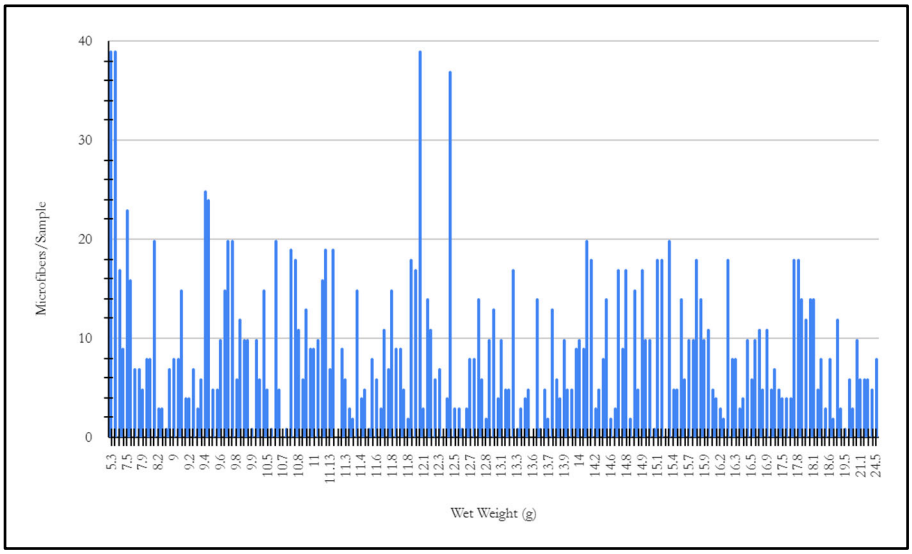

Figure 4. Graphical representation of the variation in wet weight and corresponding microfiber quantity.

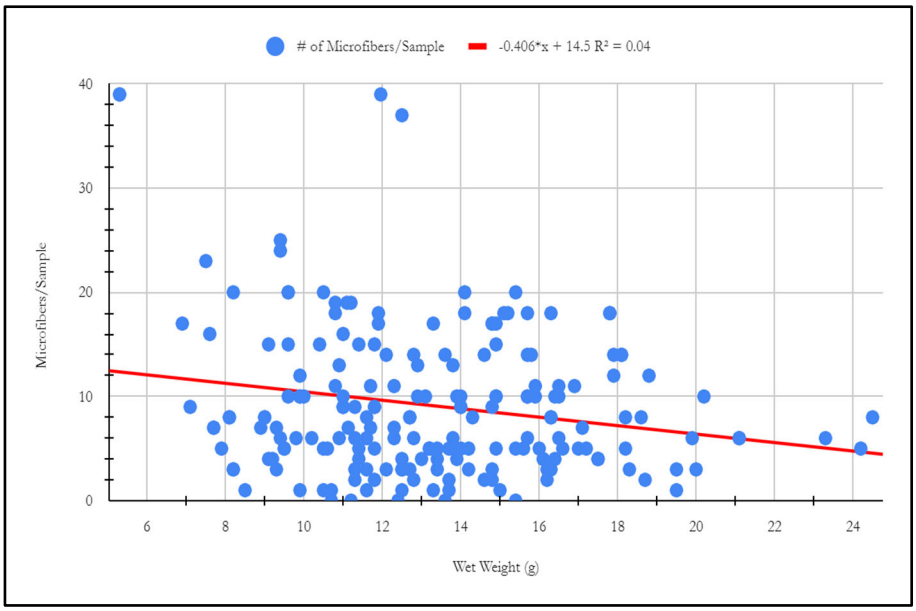

Figure 5. Linear regression comparing wet weight (g) and microfibers/sample ($r^2 = 0.04$). The red line represents the line of best fit (Microfibers/Sample = –0.406 * (wet weight) + 14.5).

Oyster shell length varied with a difference of 35.0 mm between the lowest recorded length (50.0 mm) and the highest (85.0 mm). The quantity of microfibers also varied over the range in shell length (**Figure 6**).

A linear regression was performed using the number of microfibers recovered and the shell length of the oyster samples to determine if length may be indicative of the levels of microfiber pollution (**Figure 7**). There was no correlation found between shell length and microfiber quantity ($r^2 = 0.00$). The equation obtained from the line of best fit is: Microfibers/Sample = 1.26E–3 * (shell length) + 9.04.

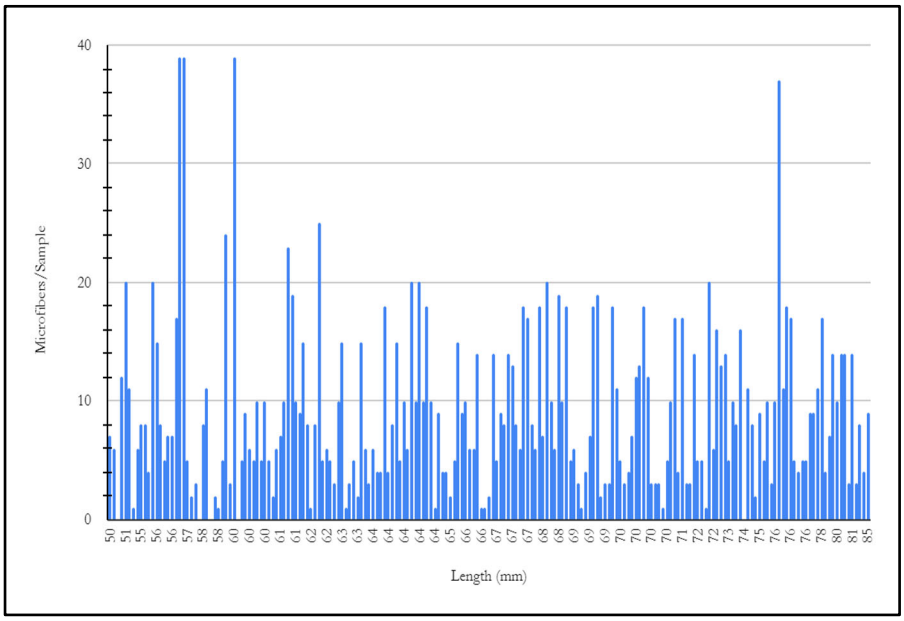

Figure 6. Graphical representation of the variation in shell length and corresponding microfiber quantity.

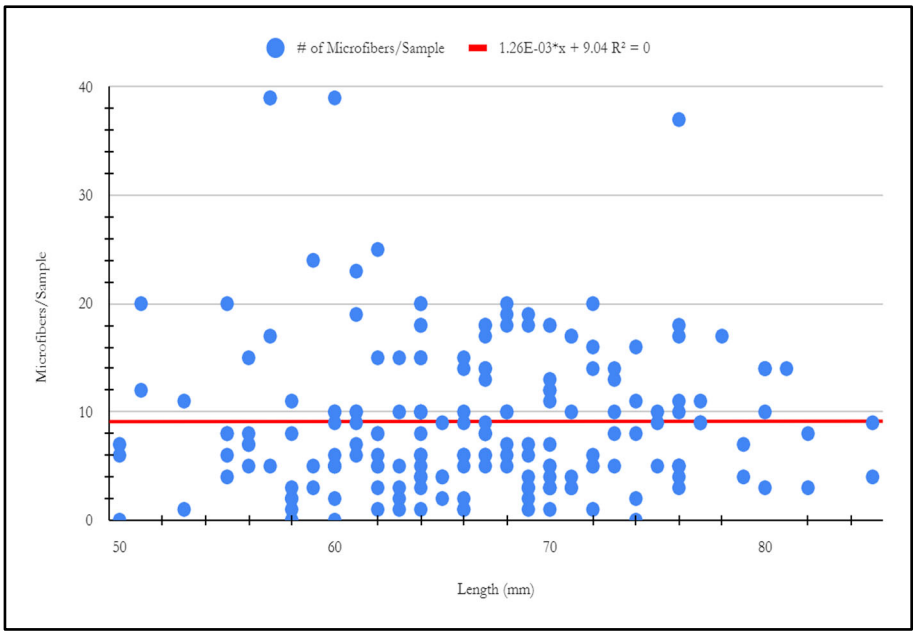

Figure 7. Linear regression comparing shell length (mm) and Microfibers/sample (r^2 = 0.00). The red line represents the line of best fit (Microfibers/Sample = 1.26E–3 * (shell length) + 9.04).

The colors of microfibers were compared to determine what color was most prevalent (**Figure 8**). Black microfibers were expected to be most prevalent, so the quantity of black microfibers was compared to the other colors.

The colors of the microfibers were vibrant, and all clearly stood out in contrast to the white filter paper. The only colors observed were black, blue, red, and green, all of which have been included in the data analysis. There were significantly more black microfibers than green (p = 2.68E–11) and red (p = 5.60E–24), but not blue (p = 0.22). 50.1% of the microfibers quantified were black (n = 900), 37.5% were blue (n = 673), 8.1% were green (n = 146), and 4.3% were red (n = 78) (**Figure 9**).

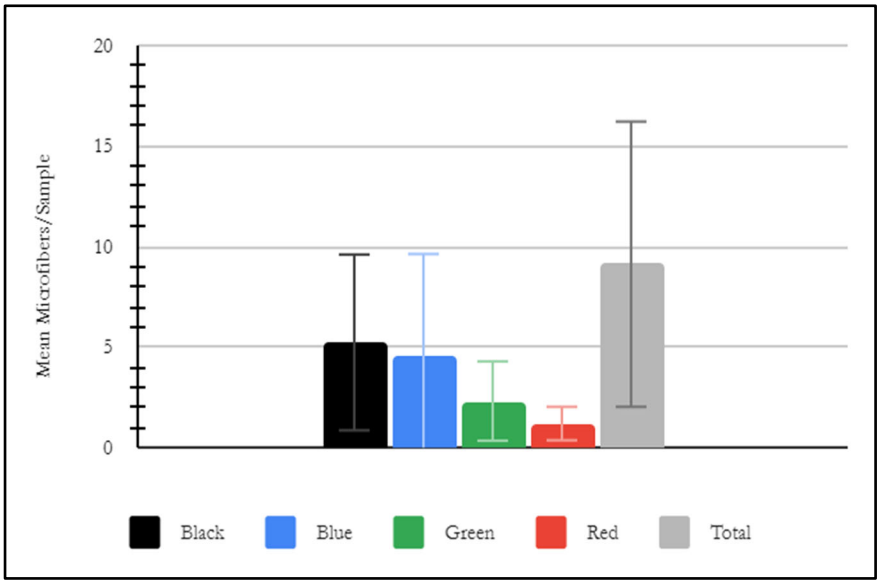

Figure 8. Mean number of black ($\bar{x}$ = 5.23 ± 4.37 microfibers/sample), blue ($\bar{x}$ = 4.58 ± 5.05 microfibers/sample), green ($\bar{x}$ = 2.32 ± 1.97 microfibers/sample), red ($\bar{x}$ = 1.20 ± 0.83 microfibers/sample), and total ($\bar{x}$ = 9.12 ± 7.09 microfibers/sample) microfibers recovered per oyster (n = 197). Error bars represent the standard deviation.

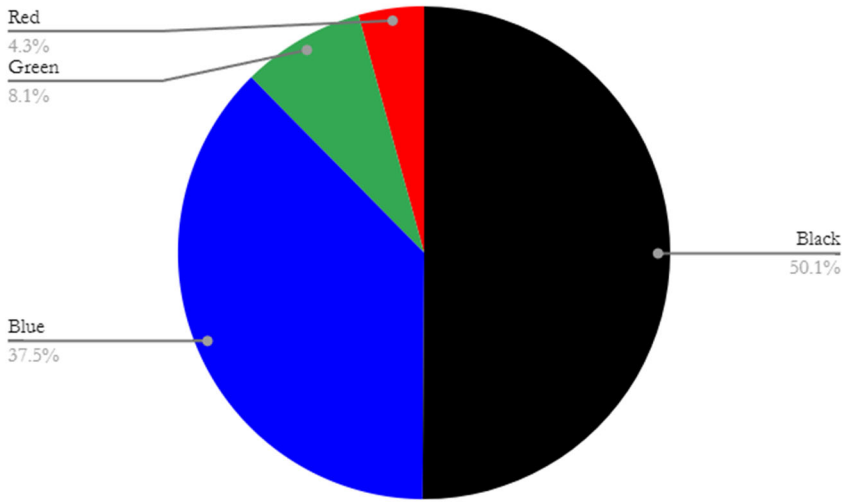

Figure 9. The percentage of black, blue, green, and red microfibers out of the total amount of microfibers (n = 1,797) recovered from all sampled oysters (n = 197).

DISCUSSION

The purpose of this study was to quantify microfiber pollution in Pacific oysters farmed for human consumption and determine if wet weight and shell length were indicative of microfiber quantity. Very few studies have been conducted quantifying microfibers using Pacific oysters sourced from Morro Bay, California. This study recovered a total of 1,797 microfibers with an average of 9.12 microfibers per oyster sample and an average of 0.79 microfibers/g ww. While oysters with less wet were found to contain more microfibers/sample compared to larger oysters, the relationship was not significant. There was no correlation between shell length and microfiber quantity.

There were significantly more black microfibers observed compared to green or red microfibers. There was no significant difference between black and blue microfibers.

Other studies along the West Coast of the United States using oysters and other bivalves have reported varied quantities of average microfibers compared to this study. While quantities were varied, lower average quantities of microfibers/sample were recovered at other locations including in commercial bivalves harvested from the coast of Baja California, Mexico ($\bar{x}$ = 0.14–0.36 microfibers/sample),[26] bivalves from San Francisco, California ($\bar{x}$ = 0.87–1.4 microfibers/sample),[27] and oysters from Washington State, USA ($\bar{x}$ = 0.77 microfibers/sample).[28] These studies were all conducted during the years 2018 and 2019, while the present study was conducted between 2021 and 2022. Due to the accumulation of microfibers over time,[12] the current study being conducted years after the mentioned West Coast studies may contribute to the greater microfiber quantities found in the present study. The variation between bivalves along the Pacific coast indicates that sample location may be a contributing factor to microfiber quantities and should be a consideration when consuming seafood. While there is variation in the amount of microfibers in seafood, filter feeders have been found to contain more microfibers than fish,[29] which increases health-related risks for communities that rely on seafood, and in particular filter feeders.

Although few studies have focused on the effects of microfiber ingestion in humans, persistent organic pollutants (POPs) that have been found in microfibers have presented a public health concern due to their contribution to metabolic diseases including type 2 diabetes as well as birth defects and dysfunctions in the endocrine and immune systems.[7, 30, 31] The limited data regarding the effect of microfibers and the chemicals they leach may give rise to uncertainty about food safety.

This study found no correlation between oyster shell length and levels of microfiber content. Oysters harvested from the coast of Oregon, U.S.A. were also found to bear no significant correlation between oyster length or weight.[32] This study found no significant correlation between microfiber quantity and wet weight, although a negative trend with smaller oysters containing more microfibers was noted. A similar result was noted in bivalves harvested from Italy with smaller oysters (4.00–5.75 g, $\bar{x}$ = 1.69 microplastics/g ww) containing more microplastics/g ww compared to large oysters ($\bar{x}$ = 0.78 microplastics/g ww).[4]

The average quantity of microfibers/g ww varies depending on the global location. The present study recovered an average of 0.79 microfibers/g ww. However, bivalves harvested from the French-Belgian-Dutch coastline found an average of 0.2 microplastics/g ww,[33] while commercial bivalves collected from the Tyrrhenian Sea found an average of 1.33 microplastics/g ww,[4] and an average of 0.04–0.07 microplastics/g ww were found in bivalves from Baja California, Mexico.[26] The variation in microplastics/g in both commercial and wild bivalves also supports the implication that the location of oyster harvest contributes to levels of microfiber pollution.

Oyster ingestion of microfibers being a factor of location rather than shell length or wet weight has ramifications for human consumption. In order to limit microfiber intake, consumers should consider the location of oyster growth and harvest. Bivalves harvested in Asia have been found to contain increased levels of microplastic contamination.[19] Three times more anthropogenic debris have been recovered in fish and bivalves from Indonesia compared to California.[5] An average of 13.3 microplastics/oyster was found in oysters collected in the Philippines and an average of 57.2 microplastics/oyster was quantified in bivalves from China.[34, 3] Contributing factors for higher levels of microfiber contamination in Asia include plastic mismanagement, population size, and major rivers that flow into the ocean.[35, 36] This bears implications for our study in Morro Bay and other locations in contact with the Pacific Ocean due to ocean currents.

Microplastics are distributed across the ocean with accumulation sites where ocean currents converge.[37, 38] The connection between continents via ocean currents makes microplastics contamination a global issue rather than a regional issue and illustrates the need for a standardized method of wastewater treatment and plastic disposal.[39]
There was no significant difference between the quantities of black and blue microfibers. However, there were significantly more black microfibers than green and red microfibers, which is consistent with initial expectations. Black and blue microfibers have been found to be more than 50% more common than other colors of microfibers in oysters from the Salish Sea, Washington,[28] Baja California, Mexico,[26] and Florida.[40] Black and blue microfibers are also more common than other colors year-round.[25]

The dominance of blue and black clothing preferences during summer and winter may contribute to why black and blue microfibers were consistently more common overall.[22] The present study was performed over the course of a year, and black and blue microfibers were consistently found to be the most common regardless of when the oysters were harvested (one harvest occurred during summer and another during mid-winter). The results indicate that synthetic black and blue fabric is a prominent contributor to microfiber pollution. To help reduce such pollution, initial efforts can be taken by fabric producers to use natural fibers for black and blue clothing. Not only are natural fibers such as cotton, hemp, linen, and jute more eco-friendly in terms of biodegradability, but also are more sustainable, renewable, and lower-cost.[41] Spreading awareness of such properties can incentivize fabric producers and other industrial companies to increase their usage of natural plant fibers.

CONCLUSIONS

The ubiquity of plastic pollution makes it both an environmental and a human health issue. Quantifying plastic pollution is imperative to drawing awareness. For this reason, it is important that microfibers be quantified. While there have been studies of microfibers quantities across the world,[3–6, 26, 33] few studies have focused on oysters found on the coast of California. The findings of this study provide a clearer number of how many microfibers a consumer may ingest. A total of 1,797 microfibers were recovered in 197 sample oysters with an average of 9.12 microfibers/oyster. Additionally, 0.79 microfibers/g ww were quantified with oysters with less wet weight containing more microfibers. Microfiber quantity has been found to vary depending on location, wet weight, and shell length with a wide range of microfibers in oysters harvested from the Pacific coast of the United States as well as from various global locations including Mexico,[26] China,[3] and France.[33]

While there is a limited number of studies that have identified precisely the effects of microfibers on humans, there is evidence of a multitude of consequences including metabolic, reproductive, and cardiovascular difficulties stemming from microfiber ingestion.[30, 31] Future research related to microfiber consumption and human health should study the range at which microfiber quantities become hazardous to human health.

Microfiber pollution can be decreased by strengthening wastewater treatment infrastructure, which will increase the amount of microfibers isolated from water that is later drained into the ocean. Furthermore, a shift towards including natural plant fibers in textiles will decrease the amount of microfibers being shed from clothing and other fabrics. Shifting from synthetic fibers to

natural fibers can be initiated by drawing awareness to the benefits of natural fibers including low density, versatility, and strength.[41]

ACKNOWLEDGEMENTS

The author would like to thank California Lutheran University for providing the opportunity and lab to undertake this research. She thanks Keury Ortiz Hernandez, Catherine Ortiz Hernandez, and Yuliana Montes for assistance with data collection.

REFERENCES

1. Organization for Economic Co-operation and Development. Plastic pollution is growing relentlessly as waste management and recycling fall short, says OECD, Release 2022, *https://www.oecd.org/environment/plastic-pollution-is-growing-relentlessly-as-waste-management-and-recycling-fall-short.htm* (accessed April 2023)
2. Ocean Conservancy. Trash Travels, Release 2010, *https://oceanconservancy.org/wp-content/uploads/2017/04/2010-Ocean-Conservancy-ICC-Report.pdf* (accessed April 2023)
3. Li, J., Yang, D., Li, L., Jabeen, K., and Shi, H. (2015) Microplastics in commercial bivalves from China, *Environmental Pollution*, 207, 190–195. *https://doi.org/10.1016/j.envpol.2015.09.018*
4. Santonicola, S., Volgare, M., Di Pace, E., Cocca, M., Mercogliano, R., and Colavita, G. (2021) Occurrence of potential plastic microfibers in mussels and anchovies sold for human consumption: Preliminary results, *Italian journal of food safety*, 10(4), 9962. *https://doi.org/10.4081/ijfs.2021.9962*
5. Rochman, C., Tahir, A., Williams, S., Baxa, D., Lam, R., Miller, J., Teh, F., Werorilangi, S., and Teh, S. (2015) Anthropogenic debris in seafood: Plastic debris and fibers from textiles in fish and bivalves sold for human consumption, *Scientific Reports*, 5, 14340. *https://doi.org/10.1038/srep14340*
6. Aung, T., Batish, I., and Ovissipour, R. (2022) Prevalence of Microplastics in the Eastern Oyster *Crassostrea virginica* in the Chesapeake Bay: The Impact of Different Digestion Methods on Microplastic Properties, *Toxics*, 10(1), 29. *https://doi.org/10.3390/toxics10010029*
7. Smith, M., Love, D.C., Rochman, C.M., and Neff, F. A. (2018) Microplastics in Seafood and the Implications for Human Health, *Current Environmental Health Reports*, 5, 375–386. *https://doi.org/10.1007/s40572-018-0206-z*
8. Yang, L., Qiao, F., Lei, K., Li, H., Kang, Y., Cui, S., and An, L. (2019) Microfiber release from different fabrics during washing, *Environmental Pollution*, 249, 136–143. *https://doi.org/10.1016/j.envpol.2019.03.011*
9. Mishra, S., Rout, P. K., and Das, A. P. (2021) Emerging microfiber pollution and its remediation, *Environmental Pollution and Remediation*, 247–266. *https://doi.org/10.1007/978-981-15-5499-5_9*
10. Courtene-Jones, W., Clark, N. J., Fischer, A. C., Smith, N. S., and Thompson, R. C. (2022) Ingestion of microplastics by marine animals, *Plastics and the Ocean: Origin, Characterization, Fate, and Impacts*, 349–366. *https://doi.org/10.1002/9781119768432.ch12*
11. Liu, K., Courtene-Jones, W., Wang, X., Song, Z., Wei, N., and Li, D. (2020) Elucidating the vertical transport of microplastics in the water column: a review of sampling methodologies and distributions, *Water Research*, 186, 116403. *https://doi.org/10.1016/j.watres.2020.116403*
12. Yarsan, E., and Yipel, M. (2013) The important terms of marine pollution "biomarkers and biomonitoring, bioaccumulation, bioconcentration, biomagnification", *Journal of Molecular Biomarkers & Diagnosis*, 1(2). *http://doi.org/10.4172/2155-9929.S1-003*
13. Yong, C.Q.Y., Valiyaveettil, S., and Tang, B.L. (2020) Toxicity of Microplastics and Nanoplastics in Mammalian Systems, *International Journal of Environmental Research and Public Health*, 17, 1509. *https://doi.org/10.3390/ijerph17051509*
14. Christoforou, E., Dominoni, D. M., Lindström, J., Stilo, G., and Spatharis, S. (2020) Effects of long-term exposure to microfibers on ecosystem services provided by coastal mussels, *Environmental Pollution*, 266(3), 115184. *https://doi.org/10.1016/j.envpol.2020.115184*
15. Sanjeeva Raj, P. J. (2008) Oysters in a new classification of keystone species, *Resonance*, 13(7), 648–654. *https://doi.org/10.1007/s12045-008-0071-4*
16. Kaplan, D. A., Olabarrieta, M., Frederick, P., and Valle-Levinson, A. (2016) Freshwater detention by oyster reefs: quantifying a keystone ecosystem service, *Public Library of Science One*, 11(12), e0167694. *https://doi.org/10.1371/journal.pone.0167694*
17. Guo, X., Wang, Y., Wang, L., and Lee, J. H. (2008) Oysters, in *Genome mapping and genomics in fishes and aquatic animals* (Kocher, T. D. and Kole, C. Eds.) vol. 2, 163–175, Springer Berlin Heidelberg, Berlin.
18. Cauwenberghe, Van L., and Janssen, C. R. (2014) Microplastics in bivalves cultured for human consumption, *Environmental Pollution*, 193, 65–70. *https://doi.org/10.1016/j.envpol.2014.06.010*
19. Nicole, W. (2021) Microplastics in seafood: how much are people eating?, *Environmental Health Perspectives*, 129(3), 034001. *https://doi.org/10.1289/EHP8936*
20. Prata, J. C., da Costa, J. P., Lopes, I., Duarte, A. C., and Rocha-Santos, T. (2020) Environmental exposure to microplastics: An overview on possible human health effects, *Science of the total environment*, 702, 134455. *https://doi.org/10.1016/j.scitotenv.2019.134455*
21. Ehrich, M. K., and Harris, L. A. (2015) A review of existing eastern oyster filtration rate models, *Ecological Modelling*, 297, 201–212. *https://doi.org/10.1016/j.ecolmodel.2014.11.023*

22. Octavina, C., Yulianda, F., Krisanti, M., and Muchlisin, Z. A. (2015). Length-weight relationship of Ostreidae in the Kuala Gigieng estuary, Aceh Besar District, Indonesia. *Aquaculture, Aquarium, Conservation and Legislation*, 8(5), 817-823.
23. Grassy Bar Oyster Company [@grassybaroyster]. (2020, January 27). *Low tide! #morrorock*. [Photograph]. Instagram. *https://www.instagram.com/grassybaroyster/?hl=en*
24. Hidalgo-Ruz, V., Gutow, L., Thompson, R. C., and Thiel, M. (2012) Microplastics in the marine environment: a review of the methods used for identification and quantification, *Environmental science & technology*, 46(6), 3060–3075. *https://doi.org/10.1021/es2031505*
25. Zhang, Q., Zhao, Y., Du, F., Cai, H., Wang, G., and Huahong Shi, H. (2020) Microplastic Fallout in Different Indoor Environments, *Environmental Science and Technology*, 54(11), 6530–6539. *https://doi.org/10.1021/acs.est.0c00087*
26. Lozano-Hernández, E. A., Ramírez-Álvarez, N., Mendoza, L. M. R., Macías-Zamora, J. V., Sánchez-Osorio, J. L., and Hernández-Guzmán, F. A. (2021) Microplastic concentrations in cultured oysters in two seasons from two bays of Baja California, Mexico, *Environmental Pollution*, 290, 118031. *https://doi.org/10.1016/j.envpol.2021.118031*
27. Miller, E., Klasios, N., Rochman, C., Lin, D., Sedlak, M., and Sutton, R. (2019) Microparticles, Microplastics, and PAHs in Bivalves in San Francisco Bay, *SFEI Contribution*, 976.
28. Martinelli, J., Phan, S., Luscombe, C., and Padilla-Gamino, J. (2020) Low incidence of microplastic contaminants in Pacific oysters (*Crassostrea gigas Thunberg*) from the Salish Sea, USA, *Science of the Total Environment*, 715, 136826. *https://doi.org/10.1016/j.scitotenv.2020.136826*
29. Hantoro, I., Löhr, A. J., Van Belleghem, F. G., Widianarko, B., and Ragas, A. M. (2019) Microplastics in coastal areas and seafood: implications for food safety, *Food Additives & Contaminants: Part A*, 36(5), 674–711. *https://doi.org/10.1080/19440049.2019.1585581*
30. Ruzzin, J. (2012) Public health concern behind the exposure to persistent organic pollutants and the risk of metabolic diseases, *BMC public health*, 12, 1–8. *https://doi.org/10.1186/1471-2458-12-298*
31. Guo, W., Pan, B., Sakkiah, S., Yavas, G., Ge, W., Zou, W., and Hong, H. (2019) Persistent organic pollutants in food: contamination sources, health effects and detection methods, *International journal of environmental research and public health*, 16(22), 4361. *https://doi.org/10.3390/ijerph16224361*
32. Baechler, B. R., Granek, E. F., Hunter, M. V., and Conn, K. E. (2020). Microplastic concentrations in two Oregon bivalve species: Spatial, temporal, and species variability. *Limnology and Oceanography Letters*, 5(1), 54-65.
33. Van Cauwenberghe, L., Claessens, M., Vandegehuchte, M. B., and Janssen, C. R. (2015) Microplastics are taken up by mussels (*Mytilus edulis*) and lugworms (*Arenicola marina*) living in natural habitats, *Environmental pollution*, 199, 10–17. *https://doi.org/10.1016/j.envpol.2015.01.008*
34. Jambre, K. G. E. (2022) Density of microplastics in Philippine cupped oyster (*Crassostrea iredalei*), *International Journal of Advanced Multidisciplinary Studies*, 1(4), 286–294.
35. Sotelo, T. J., Satoh, H., and Mino, T. (2019) Assessing wastewater management in the developing countries of Southeast Asia: Underlining flexibility in appropriateness, *Journal of Water and Environment Technology*, 17(5), 287–301. *https://doi.org/10.2965/jwet.19-006*
36. Meijer, L. J. J., Emmerik, T. V., Van Der Ent, R., Schmidt, C., Lebreton, L. (2021) More than 1000 rivers account for 80% of global riverine plastic emissions into the ocean, *Science Advances*, 7 (18), eaaz5803. *https://doi.org/10.1126/sciadv.aaz5803*
37. Lima, A. R., Ferreira, G. V., Barrows, A. P., Christiansen, K. S., Treinish, G., and Toshack, M. C. (2021) Global patterns for the spatial distribution of floating microfibers: Arctic Ocean as a potential accumulation zone, *Journal of Hazardous Materials*, 403, 123796. *https://doi.org/10.1016/j.jhazmat.2020.123796*
38. Barrows, A. P. W., Cathey, S. E., and Petersen, C. W. (2018) Marine environment microfiber contamination: Global patterns and the diversity of microparticle origins, *Environmental pollution*, 237, 275–284. *https://doi.org/10.1016/j.envpol.2018.02.062*
39. The Earth Observatory, NASA. The Pacific or "Peaceful" Ocean, Release 2014, *https://earthobservatory.nasa.gov/blogs/fromthefield/2014/04/24/the-pacific-or-peaceful-ocean/* (accessed Dec 2023)
40. Waite, H. R., Donnelly, M. J., and Walters, L. J. (2018) Quantity and types of microplastics in the organic tissues of the eastern oyster *Crassostrea virginica* and Atlantic mud crab *Panopeus herbstii* from a Florida estuary, *Marine Pollution Bulletin*, 129(1), 179–185. *https://doi.org/10.1016/j.marpolbul.2018.02.026*
41. Rana, S., Pichandi, S., Parveen, S., and Fangueiro, R. (2014) Natural Plant Fibers: Production, Processing, Properties and Their Sustainability Parameters, in *Roadmap to sustainable textiles and clothing: Eco-friendly raw materials, technologies, and processing methods* (Muthu, S. S., Ed.) 1st vol., 1–35. Springer, Singapore.

ABOUT THE STUDENT AUTHOR

Julia Bures graduated in 2024 from California Lutheran University with a BS in Biology. She will pursue a degree in veterinary medicine.

PRESS SUMMARY

One form of plastic pollution is microfibers, which are synthetic fibers five μm or smaller that are shed by synthetic-based clothing. Once in the ocean, microfibers are ingested by a variety of marine organisms including oysters. Oysters are filter feeders and a major aquaculture asset, which presents a concern for the effects of microfiber ingestion on human health. This study quantifies microfiber pollution in Pacific oysters farmed for human consumption from Morro Bay, California.

An average of 9.12 microfibers were recovered per oyster sample with no significant correlation between microfiber content and oyster visceral wet weight or shell length. Black and blue microfibers were recovered in higher quantities than red and green microfibers. The results of this study indicate that a large number of microfibers are present in commercial oysters, but more research needs to be conducted to determine how this will impact human health.

Autoregressive Bandits in Near-Unstable or Unstable Environment

Uladzimir Charniauski & Yao Zheng*

Department of Statistics, University of Connecticut, Storrs, CT

https://doi.org/10.33697/ajur.2024.116

*Students: uladzimir.charniauski@gmail.com**
Mentor: yao.zheng@uconn.edu

ABSTRACT

AutoRegressive Bandits (ARBs) is a novel model of a sequential decision-making problem as an autoregressive (AR) process. In this online learning setting, the observed reward follows an autoregressive process, whose action parameters are unknown to the agent and create an AR dynamic that depends on actions the agent chooses. This study empirically demonstrates how assigning the extreme values of systemic stability indexes and other reward-governing parameters severely impairs the ARBs learning in the respective environment. We show that this algorithm suffers numerically larger regrets of higher forms under a weakly stable environment and a strictly exponential regret under the unstable environment over the considered optimization horizon. We also test ARBs against other bandit baselines in both weakly stable and unstable systems to investigate the deteriorating effect of dropping systemic stability on their performance and demonstrate the potential advantage of choosing other competing algorithms in case of weakened stability. Finally, we measure the discussed bandit under various assigned values of key input parameters to study how we can possibly improve this algorithm's performance under these extreme environmental conditions.

KEYWORDS

Reinforcement Learning; Machine Learning; Autoregressive Processes; Bandit Algorithms; Non-Stationary Bandits; Online Learning

INTRODUCTION

Multi-Armed Bandits (MABs)[2] is a simplified reinforcement learning problem where an agent must choose among available actions (arms) to maximize the cumulative reward over time. The goal is to develop strategies that minimize regret - the difference between the rewards obtained and those that the agent could achieve by always choosing the optimal arm. Bacchiocchi et al.[1] introduce an AutoRegressive Bandits (ARBs) setting, an extension of traditional MABs and a novel representation of a particular class of continuous reinforcement learning problems, where the reward is determined by the autoregressive (AR) process, whose parameters depend on the actions the agent chooses. The AR process[3] is one of the most widely used class of stochastic processes to model temporal dependencies in real-world phenomena (e.g. stock markets, weather forecasting, etc.).[18, 19] Bacchiocchi et al.[1] employ an optimistic algorithm for online-learning, AutoRegressive Upper Confidence Bounds (AR-UCB), designed to pursue the reward maximizing action sequence, or optimal policy, within the ARBs setting in an online fashion. The AR-UCB can be used to in dynamic e-commerce pricing to model and forecast price changes over time based on historical pricing data, as the AR models assume that the current price is a linear function of past prices and an error term.[22] This algorithm has empirically proven to be advantageous with respect to existing methods in displaying its regret-minimizing abilities when tested under the same conditions(see the *Baselines Comparison* section for details). The authors demonstrated that AR-UCB always suffers the smallest cumulative regret and, unlike its competitors, displays the sublinear behavior, indicating its dominating efficiency in optimizing the sequence of played actions compared to other methods.

Standard bandit algorithms typically assume a stationary environment. However, in many real-world applications, the underlying conditions affecting the reward distribution of the arms may change over time.[20] As Granger et al.[17] note, "Many economic and business time series are non-stationary and, therefore, the type of models that we have studied cannot (directly) be used." This implication spurs the interest in developing bandit algorithms tailored for non-stationary environments.[7, 9] Particularly, in real-world applications of AR processes, unit-root non-stationarity is frequently observed. This type of non-stationarity is characterized by a stochastic trend, where the time series develops indefinitely, without returning to a fixed mean or trend line.[3, 10, 23] Failing to account for unit roots can lead to spurious regressions and invalid statistical inferences, so it is important to address unit-roots before modeling AR processes.[21] However, the important question is how the unit-root non-stationarity influences the quality of learning the optimal policy within the ARB setting and whether the AR-UCB can still remain competitive compared to other bandit algorithms under such conditions.

Existing works mostly focus on addressing non-stationarity in the standard MABs setting, without incorporating autocorrelations in the processes. For example, Besbes et al.[11] propose an algorithm that achieves the optimal regret bound, which adapts to the degree of non-stationarity in the reward process. The non-stationary bandit problem involves scenarios where the environment is dynamic, leading to fluctuations in rewards and potentially altering the optimal strategy over time.[8] Komiyama[12] propose a new bandit algorithm class named the Adaptive Resetting Bandit (ADR-Bandit) that can achieve the optimal performance in stationary and non-stationary environments, accounting for its abrupt or gradual changes, which the author calls "global changes." Furthermore, Liu et al.[13] introduce the Predictive Sampling learning algorithm that can adapt to the degree of non-stationarity in the environment and empirically outperforms Thompson sampling[14] employed in stationary learning. The prevailing consensus highlights the importance of employing specialized methods for bandit learning problems to attain desired adaptive strategies.

Limited studies have proposed more specialized algorithms that can help the ARBs adapt to changes in their learning environments. Trella et al.[9] introduce a new formulation in the context of the non-stationary latent AR bandits,[15, 16] where the reward distributions of the arms follow a latent AR process with a changing according to this AR dynamics state over time. The authors propose an efficient AR OFUL algorithm, a modified version of OFUL algorithm designed for stochastic linear bandits,[5] that is capable of effectively handling changes in non-stationarity. Nonetheless, the algorithmic approach in this paper addresses the unknown nature of the latent process, which fails to encompass the setting addressed by Bacchiocchi et al.,[1] where the information about the AR process is available for the agent. The scarcity of existing literature studying the behavior of AR bandits under extreme environmental conditions has sparked the initiation of the presented study.

The goal of this paper is to investigate the AR-UCB behavior under various degrees of systemic stability, an employed measure[10] for the degree of stationarity of the autoregressive processes, in terms of generated average cumulative regrets to determine the effect of changing these environmental conditions on the algorithm's performance. We analyze the algorithm in three near-unstable, or with an extremely weakened stability that closely replicates the unit-root non-stationarity, and one strictly unstable environment and compare it to results presented in Bacchiocchi et al.[1] containing the original stability indexes. We also test AR-UCB with other baselines from the literature[4–7] in each introduced environment. Importantly, we empirically demonstrate that near-unstable environment drastically worsen and the unstable environment paralyzes the learning process for AR-UCB and other introduced bandits. Lastly, we will empirically evaluate the AR-UCB under selected values of reward-governing parameters, such as Ridge regularization parameter and the boundedness value, whose meaning we discuss along the paper, to illustrate that the algorithm minimizes the generated cumulative regret and improves the learning process for the smallest values of these controlled parameters.

THE AUTOREGRESSIVE BANDITS

Setting

The AutoRegressive Bandits setting[1] considers the sequential interactions between the learner and the environment. It conditions the reward evolution according to the autoregressive (AR) process of the order k (AR(k)).[3] Thus, at every round t, the learner chooses an action $a_t \in \mathcal{A} = [\![n]\!]$ (we define $[\![a, b]\!] = \{a, ..., b\}$ and $[\![b]\!] = \{1, ..., b\}$ for any $a \leq b \in \mathbb{N}$) among the $n \in \mathbb{N}$ available ones and observes the reward x_t of the form described in **Equation 1**.

$$x_t = \gamma_0(a_t) + \Sigma_{i=1}^{k} \gamma_i(a_t) x_{t-i} + \xi_t \qquad \textbf{Equation 1.}$$

We define the reward space as $x_t \in \mathcal{X} \subseteq \mathbb{R}$, the unknown *parameters* depending on an action a as $\gamma_0(a_t) \in \mathbb{R}$ and $(\gamma_i(a_t))_{i \in [\![k]\!]} \in \mathbb{R}^k$, and the zero-mean σ^2-subgaussian random noise conditioned to the past as ξ_t. We can also express the reward evolution in the *inner product* form $\langle \boldsymbol{x}, \boldsymbol{y} \rangle = \boldsymbol{x}^T \boldsymbol{y} = \Sigma_{i=1}^{n} x_i y_i$, where $\boldsymbol{x}, \boldsymbol{y} \in \mathbb{R}^n$ are any finite real-valued vectors, as shown in **Equation 2**.

$$x_t = \langle \gamma(a_t), \boldsymbol{z}_{t-1} \rangle + \xi_t \qquad \textbf{Equation 2.}$$

In this equation, we have $\boldsymbol{z}_{t-1} = (1, x_{t-1}, ..., x_{t-k})^T \in \mathcal{Z} = \{1\} \times \mathcal{X}^k$ - the *context vector* expressing the past history of reward observations, and $\gamma(a) = (\gamma_0(a), ..., \gamma_k(a))^T \in \mathbb{R}^{k+1}$ - the *parameter vector* for every $a \in \mathcal{A}$.

Every $\gamma_i(a_t)$ parameter fulfills three following assumptions[1] labeled in order: **Assumption 1** (Non-negativity) requires that the coefficients of are non-negative (i.e. $\gamma_i(a) \geq 0$ for every $i \in [\![0, k]\!]$) for producing realistic results in observing the real-world phenomena. **Assumption 2** (Stability) establishes that the sum of action parameters $\Sigma_{i=1}^{k} \gamma_i(a)$ is limited to a stability coefficient value $\Gamma \in [0, 1)$. **Assumption 3** (Boundedness) enforces the boundedness to $\gamma_0(a)$ with a finite value $m = \max_{a \in \mathcal{A}} \gamma_0(a)$.

Assumption 2 and **3** guarantee the inability of the underlying autoregressive processes to diverge in expectation for any action sequence played by the agent.[1] On the other hand, the near-unstable environments with $\Gamma \approxeq 1$ and/or large values of m aggravate the learning process within the ARB setting, requiring more time for the agent to develop the optimal policy. Finally, the unstable environment $\Gamma = 1$ completely eliminates the systemic stability, in which case the learner is unable to choose the most optimal action sequence to maximize its results regardless of values of other presented parameters. In this work, we show the importance of employing these two assumptions in the learning process by empirically demonstrating that the AR-UCB suffers numerically larger regrets due to losses in learning abilities occurring in the environments, where either of these two assumptions (or both) are relaxed.

Policy and Performance

Since our studies concern the empirical analysis of the achieved regret, we provide the formal regret definition. The policy π models the learner's behavior and the regret R imposes the loss of not choosing an optimal action on a learner. The deterministic learner's policy $\pi = (\pi_t)_{t \in \mathbb{N}}$, defined for each round $t \in [\![T]\!]$ as the mapping function from the history of observations $H_{t-1} = (x_0, a_1, x_1, ..., a_{t-1}, x_{t-1})$ to the action space $\mathcal{A}$, demonstrating that $a_t = \pi_t(H_{t-1})$.

The policy performance is evaluated through the expected cumulative reward $J_T(\pi) = \mathbb{E}[\Sigma_{t-1}^{T} x_t]$ over the horizon $T \in \mathbb{N}$ with respect to the random reward noise ξ_t. The learner objective is to minimize the expected cumulative regret $R(\pi, T)$ by playing a policy π against the *optimal policy* π^* satisfying $\pi^*(H_{t-1}) = \arg\max_{a \in \mathcal{A}} \langle \gamma(a), \boldsymbol{z}_{t-1} \rangle$[1] (from **Assumption 1**) over a learning horizon $T \in \mathbb{N}$, where where $r_t = x_t^* - x_t$ is the *instantaneous policy regret* and $(x_t^*)_{t \in [\![t \in \mathbb{N}]\!]}$ is the sequence of rewards from playing π^* from **Equation 3**.

$$R(\pi, T) = J_T^* - J_T(\pi) = \mathbb{E}[\Sigma_{t=1}^{T} r_t] \quad \textbf{Equation 3.}$$

We find that the presence of weak systemic stability impedes the agent in completing the regret minimization objective. Specifically, we demonstrate the positive trend between dropping the robustness of systemic stability and the number of rounds required to develop the optimal policy under these aggravating conditions.

The AR-UCB

For the ARB setting, we devise AR-UCB that suffers sublinear regret[1] of order $\mathcal{O}\left(\frac{(m+\sigma)(k+1)^{3/2}\sqrt{nT}}{(1-\Gamma)^2}\right)$, where T is the exploration horizon, n is number of actions, m and σ are the $\max \gamma_0(a)$ and noise values, respectively, and Γ is the index of systemic stability. This formula suggests that higher autoregressive orders k, larger values m and stability indexes Γ increase the complexity of learning for this algorithm. Thus relaxing **Assumption 2** and **Assumption 3** exasperate the learning process by allowing higher values for m and Γ parameters.

At each round $t \in [\![T]\!]$, the AR-UCB algorithm computes the *Upper Confidence Bound* for every $a \in \mathcal{A}$ to play this action and observe the reward x_t as in **Equation 2**. The formal computation is defined as follows in the **Equation 4**.

$$a_t \in \arg\max_{a \in \mathcal{A}} \mathrm{UCB}_t(a) := \langle \hat{\gamma}_{t-1}(a), \boldsymbol{z}_{t-1} \rangle + \beta_{t-1}(a) ||\boldsymbol{z}_{t-1}||_{\boldsymbol{V}_t(a)} \quad \textbf{Equation 4.}$$

The AR-UCB computes $\hat{\gamma}_t(a) = \boldsymbol{V}_t(a)^{-1}\boldsymbol{b}_t(a)$, where it consistently updates the required Gram matrix $\boldsymbol{V}_t(a)$ and the vector $\boldsymbol{b}_t(a)$ ($\boldsymbol{V}_0(a) = \lambda \boldsymbol{I}_{k+1}$ and $\boldsymbol{b}_0(a) = \boldsymbol{0}_{k+1}$ at $t = 0$), as $\boldsymbol{V}_t(a) = \boldsymbol{V}_{t-1}(a) + \boldsymbol{z}_{t-1}\boldsymbol{z}_{t-1}^T \mathbb{1}_{\{a=a_t\}}$ and $\boldsymbol{b}_t(a) = \boldsymbol{b}_{t-1}(a) + \boldsymbol{z}_{t-1}x_t \mathbb{1}_{\{a=a_t\}}$ for every $a \in \mathcal{A}$ after observing the reward x_t. In this equation, we also define the exploration coefficient $\beta_{t-1}(a) \geq 0$ for every action $a \in \mathcal{A}$ and round $t \in [\![0, T-1]\!]$ as it follows in **Equation 5**.

$$\beta_t(a) = \sqrt{\lambda(m^2+1)} + \sigma\sqrt{2\log(\frac{n}{\delta}) + \log(\frac{\det \boldsymbol{V}_t(a)}{\lambda^{k+1}})} \quad \textbf{Equation 5.}$$

The first term in this equation is the *bias* term and the second one is the *concentration* term.[1] From this form of $\beta_t(a)$, it follows that smaller input values of λ and m reduce the *bias* term in computing $\beta_t(a)$. This way the algorithm more precisely estimates the action played, which helps achieve lower instantaneous regret r_t from playing the computed action a_t, while larger values of these parameters make the AR-UCB produce more biased calculations of a_t. However, because there is a trade-off between two terms of this equation with respect to λ, the value of $\beta_t(a)$ may evolve differently for smaller m under the same λ.

In practice, the actual value of m is unknown, so we may replace this value with a user-specified upper bound $\bar{m}$ to compute $\beta_t(a)$ in **Equation 5**. For example, in the simulation on the AR-UCB performance under different parameters λ, we allow $\bar{m}$ to differ from the actual value m. We will demonstrate that the AR-UCB suffers smaller regrets with $m = 20$ and $\bar{m} = 100$ as values of λ decrease to 0. However, the relationship between the regret and λ behaves quite differently under $m = \bar{m} = 1$. Moreover, we conduct another experiment to investigate the effect of m on the regret evolution when λ is fixed, and to avoid the ambiguity due to possible misspecification, we simply set $\bar{m} = m$.

SIMULATION DESIGN

In our experiments, we measure the AR-UCB and other baselines performance in terms of average cumulative regret over the optimization horizon $T = 10000$ rounds in a range of provided settings distinguished by the assigned systemic stability or the algorithm's key parameters. We evaluate all the experiments within three specific near-unstable environments, each carrying $\Gamma \in \{0.95, 0.98, 0.999\}$ stability indexes, and the unstable environment with a stability index

$\Gamma = 1$. We run a range of Python simulations, where each complies to the values in every respective setting, and provide the graphs of cumulative regrets achieved by the AR-UCB on alone or other introduced bandit baselines in each of discussed settings. All the algorithms are implemented in Python 3.12, and run over an Apple M1 with 8 GB RAM.

AR-UCB Performance

We first observe and analyze the AR-UCB cumulative regret on alone under systemic near-instability and instability. We consider three experimental settings containing autoregressive orders $k \in \{2, 4\}$, number of actions $n \in \{2, 7\}$, actual values $m \in \{1, 20, 920\}$, and noise parameters $\sigma = \{0.75, 1.5, 10\}$, respectively. We also compare our results to cumulative regret plots for every bandit generated under the original systemic stability indexes $\Gamma_{orig} = \{0.5, 0.7, 0.82\}$ using the same parameters to visually demonstrate the impact of weak stability on the AR-UCB performance. To specify the details of the learning process, we select hyper-parameters $\lambda = 1$, a Ridge regularization parameter value, and boundaries $\bar{m} = \{10, 100, 1000\}$ for the equivalent magnitudes of corresponding values of m (i.e. every $\bar{m}$ is sequentially selected for each m). **Table 1** summarizes the settings details.

	Parameters				
Setting	Γ_{orig}	k	n	m	σ
A	0.5	2	2	1	0.75
B	0.82	4	7	20	1.5
C	0.7	4	7	920	10

Table 1. Settings description.

Baselines Comparison

We test and compare AR-UCB performance in near-unstable and unstable environments against the following selected baselines: UCB1, EXP3, B-EXP3, and AR2. UCB1[4] is a widely-adapted solution for stochastic MABs. EXP3[6] is an algorithm designed for adversarial MABs and its extension to finite-memory adaptive adversaries B-EXP3.[5] AR2[7] is an algorithm that operates within a non-stationary MAB framework with an autoregressive reward structure of the first order (AR(1)). For this experiment, we utilize the same parameters as in the study on *AR-UCB Performance*. We also compare our results to cumulative regret plots for every bandit generated by Bacchiocchi et al.[1] under the original systemic stability indexes $\Gamma_{orig} = \{0.5, 0.7, 0.82\}$ using the same parameters to visually demonstrate the gravity of the impact of weak stability on the baselines performance. However, since we experiment on several baselines altogether, we display our results in three settings consisting of five graphs, where each corresponds to a stability index from Γ_{orig} to $\Gamma = 1$. **Table 1** precisely summarizes the parameters utilized in each setting.

On the AR-UCB Performance Under Different Parameters λ

We experimentally measure the AR-UCB performance under different regularization parameters λ. For our experiments on λ, we test this algorithm for selected $\lambda \in \{0.001, 0.01, 0.05, 0.2, 0.6, 1.2, 1.6, 3, 5\}$ against its performance for the originally utilized by Bacchiocchi et al.[1] choice $\lambda = 1$. We first employ $n = 7$, $k = 4$, $m = 20$, and $\sigma = 1.5$ in every near-unstable and unstable setting (**Figure 3**). Then we repeat this experiment with $m = 1$ (**Figure 4**) to analyze trade-off between the *bias* and *concentration* terms from **Equation 5** with respect to λ. We also select $\bar{m} = 1$ and $\bar{m} = 100$ as our hyper-parameter for $m = 1$ and $m = 20$, respectively. The goal of this experiment is to analyze how each assigned λ impacts the AR-UCB regret evolution with respect to its original value, and what regularization value helps the algorithm minimize it.

On the AR-UCB Performance Under Different Parameters m

We test the AR-UCB under several values of m. For our experiments on m, we consider an array of values $m \in \{0, 0.25, 0.5, 1, 10, 100, 500, 1000\}$. We utilize $n = 7$, $k = 4$, $\sigma = 1.5$, and $\lambda = 1$ in every near-unstable and unstable setting. To avoid the misspecification[1] of presented boundary parameters, each $\bar{m} = m$ for every action $a \in \mathcal{A}$ for its respective scenario (Ex. $\bar{m} = 10$ if $m = 10$), since we do not investigate in this study how the erroneous

estimation of the boundary influences the algorithm's performance. We only aim to establish the general relationship between the m value and the achieved AR-UCB cumulative regret in the learning process.

RESULTS

AR-UCB Performance

Figures 1 shows the average cumulative regrets for AR-UCB under different stability indexes. We may observe that the AR-UCB regret rapidly degenerates from the sublinear to higher forms under $\Gamma \in \{0.95, 0.98, 0.999\}$ in every respective scenario. Thus, under falling stability, the AR-UCB requires drastically more time to learn the optimal action sequence for adapting to its environment. This notion is especially highlighted under $\Gamma = 0.999$ in every experiment, where the AR-UCB achieves the exponential regret in the first stages of the simulations under the $\Gamma = 0.999$ stability index. This way we observe that the extremely low systemic stability makes the algorithm temporarily lose the learning ability within the limited exploration.

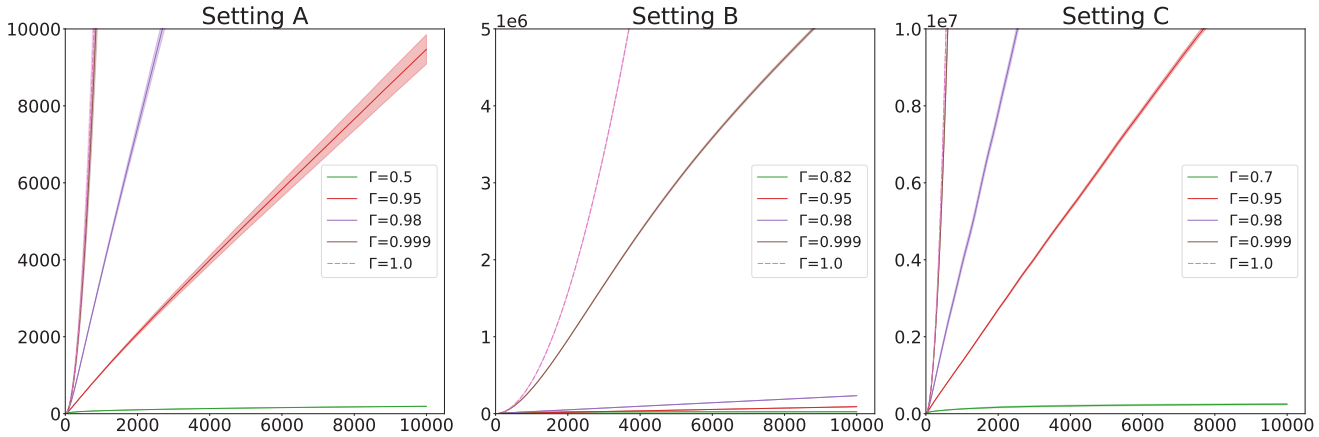

Figure 1. Cumulative regret of AR-UCB across stable, near-unstable, and unstable environments.

The AR-UCB performance under $\Gamma = 1$ is fundamentally different. First, we immediately observe the cumulative regret to be exponentially increasing in every introduced experiment. This indicates that AR-UCB completely loses its ability to acquire information in the unstable environment, making less optimal choices at every round over the learning horizon T. We may similarly observe precisely the same AR-UCB behavior under $\Gamma = 0.999$ at earlier stimulation stages, since this index value closely recreates this effect of the systemic instability on learning. However, it is still possible for the algorithm to achieve the optimal policy even under the infinitely close to 1 value of Γ over a large number of rounds, which is especially seen in a Setting **B**, whereas the unstable environment completely annihilates this possibility by paralyzing the learning process.

The above experiments highlight the importance of employing **Assumption 2** in the learning process. This assumption ensures the efficiency of learning for the algorithm by creating a stable environment s.t. Γ is far within the radius of 1. We observe that weakening this assumption with any $\Gamma \approxeq 1$ consequently weakens the algorithm's ability to process the information from its setting and develop the optimal action sequence that reduces regrets to a sublinear form. This way the more Γ approaches 1, the more this index complicates the ongoing learning for the algorithm. Finally, the unstable $\Gamma = 1$ completely abolishes the learning, so that the algorithm plays sub-optimal actions at all rounds.

Baselines Comparison

Figures 2 illustrates the average cumulative regret of all tested baselines for $\Gamma \in \{0.95, 0.98, 0.999\}$ in three settings. The cumulative regret achieved by many tested bandit baselines progressively degenerates to higher forms with increasing values of Γ. Every bandit suffers precisely the same numerical regret, except for a particular case depicted in the Setting **B** in scenario with $\Gamma = 0.999$, where UCB1 significantly outperforms every other baseline under this stability index. We also see that every baseline achieves the exponential regret under $\Gamma = 0.999$ in every experiment during the

first stages of simulations, which occurs due to the limited exploration. Amongst all the baselines, AR-UCB demonstrates near-identical performance compared to UCB1 in every experiment in all near-unstable scenarios, except for the Setting **B** under $\Gamma = 0.999$. On the other hand, AR2 is able to significantly outperform AR-UCB and other bandits in the experiment in the Setting **C**, although their achieved regrets converge in value across every scenario as the stability weakens. Both EXP3 and B-EXP3 suffer near-identical regret in every presented experiment with near-unstable indexes, achieving the largest cumulative regrets with respect to other baselines.

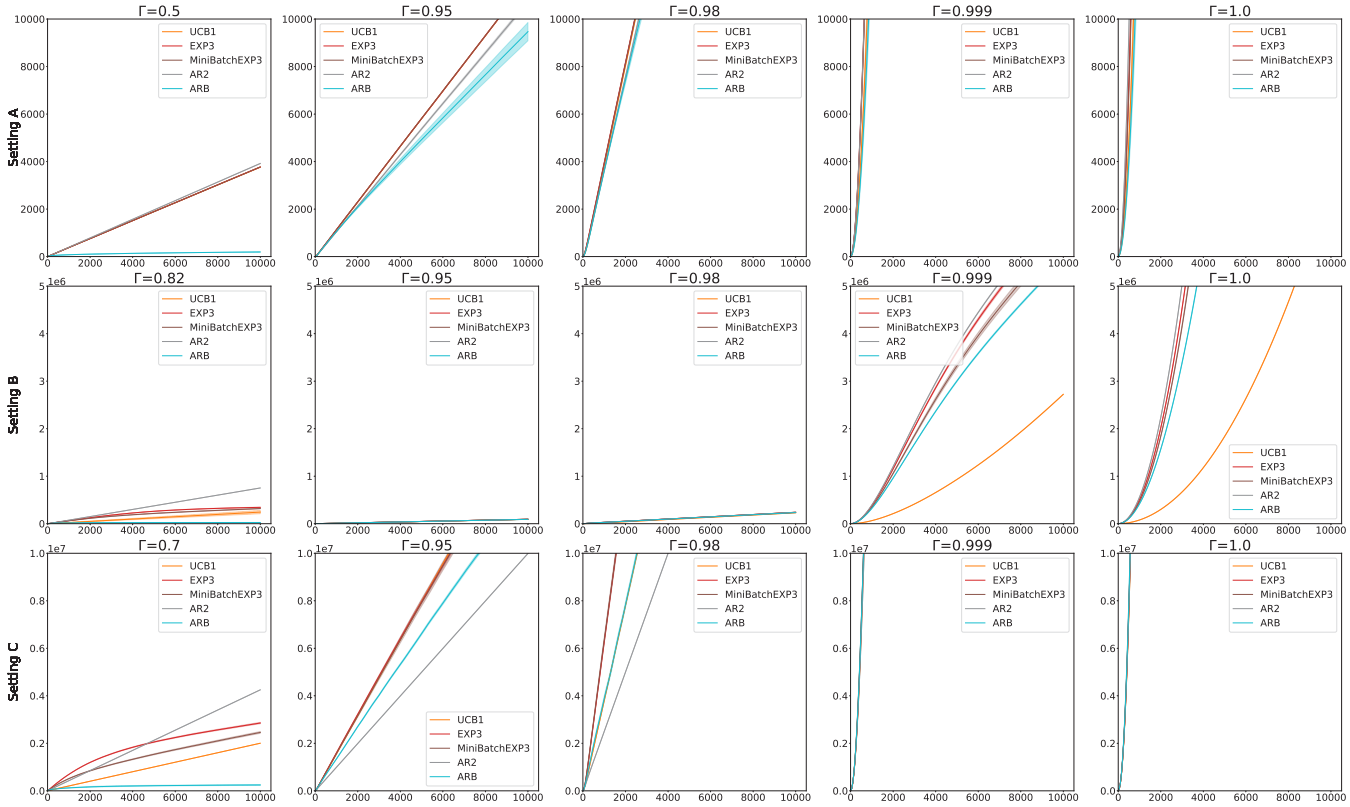

Figure 2. Comparison of cumulative regret for different baselines across stable, near-unstable, and unstable environments.

Unlike in case of near-instability, every experimented baseline displays strictly exponential behavior within the unstable environments in every presented scenario. We may observe that baselines suffer close-in-value exponential cumulative regret in every experiment, except for the one in the Setting **B**, in which UCB1 achieves the lowest regret out of all the bandits, showcasing its least sensibility to the systemic stability. Nonetheless, the AR-UCB again replicates UCB1 in terms of their regret in unstable scenarios in other two experiments (**A** and **C**). Meanwhile, the unstable environment significantly suppressed the AR2 performance, making this baseline to suffer the largest regret in every experiment. Both EXP3 and B-EXP3 again achieve a closely similar exponentially growing cumulative regret under the instability in all presented experiments.

These experiments illustrate the dependence of introduced bandits on the robustness of the systemic stability conditioned by **Assumption 2**. We demonstrated that every baseline develops the same regret behavior depending on the introduced value of a stability index Γ in the respective environment. Thus we showed that all the baselines equivalently lose their learning ability and require more additional time to optimize their action policy under near-unstable $\Gamma \approxeq 1$ values, where . Finally, the unstable index $\Gamma = 1$ disables learning processes for every baseline, making them inefficiently operate within such an environment regardless of other selected parameters.

On the AR-UCB Performance Under Different Parameters λ

Figures 3 and 4 show the average cumulative regret in the near-unstable and unstable environments for each considered λ under $m = 20$ and $m = 1$. We immediately observe that the AR-UCB achieves the best performance under the smallest $\lambda = 0.0001$ for all settings with $m = 20$, whereas the optimal choice of λ in experiments with $m = 1$ varies depending on the stability coefficient: $\lambda = 0.2$ when $\Gamma = \{0.95, 0.98\}$, $\lambda = 0.01$ when $\Gamma = 0.999$, and $\lambda = 1$ when $\Gamma = 1$. In **Figure 3**, we see that the algorithm achieves significantly smaller regrets with choices $\lambda < 1$ with respect to other selections. However, the regrets in **Figure 4** are more clustered, indicating their lesser sensitivity to the choice of λ when m is smaller. We also observe that the AR-UCB enjoys sublinear regret in settings with $\Gamma \leq 0.98$ across all choices of λ. Meanwhile, the severely weakened stability under $\Gamma = 0.999$ conditions the exponential regret evolution at some initial rounds under every λ. Still the algorithm is able to quickly reduce the regret to lower forms over more rounds, especially for optimal choices of λ. It's also worth noting that the AR-UCB can achieve smaller regret in the same fashion across selected λ under $\Gamma = 1$. Nonetheless, because the systemic instability completely disables learning processes, the algorithm does not achieve the sublinear regret in this setting regardless of other parameters.

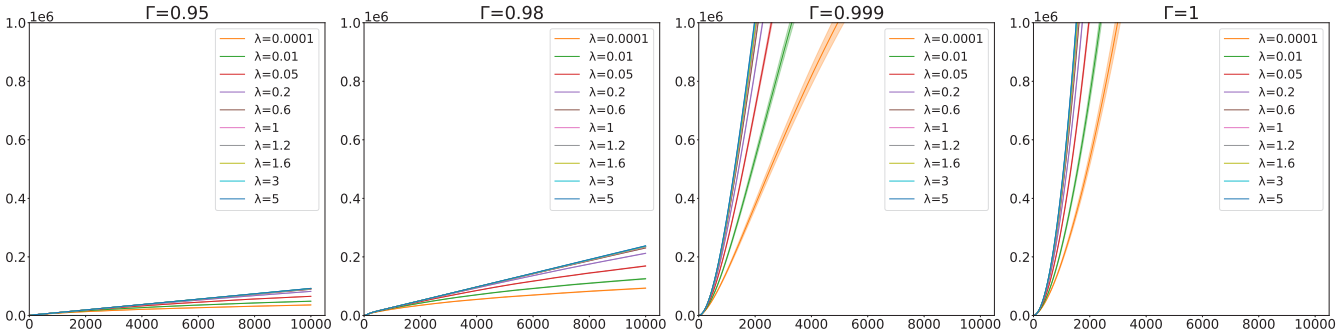

Figure 3. Effect of the choice of λ on the AR-UCB cumulative regret in near-unstable and the unstable environments ($m = 20$).

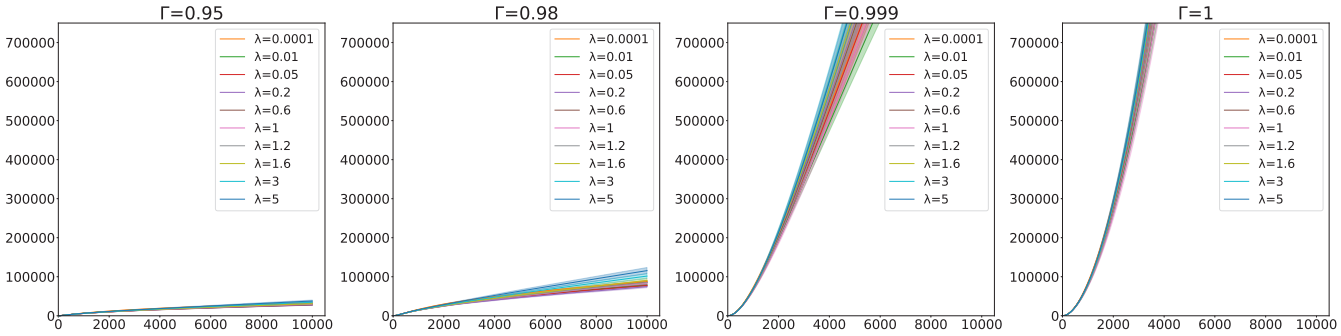

Figure 4. Effect of the choice of λ on the AR-UCB cumulative regret in near-unstable and the unstable environments ($m = 1$).

The experiments on the manipulation of the Ridge regularization parameter λ empirically illustrates the role of $\beta_t(a)$ components from **Equation 5** in the AR-UCB learning process. We can explain the different findings from **Figures 3 and 4** can be explained via the formula for this coefficient. According to this equation, the *bias* term increases with λ, while the concentration term decreases with this parameter. When m is large (ex. $m = 20$), the *bias* will dominate the *concentrtion* term even for extremely small λ choices. Consequently, in **Figure 3**, the smallest $\lambda = 0.0001$ is the most optimal across all the experiment. On the other hand, when m is relatively small, the *bias* term does not necessarily dominate the *concentration* term, and then the optimal choice of λ will depend on the trade-off between the two terms. As a result, in **Figure 4**, the cumulative regret is not monotonic in λ, and the specific optimal choice of lambda depends on the stability parameter.

On the AR-UCB Performance Under Different Parameters m

Figures 5 shows the average cumulative regrets of AR-UCB under different values m. The AR-UCB achieves the minimal regret under every $m = 0$, with a progressive increase as values m get larger across all four experiments. Across all

the experiments, the regrets under $m \in [0, 1]$ are more clustered, while the regret values under $m > 1$ are drastically different. Also, in scenarios with $\Gamma \in \{0.95, 0.98\}$, $m \in [0, 1]$ condition sublinear regret evolution over the entire learning interval, while any $m > 1$ reduces regrets to linear, allowing the sublinear behavior only during the initial stages of simulations. In the scenario with $\Gamma = 0.999$, the AR-UCB seems to exhibit the exponential regret due to severely weakened stability, especially when m is large. Meanwhile, the AR-UCB displays strictly exponential average cumulative regrets for every m within the $\Gamma = 1$ environment. Due to systemic instability, the algorithm will never achieve the optimal policy and continue to suffer this regret regardless of the provided values of m. Thus AR-UCB is only able to minimize the achieved regret with the lowest value of m, as any value $m > 0$ only leads to larger regrets.

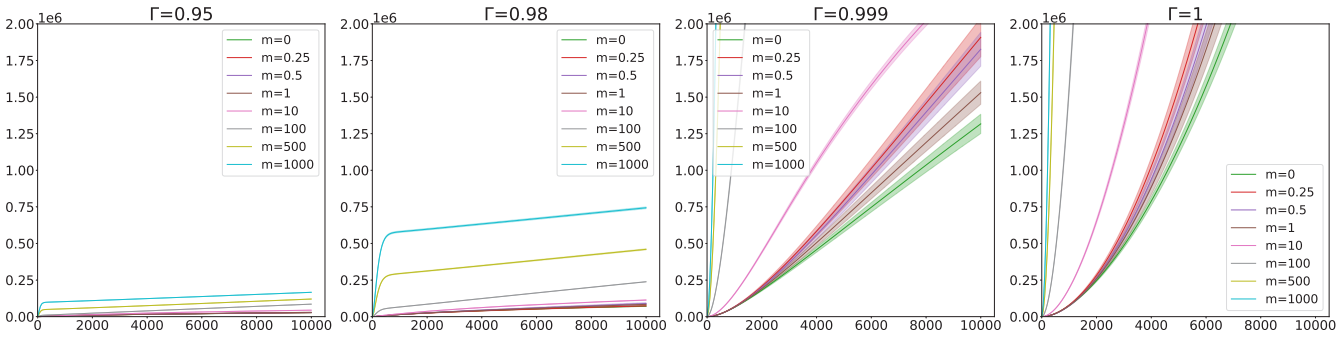

Figure 5. Cumulative regret for AR-UCB in the stable vs. near-unstable and the unstable environments.

These experiments illustrate that larger values of m substantially increase the AR-UCB regrets, while the value $m = 0$ helps produce the smallest regret across our experimental scenarios. However, in the presence of severely weakened stability (i.e $\Gamma = 0.999$), the algorithm under higher values of m can sooner optimize its performance in a trade-off with the size of the regret. Thus we empirically demonstrate that relaxing **Assumption 3** with introducing very high values of m within the weak (or eliminated) systemic stability further reduces the algorithm's performance by enlarging the *bias* in calculating $\beta_t(a)$ for each action, as shown in **Equation 5**.

CONCLUSION AND DISCUSSION

In this research, we experimentally tested the AR-UCB and other bandit baselines' behavior under varying degrees of systemic near-instability $\Gamma \in \{0.95, 0.98, 0.999\}$ and under a definite degree of systemic instability $\Gamma = 1$. First, we measured the AR-UCB performance under the near-instability and instability on alone against its stable performance, demonstrating the differences in the regret evolution within the presented settings. We then repeated our measures under the same selected near-unstable and unstable settings on several other baselines introduced in the original paper. We observed that the presented algorithm achieve precisely the same regret evolution as the AR-UCB and highlighted the performative advantages of some baselines relative to the original one under specific values of systemic near-instability and instability. Finally, we provided a series of experimental measures of AR-UCB under different Ridge regularization parameters λ and values of m to empirically analyze the improvements in the AR-UCB performance by finding the optimal values for these parameters.

Our work highlights the need for a more robust alternative to the AR-UCB algorithm capable of adapting to potentially unstable environments, such as those characterized by (near) unit-root autoregressive processes. Additionally, while our research primarily focuses on numerical investigation, it would be valuable to theoretically analyze the phase transition behavior of the AR-UCB algorithm across stable and unstable regimes. This analysis would provide insights into its capabilities and limitations. Furthermore, it is interesting to extend our study to dynamic linear bandits[24], which assumes an environment evolving according to a stable linear dynamic system. Investigating how the possible violation of stability, characterized by the unit-rootness of the transition matrix, impacts the algorithm's performance remains an open question that warrants further exploration.

REFERENCES

1. Bacchiocchi, F., Genalti, G., Maran, D., Mussi, M., Restelli, M., Gatti, N., & Metelli, A. M. (2024) Autoregressive bandits. In *International Conference on Artificial Intelligence and Statistics*, 937–945. *https://doi.org/10.48550/arXiv.2212.06251*
2. Sutton, R. S., & Barto, A. G. (2005) Reinforcement Learning: An Introduction. 2nd ed., MIT Press, Cambridge, MA.
3. Hamilton, J. D. (1994) *Time Series Analysis*, Princeton university press.
4. Auer, P., Cesa-Bianchi, N., Freund, Y., & R. E. Schapire. Gambling in a rigged casino: The adversarial multi-armed bandit problem. In *Processings of IEEE 36th Annual Foundations of Computer Science*, 322–331. *https://doi.org/10.1109/SFCS.1995.492488*
5. Abbasi-Yadkori, Y., Pál, D., & Szepesvári, C. (2011) Improved algorithms for linear stochastic bandits. *Advances in Neural Information Processing Systems* 24, 2312–2320. *https://doi.org/10.48550/arXiv.2309.14298*
6. Arora, R., Dekel, O., & Tewari, A. (2012) Online Bandit Learning against an Adaptive Adversary: from Regret to Policy Regret. *ICML'12: Proceedings of the 29th International Conference on Machine Learning* 29, 1747–1754.
7. Chen, Q., Golrezaei, N., & Bouneffouf, D. (2023) Non-Stationary Bandits with Auto-Regressive Temporal Dependency. *Advances in Neural Information Processing Systems (NeurIPS)*, 36.
8. Garivier, A., & Moulines, E. (2011) On Upper-Confidence Bound Policies for Switching Bandit Problems. In: Kivinen, J., Szepesvári, C., Ukkonen, E., Zeugmann, T. (eds) *Algorithmic Learning Theory. ALT 2011. Lecture Notes in Computer Science* (vol 6925), 174–183. Springer, Berlin, Heidelberg. *https://doi.org/10.1007/978-3-642-24412-4-16*
9. Trella, A. L., Dempsey, W., Doshi-Velez, F., & Murphy, S. A. (2024) Non-Stationary Latent Auto-Regressive Bandits. *https://doi.org/10.48550/arXiv.2402.03110*
10. Cryer, J. D., & Chan, K.-S. (2011) *Time Series Analysis With Applications In R*. Springer, New York.
11. Besbes, O., Gur, Y., & Zeevi, A. (2019) Optimal exploration-exploitation in a multi-armed bandit problem with non-stationary rewards. *Stochastic Systems*, 9(4), 319–337. *https://doi.org/10.1287/stsy.2019.0033*
12. Komiyama, J., Fouché, E., & Honda, J. (2021) Finite-time Analysis of Globally Nonstationary Multi-Armed Bandits. *ArXiv, abs/2107.11419*.
13. Liu, Y., Van Roy, B., & Xu, K. (2022) Nonstationary Bandit Learning via Predictive Sampling. *International Conference on Artificial Intelligence and Statistics*, 6215–6244. *https://doi.org/10.48550/arxiv.2205.0197*
14. Russo, D. J., Van Roy, B., Kazerouni, A., Osband, I., & Wen, Z. (2018) A Tutorial on Thompson Sampling. *Foundations and Trends in Machine Learning*, 11(1), 1–96. *https://doi.org/10.1561/2200000070*
15. Zhou, L., & Brunskill, E. (2016) Latent contextual bandits and their application to personalized recommendations for new users. Proceedings of the *Twenty-Fifth International Joint Conference on Artificial Intelligence*, 25, 3646–3653. *https://doi.org/10.48550/arXiv.1604.06743*
16. Hong, J., Kveton, B., Zaheer, M., Chow, Y., Ahmed, A., Ghavamzadeh, M., & Boutilier, C. (2020) Non-Stationary Latent Bandits. *ArXiv (Cornell University). https://doi.org/10.48550/arxiv.2012.00386*
17. Granger, C. W. J., & Swanson, N. R. (1997) An introduction to stochastic unit-root processes. *Journal of Econometrics*, 80(1), 35–62. *https://doi.org/10.1016/S0304-4076(96)00016-4*
18. Z. An, & Z. Feng. (2021) A Stock Price Forecasting Method Using Autoregressive Integrated Moving Average model and Gated Recurrent Unit Network. *2021 International Conference on Big Data Analysis and Computer Science (BDACS)*, 31-34. *https://doi.org/10.1109/bdacs53596.2021.00015*
19. Lai, Y., & Dzombak, D. A. (2020) Use of the Autoregressive Integrated Moving Average (ARIMA) model to forecast Near-Term regional temperature and precipitation. *Weather and Forecasting*, 35(3), 959–976. *https://doi.org/10.1175/waf-d-19-0158.1*
20. Hong, J., Kveton, B., Zaheer, M., Chow, Y., & Ahmed, A. (2021) Non-Stationary Off-Policy Optimization. *International Conference on Artificial Intelligence and Statistics. https://doi.org/10.48550/arXiv.2006.08236*
21. Das, S., & Nason, G. P. (2016) Measuring the degree of non-stationarity of a time series. *Stat*, 5(1), 295–305. *https://doi.org/10.1002/sta4.125*

22. Faehnle, A., & Guidolin, M. (2021) Dynamic Pricing Recognition on E-Commerce Platforms with VAR Processes. *Forecasting*, 3(1), 166–180. *https://doi.org/10.3390/forecast3010011*

23. Zhao, P., Zhang, L., Jiang, Y., & Zhou, Z. (2021) A simple approach for non-stationary linear bandits. In *International Conference on Artificial Intelligence and Statistics*, 746–755. *https://doi.org/10.48550/arxiv.2103.05324*

24. Mussi, M., Alberto Maria Metelli, & Marcello Restelli. (2023) Dynamical linear bandits. In Proceedings of the *40th International Conference on Machine Learning*, 25563–25587. *https://doi.org/10.48550/arXiv.2211.08997*

ACKNOWLEDGMENT

The authors express gratitude to the editor and reviewers for their insightful feedback, which enabled the authors to refine the manuscript to its current form.

ABOUT THE STUDENT AUTHOR

Uladzimir Charniauski is a second-year student at the University of Connecticut majoring in Applied Mathematics and Statistics at the University of Connecticut. After graduation, he hopes to gain several years of the industry experience before pursuing a Ph.D. in Statistics, focusing on the interdisciplinary studies of Reinforcement Learning and Time Series Analysis.

PRESS SUMMARY

AutoRegressive Upper Confidence Bound (AR-UCB) is a recently proposed online learning algorithm that has been shown to outperform other bandit algorithms in stable autoregressive environments. However, when the environment is weakly stable or unstable, our work reveals that AR-UCB loses its learning ability and may perform worse than other benchmark algorithms. This study highlights the critical dependence of AR-UCB on environmental stability, with important implications for its proper implementation in various real-world domains.

Extracts from Soil Samples around Pennsylvania Exhibit Potent Antibacterial Properties against *Bacillus anthracis*

Annalee M. Schmidt [a,c], *Shawn Xiong** [a,b], *& John N. Alumasa** [a,c]
[a] *Department of Biochemistry and Molecular Biology, The Pennsylvania State University, University Park, PA*
[b] *Department of Biochemistry and Molecular Biology, Dalhousie University, Halifax, Nova Scotia, Canada*
[c] *Department of Chemistry and Biochemistry, Miami University, Oxford, OH*

https://doi.org/10.33697/ajur.2024.117

Student: annalee.schmidt13@gmail.com
*Mentors: shawn.xiong@dal.ca; alumasjn@miamioh.edu**

ABSTRACT
Deadly bacterial infections such as anthrax continue to pose a significant threat to human health worldwide. This disease is caused by *Bacillus anthracis,* which the CDC classifies as a Tier 1 biological agent due to its ability to form spores resistant to severe environmental stress conditions, including antibiotics. Identifying new antibiotics against this pathogen is therefore crucial for combatting anthrax infections. In this research, crude extracts from Pennsylvania soil were purified using various chromatography methods, resulting in natural products, which were assessed for their antimicrobial properties. After performing minimum inhibitory and bactericidal concentration assays, two compounds, AMS002 and AMS003, exhibited growth inhibitory and killing activity against *B. anthracis* at 0.8 mg/ml and 0.2 mg/ml, respectively. Both compounds inhibited greater than 80% of protein synthesis relative to the control samples in cell-based and *in-vitro* fluorescent reporter assays, suggesting that these compounds may target the bacterial protein synthesis pathway as their primary mode of action. The novelty of this discovery is vital due to the resistant nature of *B. anthracis* spores and their use as a potential weapon in bioterrorism.

KEYWORDS
Antibiotics; Resistance; Natural Products; Chromatography; *B. anthracis*; Minimum Inhibitory Assay; Minimum Bactericidal Assay; Reporter Assays; Course-based Undergraduate Research Experience (CURE)

INTRODUCTION

Antibiotic resistance continues to pose a significant threat to human health worldwide. There is a substantial shortage of drugs that can fight resistant bacterial infections due to the decline in research aimed at developing novel antibiotics.[1] Over one million people die from bacterial infections every year, including 200,000 newborn babies.[2,3] These alarming statistics are projected to increase to ten million annual fatalities by 2050, creating a significant problem that requires urgent resolution.[2,3]

Pathogenic bacteria develop resistance to antibiotics using different strategies, which enable them to survive and replicate in the presence of antibiotics. Common resistance mechanisms include increased efflux systems that remove the drug from bacterial cells, alterations to the drug's molecular target, and the production of drug-altering enzymes.[4] Antibiotics are critical in providing therapy for infections, but their overuse and misuse contribute to the rise of resistant strains. According to classifications by the Centers for Disease Control and Prevention (CDC), some of the highest risk priority pathogens include *Bacillus anthracis,* vancomycin-resistant *Enterococci* (VRE), methicillin-resistant *Staphylococcus aureus* (MRSA), *Pseudomonas aeruginosa*, and *Clostridium difficile*.[5] The threat posed by these pathogens is accompanied by urgent calls from the CDC for increased drug discovery-related research to identify novel antibiotic candidates to treat deadly infections caused by these pathogens.

Following the discovery of penicillin in 1928, scientists focused on synthesizing derivatives of previously existing antibiotics to combat resistance during the medicinal chemistry era.[6] Since 2017, the Food and Drug Administration (FDA) has approved eight new antibiotics for combating antibiotic-resistant infections, most of which are derivatives of traditional antibiotics.[7] For example, Eravacycline, approved by the FDA in 2018, is a fully synthetic antibacterial agent containing two chemical modifications from tigecycline, a broad-spectrum tetracycline antibiotic.[8] Using derivatized analogs to treat bacterial infections quickly led to resistance, making such drugs ineffective.[9]

As resistant strains of bacteria persist, researchers have turned to natural products as a source of new antibiotics. The environment is a reliable resource for producing potential antimicrobial compounds because of the diversity of microorganisms within that ecosystem. Some microbes produce compounds with potent antimicrobial properties to compete with neighboring organisms for nutrients or fend off adversaries. For example, penicillin was discovered accidentally in 1928 by Sir Alexander Flemming from the fungal species *Penicillium chrysogenum.*[10] Similarly, actinomycin, pro-actinomycin, and streptothricin are potent antimicrobial compounds that vary in structure and function but were isolated from actinomycetes, a soil microbe.[11] Other soil-dwelling bacteria also produce natural products with therapeutic properties, making such an environment the ideal ecosystem for isolating compounds with antibacterial properties. In addition, the advent of sequencing technology also promoted scientists to proactively seek previously untapped biosynthetic pathways in soil microorganisms to produce antimicrobial molecules.[12]

Bacillus anthracis is a Gram-positive, spore-forming bacteria that lives naturally in the soil and causes anthrax infections.[13] Its pathogenicity is linked to the release of three main factors including the lethal factor, edema factor, and protective antigen.[14] The spores formed by *B. anthracis* are highly resistant to temperature, pressure, radiation, and chemical agents such as disinfectants.[14] When inhaled, these spores germinate within the macrophages of the lungs and are carried to the lymph nodes where infection occurs.[15] Because this infection mode occurs within the macrophages, the host's innate immune system does not respond, allowing the bacteria to grow while the host's adaptive immune response develops.[16] The active synthesis and production of virulence factors encoded by plasmids pXO1 and pXO2 from *B. anthracis* within the macrophage inactivates the MAP Kinase signaling pathway, releases adenosine monophosphate, and binds toxin receptors in the host cells.[17–19] These actions cause symptoms in the host, including localized pneumonia, fever, and other flu-like symptoms, which are commonly misdiagnosed.[20] Although recovery rates have increased over the years, inhalation anthrax remains the deadliest form of anthrax infection. Other types of infections by this pathogen include cutaneous, gastrointestinal, and injectional infections, which, although not as lethal, can result in death without early or proper treatment.[21]

Due to its ability to produce spores, *B. anthracis* is considered a weapon of bioterrorism since these spores can be easily aerosolized to cause inhalation anthrax in large populations of people.[22] Despite antibiotic treatment, many people may suffer re-infection due to ungerminated spores surviving the initial treatment.[23] Because the continuation of antibiotic treatment risks the emergence of resistance, a vaccine against anthrax is often also a part of the treatment regimen as it decreases the chances of reinfection from ungerminated spores following an early treatment.[23,24] These reasons underscore the continued efforts to discover and develop novel antibiotics for combating *B. anthracis* infections.

As part of the Course-based Undergraduate Research Experience (CURE) at Penn State[25], we isolated organic compounds from soil samples collected from two locations in Central Pennsylvania to extract and identify natural products exhibiting antibacterial activity against several bacterial species. Initial evaluation of growth inhibitory properties of the crude extracts demonstrated significant activity against Gram-positive bacteria. We continued to characterize the activity of the isolated compounds. Two natural products, AMS002 and AMS003, inhibited the growth of *B. anthracis* at 0.8 and 0.2 mg/ml, respectively. These compounds also exhibited bactericidal properties against this pathogen at the same concentrations. We employed fluorescence and *luminescence*-based reporter assays to elucidate these two compounds' potential mechanism of action. We observed that they inhibited protein synthesis *in vitro* and within bacterial cells. Subsequent mass spectrometry analysis identified the molecular mass and potential identify of one of the promising compounds. This discovery may provide new molecules to add to the declining arsenal of compounds that treat deadly *B. anthracis* infections.

METHODS AND PROCEDURES

Description of strains used in this study

Strain or plasmid	Strain description
DH5α	Host strain for cloning
BL21 (DE3)	Host strain for protein expression
B. subtilis 168	Common laboratory strain
B. anthracis Sterne	Attenuated strain of *B. anthracis*
***E. coli* - Wild Type**	MG1655 (K12) strain containing the TolC efflux pump
E. coli* - Δ*tolC	MG1655 (K12) strain lacking the TolC efflux pump
P. aeruginosa	Strain PAO1 – common laboratory strain

Table 1. Bacterial strains used in the current study.

Soil Sample Collection

The locations where the soil samples were collected were based on areas prone to having a high biodiversity of microbes. The first soil sample was collected at the corner of Fox and Grants Road, Jersey Shore, PA. This sample originated from an Amish field with biannual fertilization using manure rather than an artificial fertilizer. This sample was selected based on the organic nature of manure fertilization for plant growth. Manure can act as a source of nutrients for microbial life forms, which potentially produce compounds to compete with common soil microbes, such as *B. anthracis*. The soil collected from this location was lighter in color and dry, likely due to the lack of rainfall in the weeks before collection. The second sample was collected about 150-200 feet from the banks of the Little Juniata River, Tryone, PA 16686. This location had dense vegetation with low levels of human activity, as human interaction can interfere with the natural soil ecosystem. Soil samples were collected by digging a small hole about 0.5m in diameter and about 15 cm deep. Samples were collected in gallon-sized plastic bags, taken back to the laboratory, and the bags were left open to allow the soil to dry completely prior to extraction.

Solvent Extraction of Natural Compounds

The soil samples were inspected visually, and large particulates, including rocks, leaves, and sticks, were manually removed. The samples were packed halfway into 1 L bottles, and about 500 ml of 100% ethyl acetate was added to the bottles in a chemical fume hood. The contents were mixed gently by inversion with occasional venting to prevent gas build-up inside the bottles. These samples were left to soak for 72 hours to maximize the extraction of small molecules.

Filtration and Solvent Evaporation to Isolate Crude Organic Compound Extracts

A Büchner funnel was placed onto a filtration flask connected to a vacuum source. A Whatman filter paper was placed on the Büchner funnel and soaked with 100% ethyl acetate. Vacuum was applied, and pre-soaked soil samples were filtered. The filtrate was transferred into a round-bottomed flask, and the solvent was removed using a rotary evaporator under reduced pressure at 52 °C. The rotation speed of the instrument was increased gradually to prevent solvent bumping. This process was repeated until all the solvents were removed to yield the crude natural product extract, hereon referred to as the crude extract.

Crude Extract Analysis by Thin-Layer Chromatography (TLC)

The profile of compounds available in the crude extract was assessed by TLC analysis. Pre-cut glass TLC plates coated with a fluorescent indicator detectable with 254 nm or 366 nm wavelength (Millipore-Sigma, Burlington, MA) were used. A plate was marked with a pencil 1 cm from the end of the plate to outline the origin of sample spotting. A small amount of the crude extract was dissolved in the selected mobile phase and spotted onto the TLC plate using thin capillary tubes. The plate was dried and placed in a TLC chamber containing the same mobile phase at the level below the baseline. The mobile phases used were 50% dichloromethane with 50% hexanes, 80% dichloromethane with 20% hexanes, 100% dichloromethane, 100% dichloromethane with a drop of methanol, and 90% dichloromethane with 10% methanol. The solvent traveled by capillary action, and the plate was removed and dried after the mobile phase reached the plate's upper end. The crude profile was visualized with ultraviolet light using a hand-held dual-wavelength UV lamp. This technique determined the solvent system used to purify the crude extract.

Purification of Individual Compounds by Column Chromatography

A silica gel slurry in 100% dichloromethane was poured into a 60 mL chromatography column and allowed to pack by gravity. A thin layer of sand was added on top to protect the silica layer from disturbance. The crude extract was dissolved in minimal amounts of the mobile phase and loaded onto the column, forming a thin layer on top of the sand. This layer was allowed to be absorbed into the silica before more of the mobile phase was slowly added to the layer of sand, ensuring that the top layer of silica was not disturbed. The mobile phase was continually added to elute the compounds in 3 ml fractions. TLC grids were created by spotting the contents of each fraction onto a TLC plate, which was visualized using UV light (254/366 nm) to determine the number of UV-absorbing compounds. Fractions with similar TLC profiles were grouped, pooled, and concentrated for biological analyses or characterization. Because multiple compounds were eluted within the same fractions, further purification to separate all compounds in the crude was achieved using a CombiFlash flash chromatography system (Teledyne ISCO). Crude soil extracts were loaded onto pre-packed columns containing 40 g of silica gel and purified using the same solvent system determined from the TLC analyses. The automated system identified compounds using a UV detector (254 nm) and isolated them based on their polarity. The samples were concentrated on a rotary evaporator to produce five fractions: AMS001-AMS005.

*Minimum Inhibitory Concentration (MIC) and Minimum Bactericidal Concentration (MBC) Assay*s

A bacterial culture (5 ml) in lysogeny broth (LB) medium was incubated at 37 °C while shaking overnight. The optical density of a 10-fold diluted stationary phase culture was determined at 600 nm on the Spectronic Genesys 5 Spectrophotometer. A bulk working culture was prepared by diluting the overnight culture to an initial OD_{600nm} of 0.002 (lag phase) for subsequent antibacterial growth inhibitory assays. For microplate assays, 96 µl of LB broth was transferred to the first row of wells on a 96-well plate while 50 µl was added to the remaining wells on the plate. Concentrated aliquots (4 µl) of the purified compounds, or the necessary controls [chloramphenicol (positive control), kanamycin (positive control), and DMSO (negative control)], were

added to the first row of wells in triplicate. Two-fold serial dilutions were performed down each column by transferring 50 µl of the mixture from the first row to the second one. This procedure was repeated until the last row, when 50 µl was discarded, leaving all the wells with equal volumes. A 50 µl aliquot of the diluted culture was then added to each well, and the microplates were incubated at 37 °C for 24 h. A qualitative assessment of the plate was performed by visual inspection to determine the MIC values for the corresponding test compounds. The MIC was recorded as the lowest concentration of a test compound lacking visible growth. Further analyses were performed by obtaining the optical densities of samples in the 96-well plate on a SpectraMax i3 Microplate reader (Molecular Devices). The dose response data were plotted relative to the DMSO control. The bactericidal properties of the test compounds were determined from the microplate assays used to evaluate the MICs. Following visual determination of the MICs, spot cultures were created by transferring 5 µl from sample wells in the microplate lacking bacterial growth for each corresponding test compound onto the sectioned quadrants of LB-agar plates. Similar experiments were performed for the controls, and the plates were incubated overnight at 37 °C.

Disk Diffusion Assay

Using aseptic techniques, a saturated liquid culture of bacteria was spread onto an LB plate using a sterile cotton swab and allowed to dry at room temperature. Sterile 6.5 mm disks were soaked in 20 µl of purified natural products, spectinomycin (SPEC), or DMSO. These disks were placed in sectioned quadrants on LB agar plates and incubated at 37°C for 24 hours. At the end of the incubation period, the diameter of the clearance zones for each corresponding sample was measured and used to assess the growth inhibitory effect.

Fluorescence and Luminescence Reporter Strain Development

A pET28a cloning vector containing a gene encoding the Yellow Fluorescent Protein (YFP) was transformed into *E. coli* BL21 (DE3). 100 µl of the cells were plated on kanamycin-containing selective LB agar medium and incubated overnight at 37 °C. Colonies that grew on the selective media were restruck and grown in liquid broth containing kanamycin. The luminescence reporter strain was prepared similarly by transforming a pET28-nano-luc plasmid containing the nano luciferase gene into BL21 (DE3) cells. Transformants containing the pET28a-*nano-luc* were used in cell-based luminescence screening assays to assess translation inhibitors.

Cell-based Fluorescence and Luminescence Translation Reporter Assays

The fluorescence reporter assays were set up by first transferring 96 µl of LB to the top row of wells of a black 96-well plate (Corning, New York), and 50 µl was added to the remaining wells. 4 µl of the purified test compounds, or the necessary controls [chloramphenicol (positive control), and DMSO (negative control)], were then added to the top row in triplicate. Two-fold serial dilutions were performed from rows A – H by transferring 50 µl of culture from the first row to the second one. This procedure was repeated, and 50 µl was extracted from the last rows of the plate. Subsequently, an overnight culture of BL21 (DE3)-pET28a-*yfp* was diluted to an OD_{600} of 0.4 in LB broth containing 50 µg/ml of kanamycin for plasmid maintenance. Isopropyl ß-D-1-thiogalactopyranoside IPTG (1 mM) was then added to the culture to initiate the expression of YFP. 50 µl of this culture was added to each well, and the plate was incubated for 2 hours at 37 °C while shaking at 300 rpm. Fluorescence readings were then obtained to detect the translation of YFP using the SpectraMax i3 (Molecular Devices, $\lambda\ Ex_{468\ nm}/\lambda\ Em_{530\ nm}$). The data was analyzed using GraphPad Prism 9. The luminescence-based reporter assays were set up in a similar manner to the assay above using the BL21 (DE3)-pET28a-nano-luc cells.

Preparation of the Nano-luciferase mRNA Transcript

Preparation of the *nano-luc* mRNA for use as a template in the *in vitro* translation reactions was done by *in vitro* transcription. 1 ml of a 5X high-yield transcription buffer was prepared by mixing 500 µl 1 M HEPES (pH 7.5), 200 µl 1M dithiothreitol (DTT), 100 µl 1M $MgCl_2$, 70 µl 2mg/ml bovine serum albumin, 130 µl RNase-free water. The transcription reaction was initiated by combining 20 µl of 5X transcription buffer, 1.0 µl 1 M DTT, 30 µl 100 mM NTP mixture, 0.2 µg of pET28a-nano-luc plasmid, 0.25 µl inorganic pyrophosphatase (0.03 units), 5 µl T7 RNA polymerase (250 units) (New England Biolabs), 44 µl RNase-free water. This mixture was incubated for 3 h at 37 °C and treated with RNase-free DNase I to degrade the DNA template. Following the inactivation of the enzyme at 75 °C for 10 minutes, the sample was resolved on a denaturing 6 % urea-based acrylamide gel. The synthesized *nano-luc* mRNA was extracted and ethanol precipitated following standard protocols. This mRNA was used as a template in place of the *nano-luc* gene in an *in vitro* translation experiment, as described below.

In-vitro Luminescence-based Translation Assay.

A lysate of 50 ml *E. coli* BL21 (DE3) cells was prepared by sonication as previously described.[26] *In vitro* translation using the nano-Luciferase gene was accomplished by combining an *E. coli* BL21 (DE3) lysate (10 µl), freshly made polymix buffer (10 µl) (final reaction concentrations 5 mM HEPES pH 7.6, 5 mM NH_4Cl, 0.5 mM $CaCl_2$, 1.5 mm $MgCl_2$, 1 mM DTT, 8 mM putrescene, 2 mM ATP, 2 mM GTP, 1 mM CTP, 1 mM UTP, 0.3 mM each amino acid, 3 mg/ml *E. coli* tRNAs), pET28a-*nano-luc* plasmid or

nano-luc mRNA transcript (2.5 µl; ~10 ng), and 10 µl water. Finally, the corresponding inhibitors, DMSO as a negative control, and chloramphenicol as a positive control, were added to designated samples at (2 mg/mL, 0.2 mg/mL, and 0.02 mg/mL) and samples were incubated at 37 °C for 2 h. The Nano-Glo assay system (Promega) was used to detect the activity of the expressed luciferase enzyme in our reactions. Sample preparations were performed according to the manufacturer's instructions. The substrate was mixed with each sample in a 1:1 volume ratio, and luminescence was then recorded at 560 nm using the SpectraMax i3 microplate reader.

Mass Spectrometry and Compound Discoverer Analyses

Mass spectrometry analysis for ASM002 was performed at the Huck Life Sciences proteomic facility (Penn State University). The compound was dissolved in methanol and diluted to a final concentration of 10 µM. Samples were analyzed by liquid chromatography followed by electrospray ionization mass spectrometry in the positive mode (ESI-MS +) on a Waters Q-TOF Premier HPLC coupled instrument to obtain the exact mass and fragmentation profile of ASM002.[27] After obtaining the molar mass of the unknown compound, we used Compound Discoverer software (Thermo Fisher Scientific) to predict its potential molecular formula and structure.

RESULTS

Precise Collection Locations and Yield from Test Soil Samples

The crude extract obtained from the Amish field soil was named Crude 1, and the crude extract from the Little Juniata River was referred to as Crude 2 (**Table 2**).

Soil collection location	GPS location	Name	Antibacterial Compound
Fox and Grants Road, Jersey Shore, PA	Longitude: 41.146314; Latitude: -77.250216	Crude 1	ASM002
Little Juniata River, Tryone, PA	Longitude: 40.66476; Latitude: -78.21656	Crude 2	ASM003

Table 2. Summary details of the soil samples used in the current study.

Soil crude extract exhibits antibacterial properties against Gram-positive bacteria

Working stock solutions of 10 mg/ml of each crude extract were prepared in DMSO for these experiments. To determine the antibacterial activity of the crude extracts, a minimum inhibitory concentration assay was performed, where bacteria were grown in serially diluted concentrations of the crude extracts. The lowest concentration of the crude that could inhibit the growth of bacteria was considered the Minimum Inhibitory Concentration (MIC). Minimum inhibitory assays were performed initially with *Bacillus subtilis*, a Gram-positive species; *Escherichia coli*, a Gram-negative species; and an *E. coli ⊿tolC* mutant (a deletion mutant lacking the multidrug efflux pump, *tolC*). The minimum inhibitory concentration (MIC) against *B. subtilis* was observed to be 0.49 mg/mL for crude 1 and 0.24 mg/ml for crude 2. The crude extracts did not display significant activity against *E. coli* and *E. coli ⊿tolC*, with MICs greater than 3.92 mg/mL (**Figure 1, A**). This data suggests that the compounds in the crude extracts may not be able to penetrate the outer membrane of Gram-negative bacteria.

Since antibiotics can inhibit either growth or kill bacterial cells, we also evaluated the crude extracts for potential bactericidal properties against *B. subtilis*. 5 µL of culture from the MIC plates were plated onto LB agar plates and incubated overnight. The lowest concentration of the crude extract in which bacterial growth was not observed on the plates was considered the minimum bactericidal concentration (MBC). We recorded an MBC of 0.49 mg/ml for crude extract 1 and 0.24 mg/ml for crude 2, suggesting that they both contained bactericidal compounds. No MBC was observed against the *E. coli* and the *⊿tolC* mutant (**Figure 1, B**).

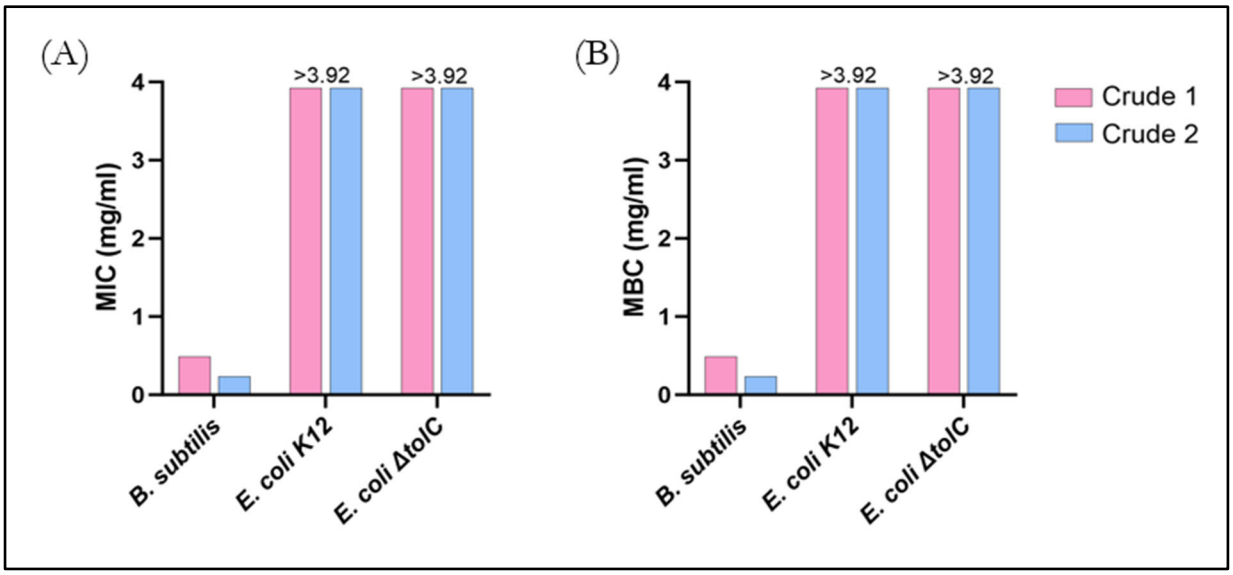

Figure 1. **Crude soil extracts showed bactericidal activity against *B. subtilis*.** **A**). Minimum inhibitory concentrations of crude extracts 1 and 2 against *B. subtilis, E. coli K12, and E. coli ⊿tolC (n=3; SD = 0).* **B**). Minimum bactericidal concentrations of crude extracts 1 and 2 against *B. subtilis, E. coli K12, and E. coli ⊿tolC (n=3; SD = 0).* SD: standard deviation.

Purification of crude extracts by column chromatography yields five compounds

The initial screens on the crude extracts indicated the presence of compounds with antibacterial properties among the mixture. We then isolated the organic compounds from the crude samples to test their individual antibacterial capabilities. First, thin-layer chromatography (TLC) was used to visualize the different compounds within the crude samples and identify the optimal mobile phase to isolate the compounds via column chromatography. Five individual compounds were observed using TLC in the crude extract derived from the Amish soil sample.

Column chromatography was used to separate the compounds in the crude extracts. For Crude 1, the column was run with 80% dichloromethane with 20% hexane before being increased to 100% dichloromethane to flush the most polar sample through the column. To separate the compounds in Crude 2, the column was started with a mobile phase of 90% hexane with 10% dichloromethane, and the polarity was increased to 100% dichloromethane. Then, the column was flushed using 50% dichloromethane with 50% methanol. During this process, the compounds were separated into fractions. Some isolated fractions, however, contained several compounds due to having very similar polarities; as a result, flash chromatography was performed to isolate the compounds with better resolution (**Figure 2, A**). Three compounds were isolated from crude 1 and two from crude 2 (**Figure 2, B**).

Isolated natural products display antibacterial properties against B. anthracis

Although we conducted our preliminary experiments using *B. subtilis*, the promising activity of the isolated compounds prompted us to transition to *B. anthracis,* which is among the most dangerous species of bacterial pathogens. The purified compounds were tested for activity against three pathogenic strains of bacteria: *B. anthracis, E. coli*, and *Pseudomonas aeruginosa*. Two compounds, AMS002 and AMS003, one from each crude extract, had inhibitory activity against *B. anthracis* at 0.8 mg/mL and 0.2 mg/mL, respectively. They did not show any significant growth inhibition activity against *E. coli* and *P. aeruginosa* (MICs > 0.8 mg/mL) (**Figure 3, A**). Experiments assessing these compounds' ability to kill *B. anthracis* cells revealed that they both possessed bactericidal properties at their respective MIC concentration (**Figure 3, B**). These results are consistent with the antibacterial effects observed from our crude extracts 1 and 2, in which only the Gram-positive bacteria such as *B. subtilis* was targeted. In contrast, Gram-negative bacteria such as *E. coli* and *P. aeruginosa* were not affected. All other isolated compounds did not show growth inhibitory activity (MICs > 0.8 mg/mL).

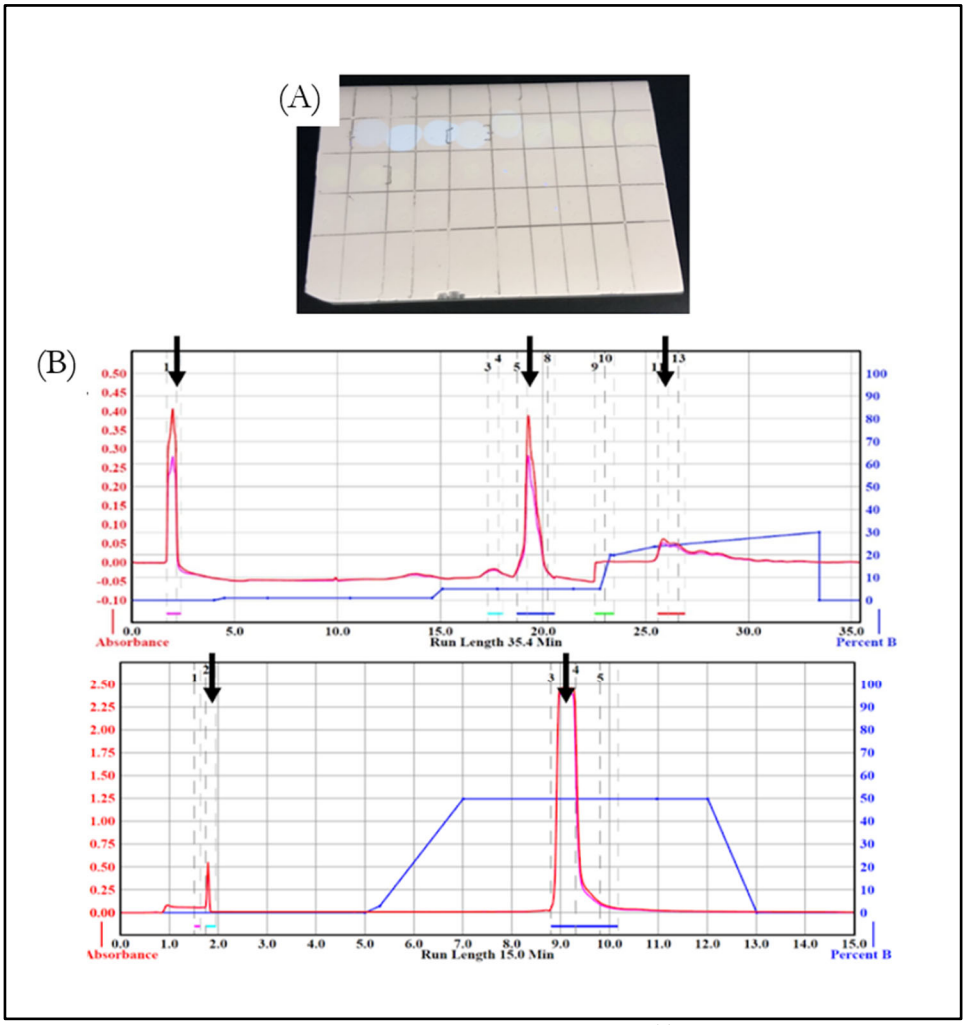

Figure 2. **Purification and analysis of compounds using chromatographic methods**. **A**). Sample TLC plate illustrating the separation strategy for crude samples and visualization under UV light. Tints of overlapping blue and green indicate fractions collected from column chromatography that were not pure. The experiment was run with a mobile phase containing 10% methanol in dichloromethane and visualized at 254 nm using a hand-held UV lamp. **B**). Crude extract purification by flash chromatography, resulting in three compounds from Crude 1 (top) and two from Crude 2 (bottom) (compounds indicated by arrows). Crude 1 (top) was purified using dichloromethane with an increasing gradient of methanol. Crude 2 (bottom) was purified using hexane with an increasing gradient of ethyl acetate. ASM002 eluted between 19 – 20 minutes (top chromatogram) while ASM003 eluted between 9 – 9.5 minutes (bottom chromatogram). NOTE: the red trace was collected at 254 nm and the pink trace at 366 nm. The blue trace indicates the concentration of the more polar solvent in the mobile phase.

We used disk diffusion assays as an alternative way to assess growth inhibition for the test compounds. Sterile disks were soaked with 5 mg/mL of AMS002 or AMS003. Bacterial lawn plates were prepared by spreading 200 µl of a *B. anthracis* culture (OD600 nm 0.3) on LB agar plates, and the disks were added on top of the lawn. The diameter of the clearance zones around the disks was measured (**Figure 3, C**). Zones of clearance for the AMS002 and AMS003 are 8.5 mm and 9.5 mm, respectively, compared to 17 mm for the positive control (**Figure 3, D**). The smaller zones of clearance observed in AMS002 and AMS003 may be due to the lack of mobility in diffusing through the agar plate. When determining the growth of bacteria as a dose-response of the inhibitors, inhibition of bacterial growth at various concentrations of AMS002 and AMS003 revealed half maximal inhibitory concentration (IC_{50}) between 10 and 50 µg/ml; data was normalized relative to the untreated controls to achieve dose-response curves (**Figure 3, E and F**).

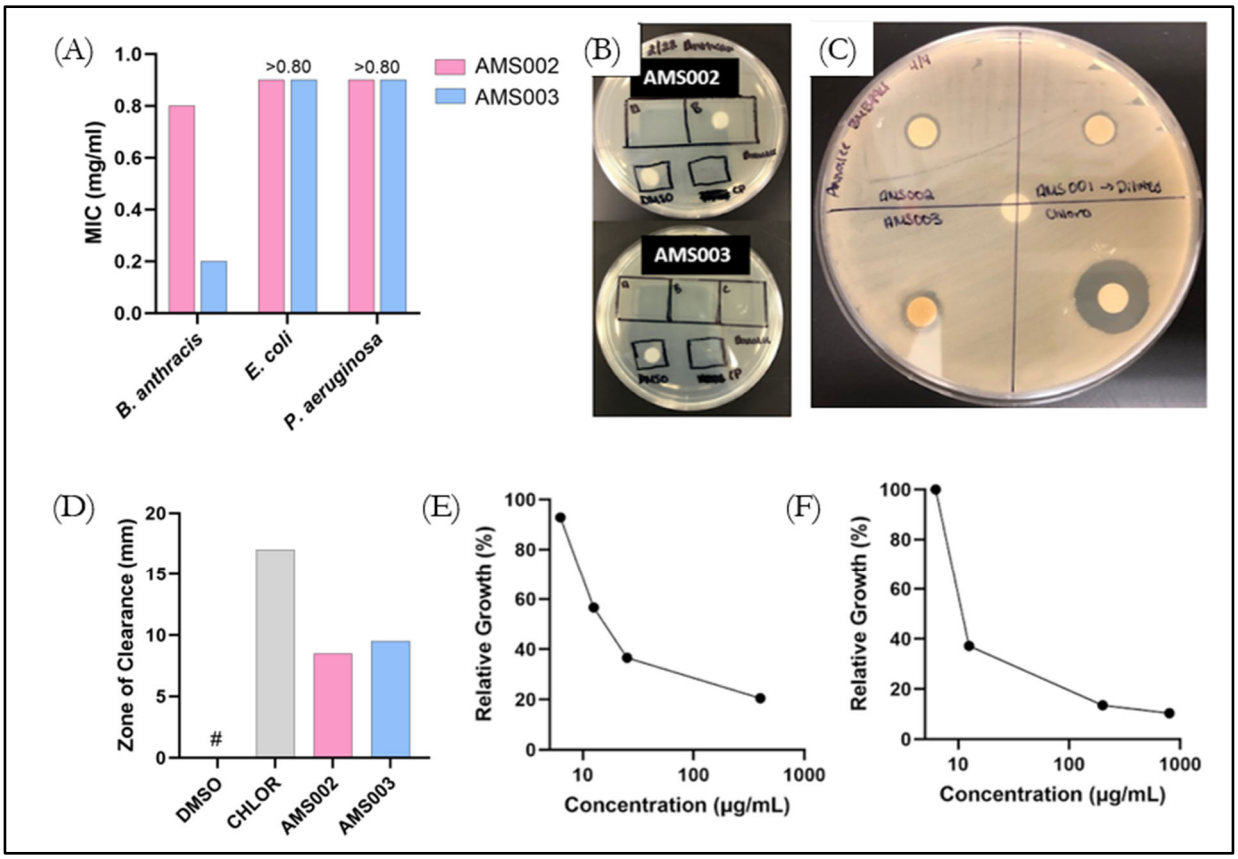

Figure 3. **Two isolated compounds, AMS002 and AMS003, showed antibacterial activity against *B. anthracis*.** **A**). Both AMS002 and AMS003 inhibited the growth of *B. anthracis* but showed no activity against *E. coli* and *P. aeruginosa* (n=1*).* **B**) MBC assay shows AMS002 at a 0.8 mg/ml concentration was bactericidal against *B. anthracis* (top plate). The top left box is 0.8 mg/ml, top right box is 0.4 mg/ml of AMS002. AMS003 at a 0.2 mg/ml concentration was bactericidal against *B. anthracis* (bottom plate). From the top left to right, the concentrations of AMS003 in each box are 0.8 mg/ml, 0.4 mg/ml, and 0.2 mg/ml. On both plates, the bottom left spot is the negative control DMSO, and the bottom right spot is the positive control, spectinomycin. **C**). Disk diffusion assay showed zones of clearance around inhibitor-soaked disks (top-left: AMS002, bottom-left: AMS003, center: top-right: AMS001, DMSO, bottom-right: Chloramphenicol). **D**). Measured diameters of the zones of clearance around AMS002 and AMS003 along with positive (CHLOR) and negative (DMSO) controls. **E**). Growth of *B. anthracis* was inhibited in a dose-dependent manner when treated with AMS002 (n=1). **F**). Growth of *B. anthracis* was inhibited in a dose-dependent manner when treated with AMS003 (n=1). Note: ASM001 was not included in subsequent analyses due to the low quantity available.

Cell-based reporter assays suggest AMS002 and AMS003 inhibit protein synthesis

We tested whether the compounds could inhibit protein synthesis in bacterial cells to elucidate the potential mechanism(s) of action for AMS002 and AMS003. To achieve this, a YFP gene was transformed into *E. coli* cells. These cells were used in an MIC-type assay where the fluorescence was detected two hours after the inhibitors were added. This assay showed a significant decrease in fluorescence, similar to the positive control, chloramphenicol at 1 mg/ml, a known protein synthesis inhibitor. Both AMS002 and AMS003 decreased the fluorescent signal in the cells to about 20% of the DMSO-treated negative control sample (**Figure 4, A**).

To confirm these results, a similar assay was performed using *E. coli* cells transformed with a *Nano-luciferase* gene, where luminescence was detected after the inhibitors were added. Luminescence produced after the treatment with AMS002 and AMS003 was decreased to nearly 30% of the DMSO-control sample for both samples (**Figure 4, B**). Taken together, both results suggested the AMS002 and AMS003 may have prevented Gram-positive bacterial growth by interfering with transcription and/or translation.

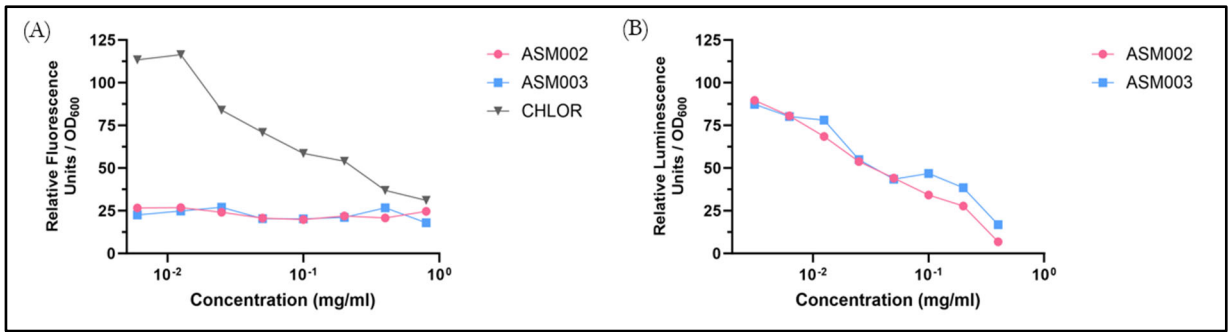

Figure 4. **Protein synthesis may be inhibited after treatment with AMS002 and AMS003**. **A**). Fluorescence-based reporter assay assessing the expression of YFP protein from a plasmid template (n=1). No increase in fluorescence was recorded for all concentrations tested with AMS002 and AMS003 while chloramphenicol reduced the YFP fluorescence signal in a dose-dependent manner. **B**). Luminescence-based assay illustrating a dose-dependent decrease in the luminescent signal by AMS002 and AMS003 from cells transformed with the *Nano-luciferase* gene (n=1). The data was normalized to the cell counts ($OD_{600\ nm}$) and plotted relative to the DMSO-treated control samples, representing 100% growth.

In-vitro luminescence-based screening confirms AMS002 and AMS003 inhibit translation

To distinguish which part of the central dogma AMS002 and AMS003 inhibit, DNA and mRNA templates encoding Nano-luciferase were mixed with an *E. coli* cell lysate and then treated with the inhibitors. Luminescence was measured to determine if the DNA or RNA templates had achieved protein synthesis. When treated with AMS002 and AMS003, synthesis of the Nano-Luciferase enzyme was halted when either the DNA or mRNA templates were added to the lysate. After adding the DNA template, the lack of luminescence suggested that transcription and/or translation was inhibited. In contrast, the lack of a luminescence signal after adding the mRNA Nano-Luciferase template indicated that translation was likely inhibited by AMS002 and AMS003 (**Figure 5, A & B**).

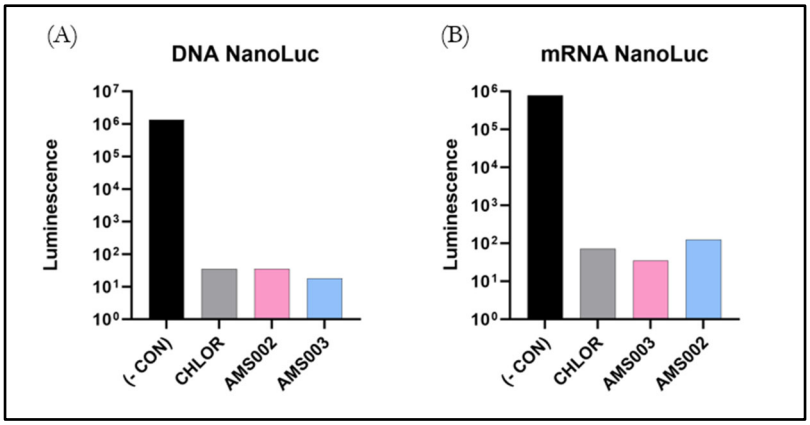

Figure 5. **AMS002 and AMS003 inhibited protein synthesis *in vitro***. **A**). Translation of a Nano-luciferase DNA template using *E. coli* 30S lysates. Chloramphenicol, AMS002- and AMS003-treated lysates show decreased luminescence signals following compound addition relative to the drug-free control (black bar) (n=1). **B**). Translation of a Nano-luciferase mRNA template using *E. coli* 30S lysates. Chloramphenicol (CHLOR), AMS002 and AMS003-treated lysates demonstrated decreased luminescence signals following compound addition relative to the drug-free control (black bar) (n=1).

Mass spectrometry analysis of compound AMS002 suggests a novel natural product

As part of our characterization of the isolated natural products, we wanted to determine whether the compounds exhibiting antibacterial properties were unique compared to known antibiotics. To achieve this, we conducted mass spectrometry and analyzed one of the promising compounds, ASM002, which had >95% purity relative to the other isolated fractions. Following the dissolution of the sample in methanol, it was analyzed by Electrospray Ionization Mass Spectrometry (ESI-MS). The obtained spectrum from the analysis revealed a compound with a base peak at m/z 157 (**Figure 6**). Upon comparing these data to known antibiotics used in the clinic, our findings suggested the discovery of a novel compound. We utilized computational methods to try and discover the potential identity of AMS002. We employed the compound discoverer software (Thermo Fisher Scientific) and searched the database for any small molecules with an identified molecular mass of 157 g/mol exhibiting antibacterial properties. This endeavor led to the identification of 5-Nitrofuran-2-carboxylic acid as a prospective candidate. Despite this finding, additional characterization studies are needed to reveal the identity of this compound. Similarly, more work is required to enhance the purity of AMS003 and determine its structural identity.

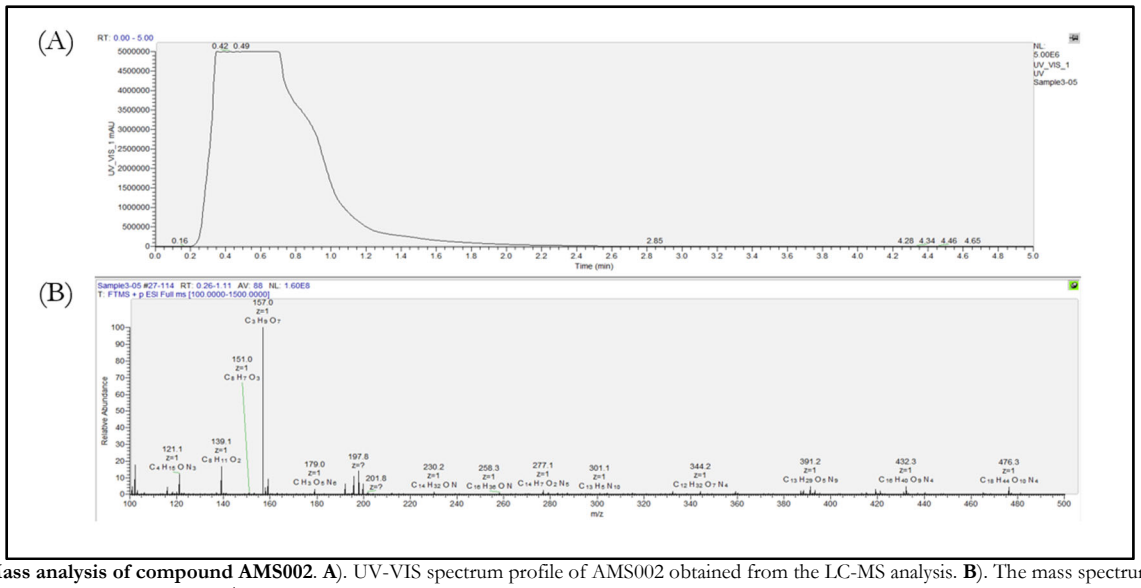

Figure 6. Mass analysis of compound AMS002. **A**). UV-VIS spectrum profile of AMS002 obtained from the LC-MS analysis. **B**). The mass spectrum for AMS002 highlighted the base peak at m/z 157 and the fragmentation pattern.

DISCUSSION

This study began by extracting organic compounds from soil samples in Pennsylvania. The first sample was collected from an Amish field, where manure was frequently applied for soil fertilization. The Amish are known for their all-natural farming, so the potential for synthetically added antibiotics was low. Manure helps facilitate plant growth as it provides a nitrogen source. Soil-dwelling bacteria may also use nitrogen containing compounds as an energy source, producing microbe-rich soil. Because microbes in the soil compete with other microbes for nutrients, inhibitory compounds are likely being produced from these organisms. The second soil sample was collected from a wooded and shaded region where human activity is low. This sample represented another soil ecosystem with a more natural source of microbes. For these reasons, we hypothesized compounds with antibacterial properties would be found in the soil of these locations.

After the isolation of the compounds and initial testing for antibacterial activity, it was found that two of the isolated compounds possessed inhibitory activity against *Bacillus anthracis*, the bacterial species causing anthrax infections. However, the observed antibacterial activity raises the question of where these compounds originated from. It may be possible that the compounds originated from other microbial life forms in the soil or nearby vegetation. Comparison of the mass spectrometry results and compound libraries in the discoverer database provided a prospective identity for AMS002, 5-Nitrofuran-2-carboxylic acid. Derivatives of this compound have been synthesized and explored for their antimicrobial activity against Gram-positive bacterial species and fungi.[28] However, we note that additional characterization experiments are needed to obtain the exact identity of the isolated compounds. Moreover, the purity of the compounds was ~ 90%, suggesting that the observed activity could have been affected by the purity. Planned experiments involve purifying these samples using HPLC to increase the purity and, hopefully, their antibacterial properties.

Our results showed that the soil samples collected from Pennsylvania locations contained potentially novel organic compounds with inhibitory activity against *Bacillus anthracis* by inhibiting translation. Inhibition by AMS002 and AMS003 was observed using MIC and disk diffusion assays. The mechanism of action was evaluated by employing *fluorescent and luminescent* reporter assays. We observed a decrease in protein synthesis after treatment with AMS002 and AMS003, and *in vitro* assays further narrowed down the mechanism as inhibition of translation. Surprisingly, both compounds completely arrested protein synthesis at concentrations below 0.01 mg/ml relative to chloramphenicol (**Figure 4, A**), which had no effect at a similar dose. These data are very promising and suggest these newly isolated compounds could be effective at inhibiting protein synthesis in pathogenic bacteria.

In the future, we would like to further characterize the mechanism of action by discovering the inhibitors' gene target(s). We plan to generate mutants of *B. anthracis* against AMS002 and AMS003 through inducing drug stress. Sequencing the genes that encode proteins involved in translation and comparing the sequences to wildtype genes would allow us to identify mutations that enable the bacteria to survive in the presence of AMS002 and AMS003, thereby identifying gene targets. This would teach us the specific inhibitory mechanisms that can effectively kill *B. anthracis* cells.

CONCLUSION

In this study, organic compounds were isolated from Pennsylvania soil samples using various chromatography methods. Two of the isolated compounds, AMS002 and AMS003, showed potent antibacterial properties against Gram-positive bacteria, including *B. anthracis*. We found that both compounds may exert their antibacterial effect by specifically inhibiting translation when using either a DNA or mRNA template, suggesting that they could target the ribosome as a mechanism of action. Mass spectrometry results indicated that one of the compounds, AMS002, may have structural similarities to a compound previously explored for its antimicrobial activity. However, further characterization of ASM002 is required to validate this hypothesis.

ACKNOWLEDGMENTS

The authors thank The Pennsylvania State University Biochemistry and Molecular Biology Department for resources and funding to support this project. We would also like to thank the teaching assistants, Tatiana McAnulty, Hannah Snoke, Rachel Swope, and Jasmine Arunachalam, for contributing to this work. We also thank the 2020 cohort of BMB205/CHEM111 for assistance with some of the experiments.

REFERENCES

1. Tacconelli, E., Carrara, E., Savoldi, A., Harbarth, S., Mendelson, M., Monnet, D.L., Pulcini, C., Kahlmeter, G., Kluytmans, J., Carmeli, Y., Ouellette, M., Outterson, K., Patel, J., Cavaleri, M., Cox, E.M., Houchens, C.R., Grayson, M.L., Hansen, P., Singh, N., Theuretzbacher, and U., Magrini, N. (2017) WHO Pathogens Priority List Working Group. Discovery, research, and development of new antibiotics: the WHO priority list of antibiotic-resistant bacteria and tuberculosis, *Lancet Infect Dis* 3, 318–327. *doi: 10.1016/S1473-3099(17)30753-3*.

2. Laxminarayan, R., Matsoso, P., Pant, S., Brower, C., Røttingen, J.A., Klugman, K., and Davies, S. (2016) Access to effective antimicrobials: a worldwide challenge, *Lancet* 387, 168–175. *doi: 10.1016/S0140-6736(15)00474-2*.

3. O'Neill, J. Tackling Drug-Resistant Infections Globally: Final Report and Recommendations. The Review on Antimicrobial Resistance https://amr-review.org/sites/default/files/160518_Final%20paper_with%20cover.pdf (accessed Jun 2023)

4. Alekshun, M.N., and Levy, S.B. (2007) Molecular mechanisms of antibacterial multidrug resistance, *Cell* 128, 1037–1050. *doi: 10.1016/j.cell.2007.03.004*.

5. Sheitoyan-Pesant, C., Abou Chakra, C.N., Pépin, J., Marcil-Héguy, A., Nault, V., and Valiquette, L. (2016) Clinical and Healthcare Burden of Multiple Recurrences of Clostridium difficile Infection, *Clin Infect Dis* 62, 574–580. *doi: 10.1093/cid/civ958*.

6. Ribeiro da Cunha, B., Fonseca, L.P., and Calado, C.R.C. (2019) Antibiotic Discovery: Where Have We Come From, Where Do We Go? *Antibiotics (Basal)* 8, 45. *doi: 10.3390/antibiotics8020045*.

7. Terreni, M., Taccani, M., and Pregnolato, M. (2021) New Antibiotics for Multidrug-Resistant Bacterial Strains: Latest Research Developments and Future Perspectives, *Molecules* 26, 2671. *doi:10.3390/molecules26092671*.

8. Zhanel, G.G., Homenuik, K., Nichol, K., Noreddin, A., Vercaigne, L., Embil, J., Gin, A., Karlowsky, J.A., and Hoban, D.J. (2004) The glycylcyclines: a comparative review with the tetracyclines, *Drugs* 64, 63–88. *doi: 10.2165/00003495-200464010-00005*.

9. Davies, J., and Davies, D. (2010) Origins and Evolution of Antibiotic Resistance, *Microbiol Mol Biol Rev* 74, 417–433. *doi: 10.1128/MMBR.00016-10*.

10. Fleming, A. (1929) On the antibacterial action of cultures of a penicillium, with special reference to their use in the isolation of B. influenzae, *Br J Exp Pathol* 10, 226-236.

11. Waksman, S.A., Schatz, A., and Reynolds, D.M. (2010) Production of antibiotic substances by actinomycetes, *Ann N Y Acad Sci.* 1213, 112–124. *doi: 10.1111/j.1749-6632.2010.05861.x*.

12. Gavrish, E., Sit, C.S., Cao, S., Kandror, O., Spoering, A., Peoples, A., Ling, L., Fetterman, A., Hughes, D., Bissell, A., Torrey, H., Akopian, T., Mueller, A., Epstein, S., Goldberg, A., Clardy, J., and Lewis, K. (2014) Lassomycin, a ribosomally synthesized cyclic peptide, kills mycobacterium tuberculosis by targeting the ATP-dependent protease ClpC1P1P2, *Chem Biol* 21, 509–518. *doi: 10.1016/j.chembiol.2014.01.014*.

13. Goel, A.K. (2015) Anthrax: A disease of biowarfare and public health importance, *World J Clin Cases* 3, 20–33. *doi: 10.12998/wjcc.v3.i1.20*.

14. Moayeri, M., Leppla, S.H., Vrentas, C., Pomerantsev, A.P., and Liu, S. (2015) Anthrax Pathogenesis, *Annu Rev Microbiol* 69, 185–208. *doi: 10.1146/annurev-micro-091014-104523*.

15. Guidi-Rontani, C., Weber-Levy, M., Labruyère, E., and Mock, M. (1999) Germination of Bacillus anthracis spores within alveolar macrophages, *Mol Microbiol* 1, 9–17. *doi: 10.1046/j.1365-2958.1999.01137.x*.

16. Park, J.M., Greten, F.R., Li, Z.W., and Karin, M. (2002) Macrophage apoptosis by anthrax lethal factor through p38 MAP kinase inhibition, *Science* 297, 2048–2051. *doi: 10.1126/science.1073163*.
17. Uchida, I., Hashimoto, K., and Terakado, N (1986). Virulence and immunogenicity in experimental animals of Bacillus anthracis strains harbouring or lacking 110 MDa and 60 MDa plasmids, *J Gen Microbiol* 132, 557–559. *doi: 10.1099/00221287-132-2-557*.
18. Tang, W.J., and Guo, Q. (2009) The adenylyl cyclase activity of anthrax edema factor, *Mol Aspects Med* 30, 423–430. *doi: 10.1016/j.mam.2009.06.001*.
19. Duesbery, N.S., Webb, C.P., Leppla, S.H., Gordon, V.M., Klimpel, K.R., Copeland, T.D., Ahn, N.G., Oskarsson, M.K., Fukasawa, K., Paull, K.D., and Vande Woude, G.F. (1998) Proteolytic inactivation of MAP-kinase-kinase by anthrax lethal factor, *Science* 280, 734–737. *doi: 10.1126/science.280.5364.734*.
20. Sweeney, D.A., Hicks, C.W., Cui, X., Li, Y., and Eichacker, P.Q. (2011) Anthrax infection, *Am J Respir Crit Care Med* 184, 1333–1341. *doi: 10.1164/rccm.201102-0209CI*.
21. Holty, J.E., Bravata, D.M., Liu, H., Olshen, R.A., McDonald, K.M., and Owens, D.K. (2006) Systematic review: a century of inhalational anthrax cases from 1900 to 2005, *Ann Intern Med* 144, 270–280. *doi: 10.7326/0003-4819-144-4-200602210-00009*.
22. Weiss, S., Kobiler, D., Levy, H., Pass, A., Ophir, Y., Rothschild, N., Tal, A., Schlomovitz, J., and Altboum, Z. (2011) Antibiotics cure anthrax in animal models, *Antimicrob Agents Chemother* 55, 1533–1542. *doi: 10.1128/AAC.01689-10*.
23. Aggarwal, S., Somani, V.K., Gupta, S., Garg, R., and Bhatnagar, R. (2019) Development of a novel multiepitope chimeric vaccine against anthrax, *Med Microbiol Immunol* 208, 185–195. *doi: 10.1007/s00430-019-00577-x*.
24. Shearer, J.D., Henning, L., Sanford, D.C., Li, N., Skiadopoulos, M.H., Reece, J.J., Ionin, B., and Savransky, V. (2021) Efficacy of the AV7909 anthrax vaccine candidate in guinea pigs and nonhuman primates following two immunizations two weeks apart, *Vaccine* 39, 1–5. *doi: 10.1016/j.vaccine.2020.10.095*.
25. Miller, D.M., Natale, A., McAnulty, T., Swope R., McNaughton, E., Becket,t A., Snoke, H., Schmidt, A., Alumasa, J.N., and Xiong, S. (2022) The Design and Implementation of an Interdisciplinary CURE as an Alternative Option for the General Chemistry Laboratory Course, *J. Chem Edu* 99, 2530–2540. *doi: 10.1021/acs.jchemed.1c01179*.
26. Aron, Z.D., Mehrani, A., Hoffer, E.D., Connolly, K.L., Srinivas, P., Torhan, M.C., Alumasa, J.N., Cabrera, M., Hosangadi, D., Barbor, J.S., Cardinale, S.C., Kwasny, S.M., Morin, L.R., Butler, M.M., Opperman, T.J., Bowlin, T.L., Jerse, A., Stagg, S.M., Dunham, C.M., and Keiler, K.C. (2021) *trans*-Translation inhibitors bind to a novel site on the ribosome and clear Neisseria gonorrhoeae in vivo, *Nat Commun* 12, 1799. *doi: 10.1038/s41467-021-22012-7*.
27. Gu, D., Ma, Y., Niu, G., Yan, Y., Lang, L., Aisa, H.A., Gao, H., Kiesewetter, D.O., and Chen, X. (2011) LC/MS evaluation of metabolism and membrane transport of bombesin peptides, *Amino Acids* 40, 669–675. *doi: 10.1007/s00726-010-0696-y*.
28. Popiołek, Ł., Rysz, B., Biernasiuk, A., and Wujec, M. (2020) Synthesis of promising antimicrobial agents: Hydrazide–hydrazones of 5-nitrofuran-2-carboxylic acid, *Chem Biol Drug Des* 95, 260–269. *doi: 10.1111/cbdd.13639*.

ABOUT THE STUDENT AUTHOR

Annalee Schmidt graduated from The Pennsylvania State University in December 2023. She now works under the direction of Dr. John Alumasa as a laboratory research technician in the Chemistry & Biochemistry Department at Miami University (OH). She will be attending graduate school at The University of North Carolina at Chapel Hill to earn a Ph.D. in biological sciences in the fall of 2024.

PRESS SUMMARY

Deadly bacterial infections such as anthrax remain a serious global health concern. Anthrax, caused by *Bacillus anthracis*, is highly dangerous as it forms spores, making it resistant to antibiotics and harsh environmental conditions. Therefore, finding new antibiotics to fight this pathogen is crucial. In this work, we purified soil extracts from Pennsylvania and found two compounds, AMS002 and AMS003, which effectively inhibited and killed *B. anthracis* cells. Our data suggests these compounds target the bacteria's protein synthesis machinery. This finding is crucial as it offers a promising solution for combating infections caused by *B. anthracis*.

Numerical Solutions for Kinematics of Multi-bar Mechanisms Using Graph Theory and Computer Simulations

*Brandon Torres & Mahdi Farahikia**

Division of Engineering Programs, State University of New York at New Paltz, New Paltz, NY

https://doi.org/10.33697/ajur.2024.118

Students: torresb4@newpaltz.edu
*Mentor: farahikm@newpaltz.edu**

ABSTRACT
A method is presented to demonstrate the application of computer simulations in the kinematic analysis of planar mechanisms, emphasizing its use in teaching the latter topic in a corresponding undergraduate course. Concepts of rigid-body dynamics are utilized in the kinematics of machines to analyze the motions (and forces in dynamics) transmitted within multiple interconnected links that make a mechanism, such as a car engine, airplane landing gear, press machine, door closer, and so on. Due to the tediousness of the analytical solutions, most textbooks limit the derivation of the equations to four-bar linkages like crank-rocker and crank-slider mechanisms. Benefiting from the advancements in computer programs, such as MATLAB, and their efficiency in solving large systems of linear and nonlinear equations, a method is proposed to facilitate teaching kinematic analysis of multi-bar linkages to undergraduate students while fostering the application of computational engineering via real-life examples. The results obtained from this method are shown to be in excellent agreement with the algebraic solution of the relative motion equations for each element in the mechanism.

KEYWORDS
Kinematics of Machines; Linkage; Numerical Solutions; Graph Theory; Machine Dynamics; Computer Simulation; Mechanism; Linkage Kinematics

INTRODUCTION

Mechanisms play important roles in a wide range of technologies, such as aircraft, steam engines, car engines, robotics, satellites, door closers, and so on[1–3]. At their core, these mechanisms are multi-body systems of interconnected links with the purpose of transmitting motion and force.

The design and synthesis of mechanisms to generate certain outputs (e.g., motion, path, or function) depend significantly on kinematics[1, 4]. The modern-day knowledge of kinematics of mechanisms and multi-body systems is based to a great extent on the works of Franz Reuleaux (German engineering scientist, considered as the "father of kinematics" by some) and his two major books, "*The Kinematics of Machinery*", and "*The Constructor*"[1, 5, 6]. Reuleaux's books and advocacy in mathematical approaches to mechanical engineering and machine kinematics inspired further development of texts in the late 19^{th} and early 20^{th} centuries, such as Kennedy, Hartmann, and Grübler[1, 7–9].

While the importance of understanding and studying the kinematics of machines is undeniable, derivation of standalone sets of governing equations for each type of linkage (four-bar, five-bar, etc.) can be mathematically "tedious", as shown by Norton[4]. As a result, the concentration of such techniques available in the literature (a summary of which

is given in the proceeding paragraphs) is limited mainly to four-bar (like crank-rocker and crank-slider mechanisms) and very few specific multi-bar linkages.

Norton and Uicker demonstrated the graphical analysis of the positions, velocities, and accelerations of linkages[4, 10]. Vector sums of the corresponding relative motion equations for two points on each link are represented graphically at a chosen scale. Although applicable, this method is not ideal for linkages with more than four bars or kinematic analysis of a linkage for its full range of motion, especially when analyzing accelerations composed of normal and tangential components.

Algebraic solutions for partial or complete kinematic analysis of specific four-bar mechanisms were explained by Norton, Uicker, and Martin[4, 10, 11]. Similar to the graphical method, vector sums of the relative motion equations are solved here for two points (typically joints) on each link based on the constraints imposed on each joint by the neighboring links. Although computer programming enables kinematic analysis of mechanisms for their full range of motion, extending this approach to linkages with more than four bars is time-consuming. Additionally, neither the graphical nor the algebraic solutions are specific to machine kinematics but an extension of the concepts of kinematics to interconnected bodies.

Analytical methods using vector loops and complex-number algebra were introduced by Norton, Uicker, Russell, Vinogradov, and Martin[4, 10–13]. At least one vector loop is constructed for a mechanism. The vector-loop equations are written in the complex-number format and expanded using Euler's identity to develop a set of n equations and n unknowns. For example, 1-DOF (Degree-of-Freedom) four-bar mechanisms lead to a set of two equations with two unknowns. The computation of the degrees of freedom (mobility) of a mechanism is demonstrated in the following section. The analytical solutions of these equations can be challenging and virtually impractical as the number of links increases[4]. Also, the number of unknowns for linkages with more than one degree of freedom exceeds the number of equations.

The vector loop approach and complex-number algebra combined with the capabilities of scientific computer programs, such as MATLAB and Python, provide an opportunity to develop a robust and efficient approach for the kinematic analysis of machines. Uicker mentioned position analysis of multi-bar linkages using numerical methods, such as Newton-Raphson, but mostly focused on abstract analytical solutions[10]. Russell introduced the application of MATLAB specific to a few examples but did not generalize it to arbitrary configurations of links[12]. A computational simulator for a five-bar "Gantry" mechanism was created using Python, Javascript, and Coördinator[14].

Despite recent advancements in scientific computer programs, for example, in solving large systems of linear and nonlinear equations and differential equations, their incorporation in relevant engineering courses remains inadequate. The current work aims to show the possibility of filling this gap in the context of developing a purely computational approach to the kinematics of machines by proposing a technique that merges classical multi-body dynamics and computer programming. The fundamentals of this method are based on generating the vector loop equations for mechanisms. However, instead of attempting to solve the large system of equations analytically, the goal here is to utilize the functionalities of MATLAB.

The advantage of the proposed method is twofold. First, it promotes the kinematic analysis of multi-bar mechanisms through a computational process of solving the vector loop equations instead of relying on commercial programs, like *Working Model*. Second, a stand-alone computer program can be produced by incorporating graph theory that identifies the vector loops automatically based on the provided input and performs a complete kinematic analysis for the full range of motion of the mechanism.

It is important to note that the goal here is not to undermine the significance of or eliminate the graphical, algebraic, and analytical methods described in the literature. An understanding of the fundamentals of classical dynamics is essential to validate the results obtained from numerical methods using in-house programs or commercial applications.

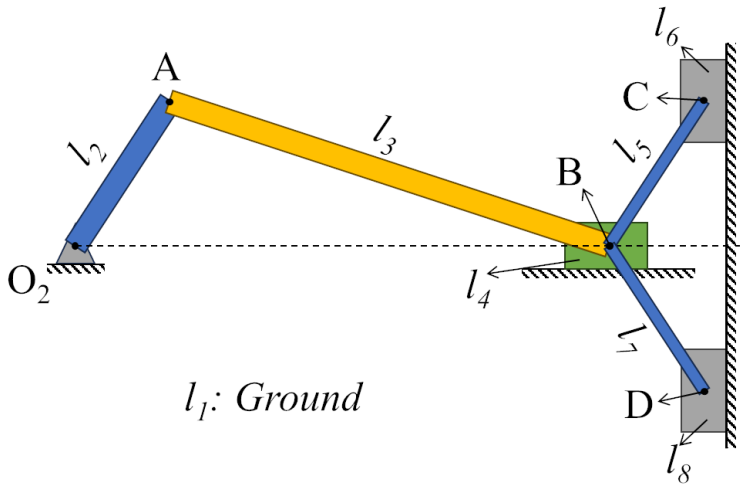

Figure 1. A schematic of an eight-bar linkage with one horizontal and two vertical sliders.

METHODS AND PROCEDURES

To demonstrate the proposed method, take the example of an eight-bar linkage shown in **Figure 1**. This mechanism consists of one horizontal slider (l_4) and two vertical sliders (l_6 and l_8.) The rotational motion of the input crank (l_2) is transferred to the horizontal slider by the connecting rod l_3. The connecting rods l_5 and l_7 transmit the horizontal translation of l_4 to the vertical translations of l_6 and l_8, respectively.

The revolute full joints O_2, A, C, and D are of Order one, whereas the Order of the revolute full joint B is three. There are three prismatic joints connecting the three sliders to the ground. In total, there are ten full joints and no half joints in this eight-bar mechanism. The mobility (Degree-of-Freedom) of this mechanism is one, given by **Equation 1**[4]

$$M = 3(L-1) - 2J_1 - J_2 = 3(8-1) - 2(10) - 0 = 1 \qquad \textbf{Equation 1.}$$

where M, L, J_1, and J_2 are the mobility, number of links, number of full joints, and number of half joints, respectively.

Vector Loop Generation

Vectors connect two joints on the same link so long as both joints connect the link to two adjacent links. The tail of each vector falls on the head of the vector representing an adjacent link. The ground link in each loop also has a vector. A local coordinate system is associated with each vector at its tail to demonstrate its direction. It is reasonable to choose a unique type of coordinate system, such as Cartesian, for all the local coordinate systems.

Ideally, a mechanism should be divided into multiple 1-DOF vector loops consisting of up to four links or two unknowns. The number of vector loops in a 1-DOF linkage is equal to the number of different joints connecting a link to the ground minus one. For example, in the eight-bar mechanism of **Figure 1**, four links (l_2, l_4, l_6, and l_8) have ground-connecting joints. Hence, this linkage can be represented by three vector loops (explained in the following), each consisting of three vectors, as shown in **Figure 2**. It is important to note that the fourth vector in each of the loops is the "offset" vector associated with sliders, all of which are set to zero for convenience but not necessity.

The first vector loop is O_2AB. This loop consist of vectors $\overrightarrow{O_2A}$, $\overrightarrow{AB}$, and $\overrightarrow{BO_2}$ whose complex-number notations are $ae^{j\theta_2}$, $be^{j\theta_3}$, and $ce^{j\theta_4}$, respectively, where $j = \sqrt{-1}$. In these equations, a, b, and c are magnitudes of the vectors, whereas θ_2, θ_3, and θ_4 represent the direction of each vector. In this loop, a, b, and $\theta_4 (= 180°)$ are constant, θ_2 is the input angular position of l_2, θ_3 is the unknown angular position of l_3, and the unknown rectilinear motion of slider l_4 is given by c.

The second vector loop, BCE, consists of vectors $\overrightarrow{BC}$, $\overrightarrow{CE}$, and $\overrightarrow{EB}$ with respective complex-number notations $de^{j\theta_5}$,

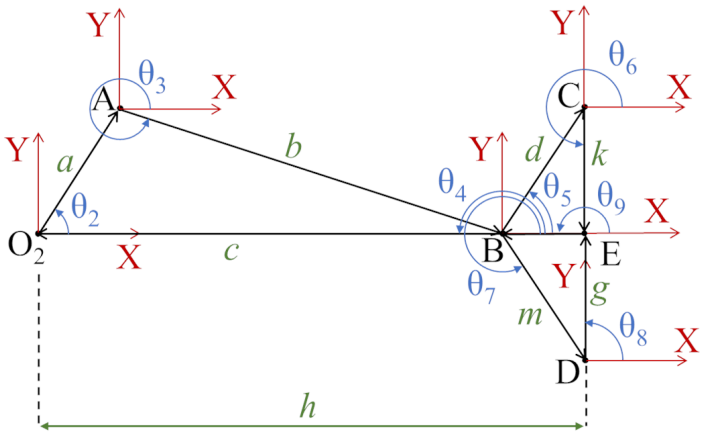

Figure 2. Corresponding vector loops for the eight-bar linkage.

$ke^{j\theta_6}$, and $(h-c)e^{j\theta_9}$. A virtual point E is chosen for this vector loop because it consists of two sliders. This virtual point can be placed anywhere; however, it is reasonable to choose a location that leads to convenient angles for the vectors. For instance, the constant angles θ_6 and θ_9 are 270° and 180°, respectively. The input to this vector loop is c, calculated in the first loop, and the two unknowns are the angular position, θ_5, of l_5 and the vertical length k. The length of the $\overrightarrow{EB}$ equals the constant h minus the input c.

The third vector loop, BDE, consists of vectors $\overrightarrow{BD}$, $\overrightarrow{DE}$, and $\overrightarrow{EB}$ represented by the complex-number notations $me^{j\theta_7}$, $ge^{j\theta_8}$, $(h-c)e^{j\theta_9}$, respectively. It is observed that vector $\overrightarrow{EB}$ is common between the second and third loops. The two unknowns in this loop are the angular position, θ_7, of l_7 and the vertical length g, while the input is the horizontal position, c, of slider l_4, as in the second vector loop. The angle θ_8 is constant at 90°.

Vector Loop Equations

For each loop in the linkage, it can be written that, due to the method of generating the vector loops, the sum of the vectors equals zero. Since there are three vector loops in the mechanism shown in **Figure 2**, three vector loop equations can be written for its position analysis in the complex-number notation.

$$\begin{cases} ae^{j\theta_2} + be^{j\theta_3} + ce^{j\theta_4} = 0 \\ de^{j\theta_5} + ke^{j\theta_6} + (h-c)e^{j\theta_9} = 0 \\ me^{j\theta_7} + ge^{j\theta_8} + (h-c)e^{j\theta_9} = 0 \end{cases} \quad \textbf{Equation 2.}$$

Equation 2 can be simplified to **Equation 3** by applying the known constants described above. Further simplification of this equation is not necessary in the development of the computational algorithm.

$$\begin{cases} ae^{j\theta_2} + be^{j\theta_3} + ce^{j\pi} = 0 \\ de^{j\theta_5} + ke^{j\frac{3\pi}{2}} + (h-c)e^{j\pi} = 0 \\ me^{j\theta_7} + ge^{j\frac{\pi}{2}} + (h-c)e^{j\pi} = 0 \end{cases} \quad \textbf{Equation 3.}$$

The six unknowns of this system of equations are θ_3, θ_5, θ_7, c, g, and k. Taking the first and second time-derivatives of **Equation 3** gives the necessary systems of equations to compute the velocity and acceleration of each link. Hence, for the three vector loops considered here, the velocity and acceleration equations are given by **Equations 4** and **5**, respec-

tively.

$$\begin{cases} ja\omega_2 e^{j\theta_2} + jb\omega_3 e^{j\theta_3} + \dot{c}e^{j\pi} = 0 \\ jd\omega_5 e^{j\theta_5} + \dot{k}e^{j\frac{3\pi}{2}} - \dot{c}e^{j\pi} = 0 \\ jm\omega_7 e^{j\theta_7} + \dot{g}e^{j\frac{\pi}{2}} - \dot{c}e^{j\pi} = 0 \end{cases} \quad \textbf{Equation 4.}$$

$$\begin{cases} ja\alpha_2 e^{j\theta_2} - a\omega_2^2 e^{j\theta_2} + jb\alpha_3 e^{j\theta_3} - b\omega_3^2 e^{j\theta_3} + \ddot{c}e^{j\pi} = 0 \\ jd\alpha_5 e^{j\theta_5} - d\omega_5^2 e^{j\theta_5} + \ddot{k}e^{j\frac{3\pi}{2}} - \ddot{c}e^{j\pi} = 0 \\ jm\alpha_7 e^{j\theta_7} - m\omega_7^2 e^{j\theta_7} + \ddot{g}e^{j\frac{\pi}{2}} - \ddot{c}e^{j\pi} = 0 \end{cases} \quad \textbf{Equation 5.}$$

Each system of equations above has two unknowns per equation, for a total of six unknowns. These unknowns are ω_3, ω_5, ω_7, $\dot{c}$, $\dot{g}$, and $\dot{k}$ for **Equation 4** and α_3, α_5, α_7, $\ddot{c}$, $\ddot{g}$, and $\ddot{k}$ for **Equation 5**. The input angular position (θ_2) and angular velocity (ω_2) of link l_2 can be calculated using dynamics principles ($\omega = \int_{t_0}^{t} \alpha dt + \omega_0$, and $\theta = \int_{t_0}^{t} \omega dt + \theta_0$.) To solve for the six unknowns, the *real* ($\mathfrak{Re}$) and *imaginary* ($\mathfrak{Im}$) components of its complex equations are set equal to zero, leading to two individual equations for each vector loop equation. For instance, the expansion of **Equation 3** is given in **Equation 6**. **Equations 4** and **5** can also be expanded similarly.

$$\begin{cases} \mathfrak{Re}[ae^{j\theta_2} + be^{j\theta_3} + ce^{j\pi}] = 0 \\ \mathfrak{Im}[ae^{j\theta_2} + be^{j\theta_3} + ce^{j\pi}] = 0 \\ \mathfrak{Re}[de^{j\theta_5} + ke^{j\frac{3\pi}{2}} + (h-c)e^{j\pi}] = 0 \\ \mathfrak{Im}[de^{j\theta_5} + ke^{j\frac{3\pi}{2}} + (h-c)e^{j\pi}] = 0 \\ \mathfrak{Re}[me^{j\theta_7} + ge^{j\frac{\pi}{2}} + (h-c)e^{j\pi}] = 0 \\ \mathfrak{Im}[me^{j\theta_7} + ge^{j\frac{\pi}{2}} + (h-c)e^{j\pi}] = 0 \end{cases} \quad \textbf{Equation 6.}$$

Although the components of a complex number can be derived using Euler's identity ($e^{j\theta} = cos(\theta) + jsin(\theta)$), corresponding built-in MATLAB functions are utilized in this method.

RESULTS

Vector Loop Generation Algorithm

The problem of automatically detecting loops for mechanisms is very similar to finding cycles (vector loops) in an undirected graph. The vectors for any cycle inherently form edges between connection points or pins on a link, which are called nodes. Any graph has a finite number of unique cycles, starting and ending with the same node. The proposed method requires that each edge in a cycle is traversed only once.

Figure 3 shows the decomposition of the mechanism in **Figure 1** in terms of edges and neighbors. Pin A on link l_2 is defined by nodes 3 (on l_2) and 4 (on l_3), and so on. Each node is attributed by the link to which it belongs and the nodes with which it neighbors. Node 3 belongs to link l_3 and neighbors nodes 2 (on l_2) and 4 (on l_3). In other words, one of the neighboring nodes belongs to the same link, and the other one belongs to an adjacent link. One edge is defined between nodes 2 and 3, both of which belong to link l_2. Another edge is defined between nodes 3 and 4, which belong to links l_2 and l_3, respectively. The edges that connect nodes on adjacent links are shown with dashed lines in **Figure 3**.

The method described here requires the minimum number of cycles to cover every node and edge in the graph that represents the mechanism. For instance, the eight-bar mechanism of **Figure 1** can be represented by six possible loops, but only three cycles are needed to cover all the nodes and edges. The *cyclebasis* function in MATLAB gives the minimum number of cycles for a given graph. This information is used to find the order of the links and directions of the vectors and is necessary when generating the vector loop equations ensuring that every link is included without redundancy.

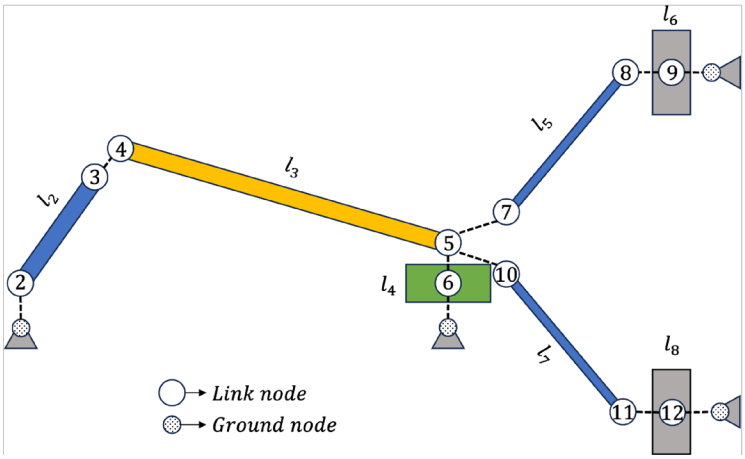

Figure 3. For each link, a node is created for points that connect to a neighboring link. Edges are formed at these connections and within the link itself. For example, l_2 would contain nodes 2 and 3, and node 3 would be neighbors with nodes 2 and 4. When defined this way, each loop can be found starting from and ending at the ground reference point, node 1. This method can be generalized for any mechanism.

For the numerical method presented here, an adjacency matrix is defined first. This is a square matrix whose rows represent a node of interest and whose columns refer to the neighboring nodes to that node. If the nodes represented by a row-column combination are connected by an edge, the corresponding element of the adjacency matrix takes a value of one. Otherwise, that element of the matrix will have a zero value. The adjacency matrix can be developed in a *for loop* as shown in the snippet below.

When the adjacency matrix is formed, it is provided as an input to the *graph* function that converts the matrix into a graphical object. The graphical object is used as the input to the *cyclebasis* function to generate the minimum number of unique cycles that represent the graph corresponding to the mechanism. The following snippet shows the MATLAB code for the steps explained above.

```
A = zeros(num_points+1); % Adjacency matrix as a square matrix of zeros
% We use the number of points +1 to account for the ground node

% Use nested for-loops to populate the elements of A
% First the link, second for each node on the link
for l = 1:length(LinkData)
   for p = 1:(LinkData(l).Point)
      currentNode = LinkData(l).Point{p}.NodeIndex;
      neighbors = LinkData(l).Point{p}.Neighbor;
      A(currentNode,neighbors) = 1; % If the nodes are connected, set the value to 1.
   end
end

G = graph(A); % Convert the matrix to graphical object.
cycles = cyclebasis(G); % Obtain the minimum unique cycles for the graph.
```

Figure 4 demonstrates the graph network defined for the eight-bar mechanism shown in **Figure 1** using the *cyclebasis* function in MATLAB. Three vector loops are automatically created for this mechanism because it can be divided into three 1-DOF linkages. Each loop has an area that does not overlap with the others and is essentially called a basis cycles.

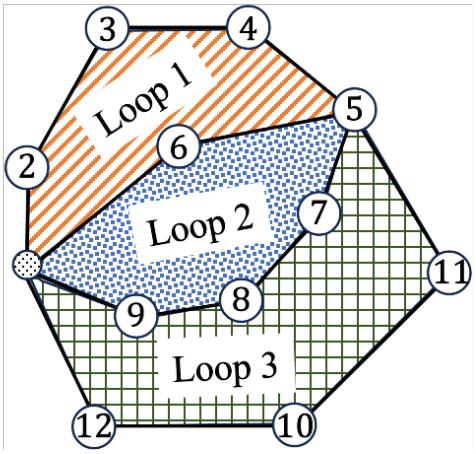

Figure 4. Graph network representation of the eight-bar linkage.

Fundamentals of Numerical Solution to the Vector Loop Equation

In this section, the steps in developing a computational solution of **Equation 6** (and similar expansion of **Equations 4** and **5**) are explained. It is assumed that the initial angular and linear positions of the links are obtained using graphical or analytical linkage synthesis methods and that the initial angular velocity and angular position of the input crank, l_2, are known.

Time values are stored in an array, e.g., `t=0:del_t:t_end`, where the variables for time interval (`del_t`) and final time (`t_end`) are previously defined. The amplitudes and angles of the vectors are stored in two arrays with the number of rows equal to the number of time points and the number of columns equal to the number of links, e.g., `L=zeros(length(t),8)` and `theta=zeros(length(t),8)`. Arrays of the same order are defined to store the velocities and accelerations. The first row of these arrays corresponds to the initial condition of the linkage at $t = 0$.

The time array is used to calculate the angular velocity and position of the input crank for all time points using a known angular acceleration, α_2. In case of a constant angular acceleration, the angular velocity and position of the input crank are stored in the first columns of their arrays using

```
alpha(:,1)=alpha_2;
omega(:,1)=alpha_2*t+omega_2i;
theta(:,1)=0.5*alpha_2*t.^2+omega(:,1).*t+theta_2i;
```

in which `omega_2i` and `theta_2i` represent variables for the initial angular velocity and position of l_2.

Since the amplitudes of the vectors representing rotating rigid rods are constant, their values are stored in all the rows of the corresponding columns of the amplitude array. Here, the constant lengths of links l_2, l_3, l_5, and l_7 are stored in the first, second, fourth, and sixth columns of the magnitude array (e.g., `L(:,1) = a;` where `a` is determined through linkage synthesis.)

Similarly, the angles of the vectors representing the sliding links are constant and can be stored in the angle array. In this case, the links l_4, l_6, and l_8 are sliders, and their angles are stored in the third, fifth, and sixth columns (e.g., `theta(:,3)=pi;`). The constant angle of the vector $\overrightarrow{EB}$ is stored in all the rows of the eighth column of this array.

The remaining elements of the arrays mentioned above are determined through an iterative numerical method which requires an initial guess as the solution for the unknowns. Here, the six unknowns in **Equation 6** are the angular positions of l_3, l_5, and l_7, and the linear positions of l_4, l_6, and l_8. Hence, the values obtained for these variables in linkage synthesis are used as the initial guess to facilitate a quick convergence for the position analysis solver.

```
pos_ini = [theta(1,2) L(1,3) theta(1,4) L(1,5) theta(1,6) L(1,7)];
```

After the successful completion of the position analysis, an initial guess for velocity analysis is made using the forward-difference method.

```
vel_ini = [(theta(2,2)-theta(1,2))/del_t (L(2,3)-L(1,3))/del_t ...];
```

Similarly, an initial guess for acceleration analysis is generated via numerical differentiation of velocity using the forward-difference method.

```
acl_ini = [(omega(2,2)-omega(1,2))/del_t (V(2,3)-V(1,3))/del_t ...];
```

Position analysis is performed, first, in a *for loop* with as many iterations as the number of time points as explained here (`for cnt=1:length(t)`). An anonymous function corresponding to the system of equations for position analysis, such as Eqn. 6, must be defined within the *for loop*. The anonymous function takes one input, which is an array with the same number of elements as the number of unknowns (six here.) The key to setting up the anonymous function properly is to represent the unknowns of the problem correctly. For instance, the complex notations of the position vectors for rotating rigid rods, such as l_3 ($l_3 e^{j\theta_3}$), and sliders, such as l_4 ($ce^{j\pi}$), are as follows.

```
L(cnt,2)*exp(x(1)*1i)
x(2)*exp(1i*pi)
```

Here, `x` is the input variable for the anonymous function whose first and second elements represent the angular position of l_3 and linear position of l_4, respectively. Consequently, the anonymous function corresponding to **Equation 6** for position analysis is constructed as shown below.

```
pos = @(x) [real(L(cnt,1)*exp(theta(cnt,1)*1i)+ ...
    L(cnt,2)*exp(x(1)*1i)+ ...
    x(2)*exp(theta(cnt,3)*1i));
      imag(L(cnt,1)*exp(theta(cnt,1)*1i)+ ...
    L(cnt,2)*exp(x(1)*1i)+ ...
    x(2)*exp(theta(cnt,3)*1i));
      real(L(cnt,4)*exp(x(3)*1i)+ ...
    x(4)*exp(theta(cnt,5)*1i)+ ...
    (h-x(2))*exp(theta(cnt,8)*1i));
      imag(L(cnt,4)*exp(x(3)*1i)+ ...
    x(4)*exp(theta(cnt,5)*1i)+ ...
    (h-x(2))*exp(theta(cnt,8)*1i));
      real(L(cnt,6)*exp(x(5)*1i)+ ...
    x(6)*exp(theta(cnt,7)*1i)+ ...
    (h-x(2))*exp(theta(cnt,8)*1i));
      imag(L(cnt,6)*exp(x(5)*1i)+ ...
    x(6)*exp(theta(cnt,7)*1i)+ ...
    (h-x(2))*exp(theta(cnt,8)*1i))];
```

This anonymous function and the initial guess are used as inputs of the *fsolve* command in MATLAB to compute the unknowns at every iteration of the *for loop*. While the initial guess may remain unchanged, updating it with the solution from the previous iteration helps with a quick convergence of the *fsolve* command.

```
if cnt > 1
   pos_ini = sol;
end
sol = fsolve(pos,pos_ini);
```

Here, `sol` is an array of six elements storing the solution of the numerical solver. At the end of each iteration, this variable is used to update the arrays that were defined for angular and linear positions of links.

```
theta(cnt,2) = sol(1);
L(cnt,3) = sol(2);
L(cnt,8) = h - sol(2);
theta(cnt,4) = sol(3);
L(cnt,5) = sol(4);
theta(cnt,6) = sol(5);
L(cnt,7) = sol(6);
```

Similar to the position analysis, an anonymous function corresponding to the expanded format of **Equation 4** is defined inside a *for loop*. The angular velocities of rotating rods and linear velocities of the sliders are unknown. All the position data are calculated in the previous step. The anonymous function for the velocities of the example here is shown below.

```
vel = @(x) [real(L(cnt,1)*omega(cnt,1)*exp(theta(cnt,1)*1i)*1i+ ...
  L(cnt,2)*x(1)*exp(theta(cnt,2)*1i)*1i+ ...
  x(2)*exp(theta(cnt,3)*1i));
    imag(L(cnt,1)*omega(cnt,1)*exp(theta(cnt,1)*1i)*1i+ ...
  L(cnt,2)*x(1)*exp(theta(cnt,2)*1i)*1i+ ...
  x(2)*exp(theta(cnt,3)*1i));
    ... % Continues like the position vector
```

Again, updating the initial guess solution at every iteration of the solution to facilitate a quick convergence is reasonable. The initial guess and the anonymous function are provided as inputs to the *fsolve* command. The results obtained from this command are used to update the corresponding elements of the velocity arrays similar to the position analysis.

An anonymous representing the expanded acceleration equations such as **Equation 5**, shown below, is used inside a *for loop* similar to position and velocity analysis to compute all the accelerations in successive iterations.

```
acl = @(x) [real(-L(cnt,1)*omega(cnt,1)^2*exp(theta(cnt,1)*1i)+ ...
  L(cnt,1)*alpha(cnt,1)*exp(theta(cnt,1)*1i)+ ...
  L(cnt,2)*x(1)*exp(theta(cnt,2)*1i)*1i- ...
  L(cnt,2)*omega(cnt,2)^2*exp(theta(cnt,2)*1i)+ ...
  x(2)*exp(theta(cnt,3)*1i));
    imag(-L(cnt,1)*omega(cnt,1)^2*exp(theta(cnt,1)*1i)+ ...
  L(cnt,1)*alpha(cnt,1)*exp(theta(cnt,1)*1i)+ ...
  L(cnt,2)*x(1)*exp(theta(cnt,2)*1i)*1i- ...
  L(cnt,2)*omega(cnt,2)^2*exp(theta(cnt,2)*1i)+ ...
  x(2)*exp(theta(cnt,3)*1i));
  ... % Continues like the position vector
```

The initial guess solution for acceleration is updated in each iteration and is provided as an input for the *fsolve* function. The output of this function is used to populate the acceleration arrays similar to the position analysis.

Algorithm for Numerical Solution

A generalized form of the anonymous functions is used to define the vectors of each link. Each link has four attributes. The first attribute is called "*Type*" and determines if the link is a rotational rod, slider, etc. The magnitude and angle of the vector for each link are used to define "*Magnitude*" and "*Angle*" attributes of the link. Then, the anonymous function is attributed to the link, called "*Fun*", which depends on the link type. This is demonstrated in the following snippet.

```
euler = @(R, theta) R*exp(1i*theta);
Vector = @(R, theta) [real(euler(R,theta)); imag(euler(R,theta))];
for l = 1:length(Link)
  ang = Link(l).Angle;
  mag = Link(l).Magnitude;
  if Link(l).Type == 0 % Rigid
      Link(l).Fun = @(x) Vector(mag,and);
  elseif Link(l).Type == 1 % Rotating Bar
      Link(l).Fun = @(x) Vector(mag,x);
  elseif Link(l).Type == 2 % Slider
      Link(l).Fun = @(x) Vector(x,mag);
  else
      % reserved for other link types
  end
end
```

In a *for loop*, the anonymous functions are summed for their real and imaginary parts in separate vector rows, resulting in a new anonymous function that is compatible with MATLAB's *fsolve* function. Like before, the *fsolve* function is called repeatedly for each time step, using results from the previous step for initial guesses, as explained in the previous section. The automatic method of generating the "*anonymous function*" is shown in the snippet below.

```
F = @(x) 0;
for l = Order{c}
  F = @(x) F(x) + Direction{c}(l) * Link(l).Fun(x(l));
end
```

Besides being shorter, the primary benefit of this approach is its ability to be generalized. The same code used to solve the eight-bar of this example linkage would also solve any other 1-DOF multi-bar linkages.

DISCUSSION

The results from the numerical algorithm are verified using the algebraic solution of the relative motion equations for interconnected rigid bodies and applying the motion constraints at each joint. For instance, in the present example, $v_{By} = v_{Cx} = v_{Dx} = 0$ and $a_{By} = a_{Cx} = a_{Dx} = 0$. The lengths and angles of the links for the eight-bar linkage shown in **Figure 1** at $t = 0$ are given in **Table 1**.

Kinematic analysis of the linkage is performed for $0 \leq t \leq 2.35$ seconds with an interval of 0.05 seconds. This ensures the input link completes at least one cycle. The angular acceleration of the input crank, l_2, is zero, and its initial angular velocity is three rad/s.

Link	Length (m)	Angle (rad)
l_2	a = 3	$\theta_2 = \pi/2$
l_3	b = 5	$\theta_3 = 5.6397$
l_4	c = 4	$\theta_4 = \pi$
l_5	d = 6.15	$\theta_5 = 0.8627$
l_6	k = 4.6715	$\theta_6 = 3\pi/2$
l_7	m = 6.15	$\theta_7 = 5.4205$
l_8	g = 4.6715	$\theta_8 = \pi/2$

Table 1. Initial values for lengths and angles of the links of the eight-bar linkage.

Angular positions, velocities, and accelerations of links l_3, l_5, and l_7 are shown in **Figure 5**. An excellent agreement between the results from the numerical algorithm and the algebraic analytical solution is observed. As expected, the kinematic parameters of links l_5 and l_7 are vertically symmetrical.

Figure 6 also shows that the results for displacements, velocities, and accelerations for sliders l_6 and l_8 agree with those derived from the analytical solution. Due to the setup of the eight-bar linkage in this example, the profiles of the kinematic parameters of these links are also vertically symmetric.

It is observed in **Figure 7** that the results for the horizontal slider l_4 obtained from the numerical algorithm match well with the analytical solution. The deviation between the analytical and numerical results shown in **Figures 5-7** is much smaller than 1% for all parameters. The largest difference may occur in reporting zero values, which is caused by rounding errors in the numerical method showing very small values such as 10^{-16} instead of absolute zero. Such an excellent agreement partially stems from choosing appropriate initial guess solutions for the numerical method in each step of the iterations, as explained earlier.

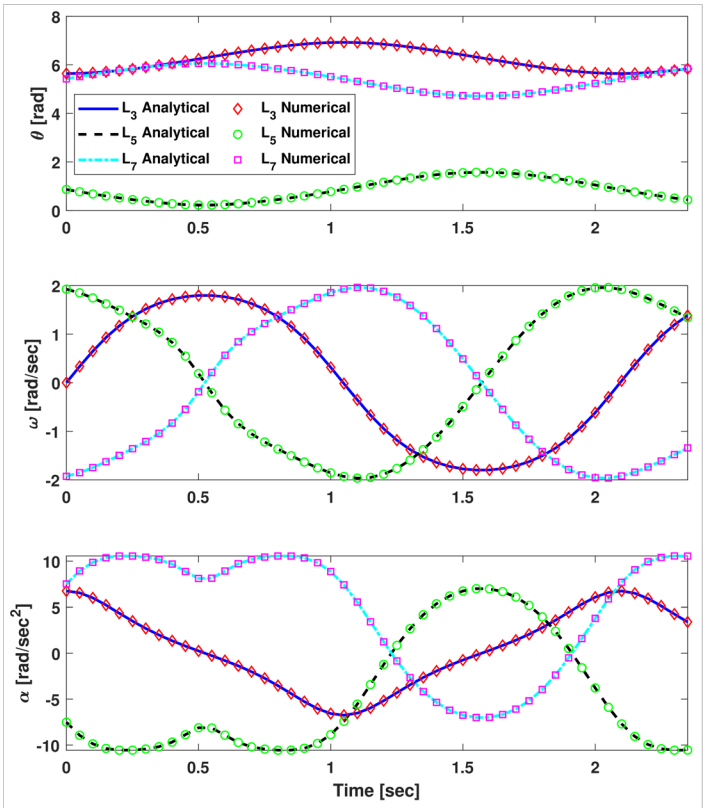

Figure 5. (Top) Angular positions, (Middle) angular velocities, and (Bottom) angular accelerations of links l_3, l_5, and l_7.

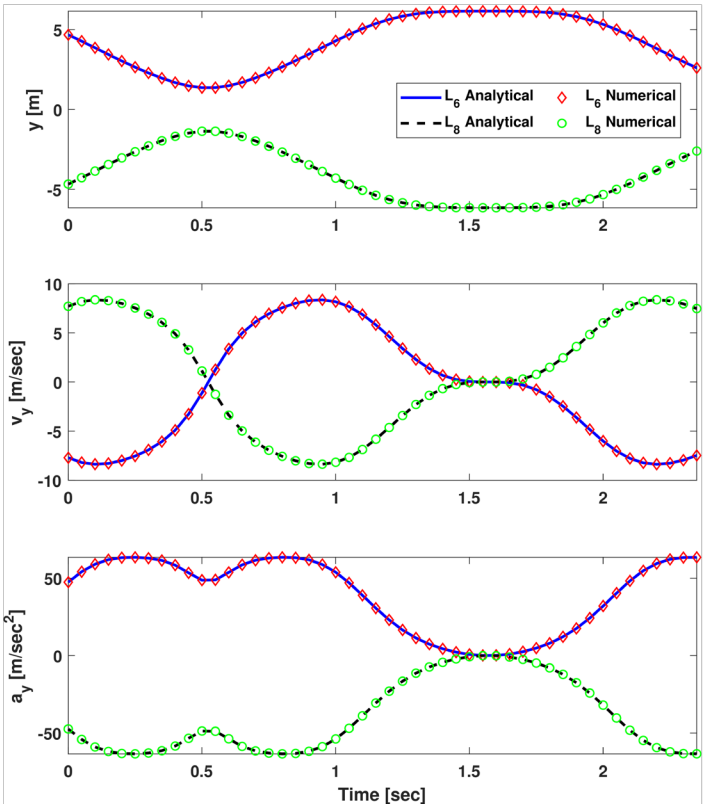

Figure 6. (Top) Positions, (Middle) velocities, and (Bottom) accelerations of sliders l_6, and l_8.

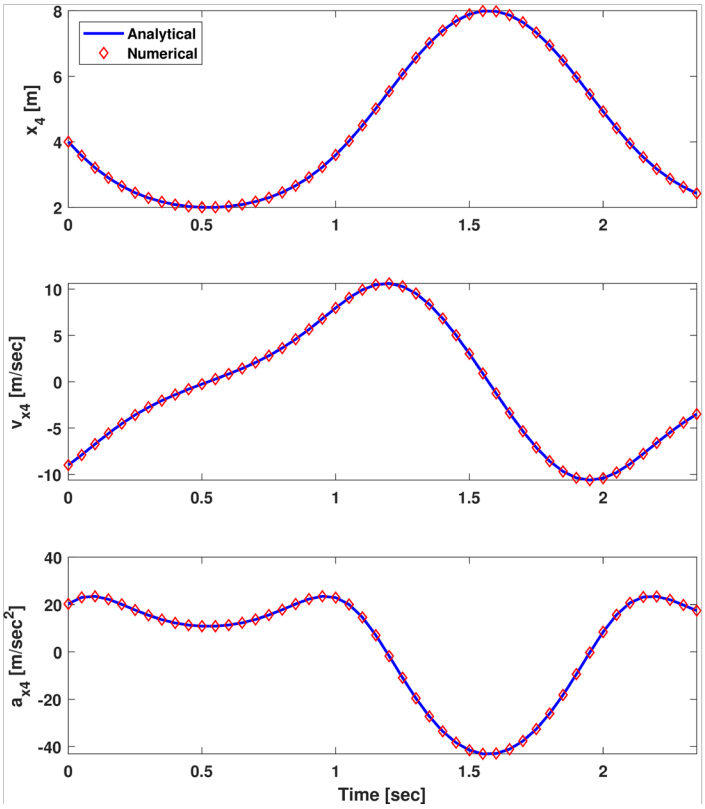

Figure 7. (Top) Position, (Middle) velocity, and (Bottom) acceleration of slider l_4.

It must be noted that the goal here is to verify the accuracy of the results from the presented numerical algorithm when compared with the algebraic solution. The excellent match between the results derived from the two methods verifies the accuracy of the numerical solution. This algorithm was tested with several other 1-DOF multi-bar linkages and exact matches were observed between the numerical and algebraic solutions.

CONCLUSIONS

An algorithm was presented for numerical analysis of the kinematics of multi-bar linkages using computer simulations in MATLAB. The algorithm is based on developing the vector loop equations for the linkages, as in an analytical solution. The vector loop equations can be generated either manually or by generating a path-finding algorithm. The numerical solution benefits from the capabilities of scientific programming languages, such as MATLAB, to find the roots of systems of nonlinear and linear equations. It was demonstrated that the presented algorithm can handle links of any order (binary, ternary, etc.) as well as links whose kinematics are related to that of an adjacent link. The results obtained using the presented algorithm for an eight-bar linkage were in excellent agreement with the analytical solution.

The method presented here can be used in teaching relevant courses such as kinematics or dynamics of machines. The authors are currently developing a complete stand-alone program with a graphical user interface for kinematic analysis of mechanisms. The next step is to include force calculations to provide a complete dynamic analysis of any linkage mainly for educational purposed.

The algorithm can be further improved to capture errors that may occur if the mechanism is physically incapable of completing a full cycle. For example, if a non-Grashof four-bar linkage is pushed beyond its limits, the solver will produce an error. Another enhancement to the method is to enable the program to analyze linkages with inverse sliders.

ACKNOWLEDGEMENTS

The authors thank the Office of Research, Scholarship, and Creative Activities at SUNY New Paltz.

REFERENCES

1. Moon, F. C., (2003), Franz Reuleaux: Contributions to 19th Century Kinematics and Theory of Machines, *Applied Mechanics Review*, **56**(2), 261–285, *https://doi.org/10.1115/1.1523427*
2. Thurston, R. H., (1878), The Steam-Engine As A Simple Machine, in *A History of the Growth of the Steam-Engine*, Vol. 24, 1–20, D. Appleton And Company, New York.
3. The Editors of Encyclopedia, (2023), Steam Engine, December 2023 URL *https://www.britannica.com/technology/steam-engine* (accessed January 2024)
4. Norton, R. L., (1998), Position Analysis, in*Design of Machinery*, 5th ed., 174–214, McGraw-Hill, Massachusetts.
5. Reuleaux, F., (2013), Sketch of the History of Machine Development, in *The Kinematics of Machinery: Outlines of a Theory of Machines*, 1st ed., 201–242, Courier Corporation, New York.
6. Reuleaux, F., (1901), The Elements of Graphostatics, in *The Constructor*, 4th ed., 22–38, HH Suplee, New York.
7. Kennedy, A. B. W., (1907), The Machine, in *The Mechanics of Machinery*, 1st ed., 1–19, Macmillan and Company, New York.
8. Hartmann, W., (1913), Introduction, in *Die Maschinengetriebe*, 1st ed., 1–2, Macmillan and Company, New York.
9. Grübler, M. F., (1917), Die Elementenpaare, in *Getriebelehre: eine Theorie des Zwanglaufes und der ebenen Mechanismen*, 1st ed., 1–7, Springer, Berlin.
10. Uicker Jr, J. J., Pennock, G. R., and Shigley, J. E., (2023), The World of Mechanisms, in *Theory of machines and mechanisms*, 6th ed., 3–54, Cambridge University Press, Cambridge.
11. Martin, G. H., (2002), Linkages, in *Kinematics and dynamics of machines*, 2nd ed., 44–68, Waveland Press, Illinois.
12. Russell, K., Shen, J. Q., and Sodhi, R., (2018), Mathematical Concepts in Kinematics, in *Kinematics and Dynamics of Mechanical Systems: Implementation in MATLAB® and SimMechanics®*, 2nd ed., 13–37, CRC Press, New York.

13. Vinogradov, O., (2000), Kinematic Analysis of Mechhanisms, in *Fundamentals of kinematics and dynamics of machines and mechanisms*, 1st ed., 15–64, CRC Press, New York.
14. Gamble, B., (2010), Software Implementation, in 5-Bar Linkage Kinematic Solver and Simulator, 1st ed., 18–23, The University of Vermont, Vermont.

ABOUT THE STUDENT AUTHOR

Brandon Torres is a Class of 2024 Mechanical Engineering undergraduate student at the State University of New York (SUNY) at New Paltz. His area of interest for research is computational engineering and programming. Brandon has been working on projects that involve modeling physical systems with MATLAB, such as fluid motion and machine dynamics problems. Brandon has also been working as a student assistant for Computer Simulations in SUNY New Paltz, hoping to teach others about the benefits of using computer programming to solve real-world engineering problems.

PRESS SUMMARY

Machines and mechanisms are all around us, from door closers, to can openers, to car engines, to aircraft landing gear, and so on. These are a tools made up of interconnected links (e.g. rods) that transfer motion and force from one source and/or form to another point and/or form. For example, the energy stored in the spring component of a door closer is converted into the kinetic energy that moves the door back to its closing state.

Understanding the behavior of these mechanisms, such as the speed at which their components move, requires a dynamic analysis of the interconnected links. Although algebraic methods from classical dynamics can be used for this purpose, the process becomes tedious as the number of components in the mechanism increases. The increasing number of links in the mechanisms makes the derivation of specific equations for any given design virtually impossible. There is a lack of a general solution method for the dynamic analysis of mechanisms of any design that can be used for education purposes.

Thanks to the advancement of computational technologies, the authors have developed a numerical method that employs mathematical concepts such as graph theory and complex numbers to perform a complete kinematic analysis of mechanisms. The proposed method is capable of analyzing mechanisms with several components, and can be taught in classroom as a means to study the motions of mechanisms for which analytical solutions are challenging.

Learning About Food Insecurity in Athens-Clarke County, Georgia Using Key Informant Interviews

*Natalie Wong[a] & Michelle Ritchie[b]**

[a]Department of Environmental Health Science, College of Public Health, University of Georgia
[b]Institute for Disaster Management, College of Public Health, University of Georgia

https://doi.org/10.33697/ajur.2024.119

Student: natalie.wong@uga.edu
*Mentor: michelle.ritchie@uga.edu**

ABSTRACT
Several studies have suggested that food insecurity rates increased during the early days of the COVID-19 pandemic. This study sought to assess the strategies employed by food relief organizations to combat this issue amidst the challenges of 2020. Specifically, the research focused on six local food organizations in the Athens, Clarke County area in Georgia. Organizations were contacted via email, and subsequent key informant interviews were conducted via Zoom with the organization's leaders to understand their responses to food insecurity relief during the 2020 COVID-19 pandemic. The findings were synthesized using a narrative qualitative approach to identify overarching themes in the organizations' strategies amid the pandemic. Overall, this study revealed a prevalent lack of emergency preparedness among the organizations, exacerbating the issue of food insecurity in the Athens-Clarke County, Georgia area. These results underscore the need for public policy interventions addressing the underlying causes of food insecurity, including the elimination of food deserts, enhancement of food procurement accessibility, improvement of food affordability, and mitigation of associated disparities by race, income, and gender. By understanding the experiences of these organizations amidst the pandemic and the pre-existing factors that contribute to food insecurity, stakeholders, including other organizations, community leaders, and locals may be able to better prepare for future crises.

KEYWORDS
Food insecurity; key informant interviews; qualitative analysis; COVID-19; health disparities; food deserts

INTRODUCTION

Much of the Athens-Clarke County (ACC), Georgia, area is identified as a food desert or food swamp, where low-income communities lack stores that sell affordable, nutritious foods.[1] Here, we use the term Low Income, Low Access (LILA) to reflect the activist language around food apartheid.[1, 3] Despite the need, relatively few studies have focused on local food relief organizations in Athens, Georgia,[4-7] and of these studies, none focus on food relief within the context of the COVID-19 pandemic.

Some data suggested food insecurity for children and adults has decreased from 2019 through 2021 in the United States.[8] However, the peer-reviewed academic literature suggested the opposite, with rates of food insecurity increasing significantly over this time period.[9] Food insecurity remained stable in 2020, and decreased slightly in 2021 due to pandemic aid, Supplemental Nutrition Assistance (SNAP) expansion, and Pandemic Electronic Benefit Transfers (P-EBT).[10] However, rates increased in 2022 when some of this federal aid ended.[10] These discrepancies may be due to differences in how food insecurity is measured. For instance, one study suggested that although the Food Security Survey Module is the most common model to measure food insecurity, it does not accurately depict the magnitude of food security.[11]

One study identified eight multi-item tools to measure food access, including the Cornell Child Food Security Measure, the Community Childhood Hunger Identification Project tool, the Hager two-item screen, the Girard four-point tool, the Kuyper past food insecurity, the Household Food Insecurity Access Scale, and the Townsend Food Behavior Checklist.[11] Similarly, a second study identified the most common models used to create psychometric properties for measuring household food security.[12] For all instruments, the studies found that food insecurity and hunger were linked to physical access and financial resources.[12] However, few of these instruments addressed questions relating to food safety.[12]

A third study suggested that understanding the role of gender disparities was key to understanding factors contributing to food insecurity because women might have experienced less access or opportunities to education, employment, and healthcare. Based

on these factors, the study found that females had reported a higher percentage of household food insecurity than males.[13] A fourth study attempted to provide a comprehensive understanding of the factors that affected food insecurity, including how the pandemic might have amplified the issue. This study evidenced that disparities such as those mentioned had further widened amid the COVID-19 pandemic.[9] The authors hypothesized that individuals with higher odds of food insecurity might have been socially, culturally, and economically disadvantaged groups, persons with more symptoms of depression or anxiety, and persons with higher levels of fear and concern about the COVID-19 pandemic.[9] Again, these studies demonstrated that more research was needed to holistically assess and respond to rates of food insecurity.

Further, some regions of the country experienced higher food insecurity rates than others during the pandemic, in part dependent on their existing emergency food resources. For example, with the rise of unemployment during the pandemic, some food relief organizations became overwhelmed, with one study suggesting that food relief organizations saw up to a 75% increase in clientele during the pandemic.[9] Indeed, this increase in clientele during the pandemic could have been due to how some local food distribution systems operated. One study suggested that food banks that depended on retailers often failed to provide food stocks due to slow supply chains during the pandemic.[14] On the other hand, food banks with wholesale suppliers were able to have a stable supply of food.[14] This highlighted the importance of diversifying supply sources and types to ensure access to food during an emergency crisis was being met.

Another study found that case studies have shown school-age children have greater difficulties meeting their dietary needs during the summer break due to school meals being unavailable. Research has shown that these school meal programs positively affect a child's dietary intake and improve food insecurity among low-income households.[15] Based on this data, the authors found that food insecurity was more prevalent during the summer.[15] With the 2020 COVID pandemic, the majority of schools were shut down, mimicking a summer season, which may have affected school-aged children's food security as many households rely on the National School Lunch Program for breakfast and lunch. Thus, amid the pandemic, there may have been increased numbers of unemployed and food-insecure children, pointing to the need for more research.[16]

In response to the literature gaps stated above, this study aimed to determine how organizations addressed food insecurity in the ACC area during the COVID-19 pandemic to understand how their responses resulted in differing outcomes for food insecurity. Namely, we asked, "How did the COVID-19 pandemic affect local organizations' response to food insecurity relief?"

METHODS AND PROCEDURES

To answer the research question, we created a set of semi-structured interview questions to guide interviews with local food relief organizations' leadership. We focused these questions on the organization's mission, how they provided food insecurity relief, how their operation was impacted during COVID-19, and how these factors may have produced differing outcomes for food insecurity relief (see Appendix A). Namely, after receiving informed consent from participants, we conducted key informant interviews via Zoom over a period of four weeks, with each interview lasting for approximately 30 minutes. We asked the interviewees if we could record the interview for later reference, and we took detailed notes during the interview. At the end of each interview, we asked the interviewees if they knew other organizations that could be referred to for interviews, in keeping with a snowball sampling approach. This procedure was repeated until all interviews were completed.

After interviewing organizational leaders, we found overarching themes regarding how the organizations handled food insecurity relief during the pandemic using a thematic and narrative analysis approach.[15-16] First, we took detailed notes during the interviews and organized them by order of question. Then, we condensed these notes into paragraph summaries by organization. We then re-listened to interviews to catch any gaps in notes. Through this process, we analyzed the gathered information to identify patterns of common themes across organizations. Namely, we used a thematic and narrative analysis to identify these themes within a framework for understanding individuals' experiences across organizations. Due to the scope of the study and the in-depth nature of the interviews, we chose to work with only six participants.[17]

Participants and Recruitment

This research focused on food relief organizations in the ACC area that funded food relief or otherwise distributed, donated, packed, or served food to community members in 2020 (See Appendix B). Before beginning, we sought approval from the Institutional Review Board at UGA. Ultimately, it was determined that this project was exempt from human subject research (PROJECT00008179). Following this determination, we assembled a list of twelve local organizations through news articles, recommendations from local experts, government officials, and website searches. We then recruited these organizations via email requesting an interview with a leader or representative, and a follow-up email was sent two weeks later when required. For organizations without emails, we called their main phone number or sent an Instagram direct message instead. These communications were sent out in October 2023. Of the twelve organizations that were contacted, six of them agreed to participate in an interview via Zoom, equaling a 50% response rate.

RESULTS & DISCUSSION

There were six common themes that we identified during our analysis of organizational leaders' responses to our interviews. These themes were discussed in turn. One such theme included emergency preparedness and response. Most of the leaders stated they were woefully unprepared for a spike in demand for food relief. The COVID-19 pandemic placed an even greater strain on their ability to meet the needs of local people. Another theme included was food justice and sovereignty. We see this in the fact that two organizations worked closely together to ensure their clients had agency over their food choices. Further, another organization highlighted how some food-insecure clients also requested food-adjacent items, pointing to the need for additional items beyond foods. Results also point to additional low-income and low-access (LILA) issues, identifying significant barriers to access. All organizations concurred that the USDA's Food Atlas map was a fair representation of the LILA area. However, barriers and solutions to food access and disparate impacts of food insecurity were identified. It was also noted that there were no noticeable changes to the demographics most impacted by food insecurity during the pandemic. Finally, food relief networks surfaced as a prominent theme in providing local food relief. All organizations were able to find ways to adapt to the COVID-19 pandemic, such as by fostering collaboration among other local organizations and businesses in Athens.

Emergency Preparedness and Response

There were many similarities between organizational leadership's emergency preparedness practices before and in response to the COVID-19 pandemic in 2020. Overall, most organizations expressed that they did not have emergency preparedness plans before the pandemic. Some organizations noted that their general emergency management operational policies were recently updated, but all noted that their policies regarding a pandemic had not been recently updated or did not exist. For example, the director of programs and services from Organization C stated, "I think the emergency handbook was from the 1970s. We certainly have policies that have been updated since then related to parts of emergency management like inclement weather, but pandemic (Participant A)?"

Despite this lack of pandemic preparedness, most organizations reported being able to recover and adapt to changes quickly. Since nonprofits and social service organizations were classified as essential workers, food relief organizations were given emergency authorization to work in person. During this time, all organizations interviewed stated that they adhered to the social distancing protocols and adjusted their program operations accordingly. For instance, most organizations implemented a mask mandate, drive-throughs or meal deliveries, to-go plates, or an appointment-only policy. All of these changes helped ensure the safety of their staff, volunteers, and guests while also adhering to COVID-19 guidelines.

Further, one noticeable difference among the organizations interviewed was how each handled emergency food production levels. Organizations A, B, and C increased their production, Organization D decreased their production, and Organizations E and F's production was reportedly unaffected. These production levels were determined based on the number of meals distributed and by how many volunteers or staff were working. For example, organizations A and B worked closely together. As such, their production increased since Organization A receives approximately 90% of its produce from Organization B, and during the pandemic, Organization B began growing and donating more crops to meet the growing demand for food. For example, Organization A stated, "We've always been close with [Organization B], so when the pandemic hit, we knew we needed to keep operating, and so we very quickly moved our operations out here to [Organization B], which is how we have continued to operate since then (Participant B)."

Notably, the pandemic significantly affected Organization C, which reportedly "saw a 4,000% increase in our meal deliveries (Participant C)" from 2020 to 2021. Despite this, using federal money from ACC, Organization C became the primary food relief program, adopting a whole community approach that involved working with many smaller nonprofits and organizations. More people also volunteered with Organization C during the pandemic than before. On the other hand, distribution decreased for Organization D because, in part, it did not allow volunteers to help during the pandemic. Instead, Organization D was run by two full-time staff members to ensure minimal social contact. Since new food relief organizations were started during the pandemic, it helped ease the burden of food insecurity relief for Organization D. As one participant from Organization D stated, "We were the main emergency food resource for last 40-50 years, but new places occurred, which eased the burden a little bit (Participant D)." These themes show the non-linear, place-based nature of food relief organizations' preparation for and response to the pandemic. Although the majority of organizations lacked an emergency response plan before the pandemic, they were able to adjust to COVID-19-related changes and challenges to continue serving the community.

Food Justice and Sovereignty

Interview responses from Organization A, Organization B, and Organization C brought attention to the importance of agency in local food relief. Agency is defined as an individual's ability to make choices for their food within the constraints of one's social, physical, and economic environment.[20] During the pandemic, Organization A and Organization B worked even more closely

together, as vegetables and fruits grown vary depending on the feedback from Organization A about what individuals prefer. For instance, Organization B used to grow eggplants during the summer, but they received feedback from Organization A that it was not desired by clients due to dietary preferences, so they scaled back the production of these crops. Instead, they focused on producing more in-demand crops, such as okra, tomatoes, green beans, collard greens, and squash, some of which come with cultural significance. For example, one participant from Organization A stated, "We are also able to give more direct feedback to [Organization B]'s staff. For example, 'mixed salad greens are great, but our clients prefer collard greens', or 'they really love okra' (Participant E)." This feedback-driven approach ensured that the community's preferences and dietary needs were considered, supporting food sovereignty, and resulting in less food waste. Here, we define food sovereignty as the peoples' right to define their own food systems by making joint decisions with food providers on food issues that benefit all.[21]

Some additional challenges during the pandemic were a result of logistical constraints. For instance, many people served by Organization C requested meat products, such as beef or chicken, but this proved difficult due to cost and limited cold food storage space. Due to this, Organization C had to mostly provide canned meat. Occasionally, however, they were able to provide some fresh or frozen meat when they worked with a catering business that prepared meals and an agribusiness that provided bacon. For example, one participant from Organization C stated,

> "We were able to provide some fresh or frozen meat during the pandemic. It was just limited. We had to focus more on canned or dry proteins, for sure, but the work with [local organizations] did offer some meat products including in prepared meals…. We also did smoked chickens for everyone the week of Christmas (Participant F)."

Organization C also recognized "food adjacent items" such as cleaning supplies, paper goods, and hygiene as being essential to an individual's overall well-being. While these were not directly food-related, it showed the interconnectedness between the right to nutritious, affordable food and the right to other essential items needed to live a healthy lifestyle. Overall, when individuals were afforded the choice to voice their food preferences, they were afforded a sense of agency, promoting food sovereignty.

Low-income and Low-access Constraints

In Athens, low-income and low-access areas presented a key barrier to access to affordable, nutritious foods. For example, one participant stated, "Clarke [County] is the hub for all these other outlying rural counties. One thing that we saw during Covid that we still see is it's worse when you get out there. The population isn't as high, but people can be more isolated because of geographical distance (Participant C)." All organizations consulted unanimously agreed that the USDA's Food Atlas map of ACC was a fair representation of this, but that it could also be expanded to better reflect lived experiences. For example, certain areas in ACC had a more limited number of grocery stores, resulting in some reliance on public transportation or less nutritious food options if access to a vehicle was a limiting factor to food procurement. While many fast food chains, gas stations, and Dollar Generals could be found throughout Athens, these stores often do not provide fresh, nutrient-dense produce. Many individuals affected by food insecurity could afford and access non-perishable or fast food items, but such food-like items lacked sufficient nutrients for a long-term, healthy, balanced diet.

Moreover, some food relief organizations argued that transportation and time emerge as key factors that further exacerbate food insecurity. While ACC has a public transit system, residents had to factor in the bus schedules, limited routes, and their limitations, such as physical mobility, work schedules, and childcare. For example, individuals that had long shifts or worked during unconventional hours had schedules that conflicted with the bus timetable and grocery store hours of operation. One participant echoed this sentiment, stating, "Transportation as a whole could mean a lot of things. The wait time for the buses is super long. Even if you could use the bus to get to work or to a food pantry, how does your schedule align with it (Participant A)?" Additionally, residents must factor in the amount of groceries they could carry while walking or taking the bus. Testimonies from participants showed how access to affordable and nutritious foods in ACC is not only hindered by geographical constraints but also logistical constraints, such as limited grocery store availability and public transportation reliability. Overall, clients faced difficulties in aligning their schedules with the bus routes and grocery store hours, further complicating their ability to obtain healthy food options.

Barriers and Solutions to Food Access

Representatives of the organizations were asked to provide their opinion on the possible barriers to access and potential solutions regarding subsequent policy, logistics, and expansion of programs. Organization E emphasized how family structure and income could influence the prioritization of needs, which could influence food insecurity. For example, if a family has limited funding or income, they may have to decide what bills to pay, ultimately forgoing meals in favor of paying a heating bill, for example. As one participant stated, "Food prices have gone up, and some people have to decide on whether to eat or pay for rent." Based on data reported by the USDA ERS, the Consumer Price Index (CPI) had a 25.0 percent increase from 2019 to 2023.[22] From 2020 to 2021, this increase was driven by changes in consumption patterns and supply chain disruptions caused by the pandemic.[22]

Organization E suggested solutions, including increasing wages to make healthy foods more affordable or reducing the cost of healthy foods. Organization F pointed out that to improve access to healthy foods, people should not have had to go through extensive paperwork for assistance. For example, unhoused individuals might not have had the necessary paperwork, such as proof of income or a social security number, to qualify for assistance. Even if individuals had the required documents, they often had to wait months before being eligible for more assistance.

Besides cost, other barriers to food security highlighted by some organizational leaders include technology, mobility, and transportation. For example, one participant from Organization C stated, "I think you see higher numbers at both ends of the age spectrum. It [hunger] can impact anybody, but I think children and seniors are where you see it the most." In ACC, one in five people were considered food insecure, with higher percentages among children and senior citizens.[23] This is particularly concerning since children and seniors were among the most vulnerable to the effects of food insecurity. Regarding senior citizens and other vulnerable populations, many at-risk individuals chose not to use public transportation when buying at grocery stores to reduce their exposure to COVID-19. Additionally, some individuals had mobility issues that caused them to be physically unable to get to any stores or food relief organizations.

Considering these key issues, during the pandemic, Organization C increased its meal delivery program and started a drive-through food drive to adjust to demand. Organization B's representative also believed that components of food insecurity relief should have been expanded to include wait times for public transportation, work schedules, and food sovereignty issues. Similarly, Organization A stated that many individuals had jobs and ended up relying on fast food due to convenience, as many grocery stores were only open for a relatively limited amount of time each week.

Disparate Impacts of Food Insecurity

Based on the results of the interview analysis, the majority of organizations noted that individuals who were food insecure were primarily those who were low-income or experiencing homelessness. Organization A, D, and E all stated that they often saw the same individuals and families seeking aid, primarily the working poor living at or below the poverty line. Amid the pandemic, some of these same people experienced tragedies, in some cases causing them to move or pass away. As a result, these organizations began to see new individuals but who shared the same demographic features as those before them. For example, many individuals who sought food relief were women and/or Black, which highlighted additional disparities within local overarching demographic and socioeconomic trends. Understanding and addressing these disparities might help create solutions for more equitable access to food in ACC by serving those most at risk. Finally, according to a representative from Organization E, of those individuals who were unhoused, many reported relying heavily on food relief organizations for sustenance, which in some cases meant only eating one healthy meal per day.

Other at-risk groups affected by food insecurity included families with children, individuals with mental health conditions, individuals experiencing other life stressors, and senior citizens. For example, Organization F and Organization C described how children are impacted by food insecurity. Before preschool and during summers, children were sometimes unable to receive breakfast and lunch, which would otherwise be supplied by their schools. Similarly, some organizations observed that, typically, more families came to the food pantry during the summer when children are out of school or are otherwise at home regularly. With the COVID-19 pandemic, however, more families with children were seeking aid because, when schools shifted to lockdown, it placed the burden of providing breakfast and lunch on the caregivers. It is important to note, though, that during the pandemic, Clarke County School District noticed this concern and was able to create a temporary distribution model for the fall semester of 2020 to keep students fed. This included free meals to all children ages 2-18 through curbside pickup at multiple school locations.[24]

Another disparity that one organization brought attention to was how senior citizens and other vulnerable populations were impacted. Many senior citizens were especially impacted during COVID-19 since they worried about the safety protocols of their grocery stores. Senior citizens with mobility issues also found it difficult to drive or otherwise coordinate getting to the grocery store. As one participant stated, "People can experience it [hunger] for a variety of reasons. For our home delivery clients, it's usually because they're living at or below the poverty line and/or they have a health condition that makes it difficult for them to get to the grocery store or they can't drive anymore (Participant D)." According to the interviews conducted, before the pandemic, demographic groups that were impacted the most by food insecurity included individuals who were low-income, unhoused, women, Black, those with mental health conditions, families with children, and senior citizens. Interviews revealed no noticeable changes to the demographics most impacted by food insecurity during the COVID-19 pandemic.

Food Relief Networks

When the COVID-19 lockdown began in March 2020, organizations had to adapt to the 'new normal' quickly. Thus, representatives of the local food relief organizations were asked to provide their insights on how they were able to implement new strategies and collaboration efforts. Organization D explained that many new organizations and programs emerged during this time to alleviate the rise in food insecurity, providing some relief. The director of Organization D noted that a surge of new initiatives and programs emerged within the past few years, which offered substantial support for relief. Having served as the primary emergency food source since 1980, Organization D benefited from this expansion of networks. This was especially crucial when they had to cut volunteers due to safety protocols. For example, Organization C created a new food relief program expanding its outreach to the entire ACC community. Other organizations had their programs expanded or adapted to include to-go plates, appointment-only visitation of food pantries, drive-through food pick-ups, and a Zoom-based cooking show. Some of these efforts, however, were only available for a finite time due to client feedback and preferences. For example, Organization E switched back to indoor eating rather than to-go plates. Organization F has stopped appointment-only visitations, although many of their clients prefer to set up an appointment rather than walk-ins now.

Another notable change after the COVID-19 pandemic was to Organization E's community kitchen resource table, which included expanding services to include Humana services, Supplemental Nutrition Assistance Program outreach, and career preparation via workshops. While these implementations were not a direct response to the COVID-19 pandemic, they were added to help their guests more holistically while they received a meal. For example, one participant stated, "We're trying to figure out ways of what we can offer guests while they are here that could help them move forward in life (Participant A)." Some of these organizations had previously collaborated with other organizations and local businesses, and during lockdown, these collaborations generally increased. For example, Organization A formed a closer partnership with Organization B and moved its primary operations to Organization B's facility. With this change, Organization B was able to receive feedback faster on what crops to produce more or less of.

Further, when Organization E decided to close their in-person dining, they partnered with local restaurants nearby to serve their to-go plates. Finally, regarding Organization C's new food relief program, some of their expanded partners included the Food Bank of Northeast Georgia, local food vendors, Epting Catering, special events companies, the Athens Farmers Market, Collective Harvest, Georgia Grown, Clarke County school districts, and the Athens Immigration Rights Coalition. These collaborative efforts highlight how the food relief community was resilient during the lockdown, uniting to fight food insecurity in the ACC area.

CONCLUSIONS

Much of the ACC area was identified as low-income and low-access, making it difficult for people to access affordable, nutritious foods needed for a healthy lifestyle.[1] Despite this, relatively few studies focus on local food relief organizations, particularly within the context of the COVID-19 pandemic. In response to these gaps in the literature, this study aimed to determine how organizations addressed food insecurity in the ACC area during the COVID-19 pandemic to understand how their responses may have resulted in differing outcomes for food insecurity relief. Namely, we asked, "How did the COVID-19 pandemic affect local organizations' response to food insecurity relief?"

To answer this research question, we aimed to determine how organizations addressed food insecurity in the ACC area during the COVID-19 pandemic to understand how their responses resulted in differing outcomes for food insecurity. Common themes were identified using a thematic and narrative qualitative approach of key informant interviews. Namely, we found interviewees discussed emergency preparedness and response; food justice and sovereignty; low-income and low-access; barriers and solutions to food access; disparate impacts of food insecurity; and food relief networks. As such, we suggest the USDA Food Atlas could be improved to better reflect lived experience of food insecurity by including additional factors, such as the number and operating hours of food stores and the amount and quality of public transportation. Solutions to decreasing current barriers to food access may also include expanding public transportation, increasing the number of grocery stores, expanding store hours, or offering healthier food options at non-grocery stores, such as at gas stations and Dollar Generals.

Together, themes uncovered pointed to areas of need for organizations to continue to address food insecurity in the ACC area, including how their missions can be supported amid change, such as was the case with the COVID-19 pandemic. By learning about food insecurity in the context of the COVID-19 pandemic, stakeholders and the people in the community may be better prepared for future crises and have a more resilient food system. Future research should explore the long-term impacts of strategies implemented by these organizations during the pandemic. Additionally, there is a need for studies that evaluate the impact of organizations serving the community and if they are helping to address underlying or root causes of food insecurity. Future research could also focus on evaluating the effectiveness of proposed solutions, such as expanding public transportation

and increasing healthy and affordable food options in non-grocery stores. Finally, investigating public perception of food insecurity by varying demographics can lead us to a better understanding of how to improve public outreach and address food insecurity in ACC and other similar communities in the United States.

ACKNOWLEDGEMENTS

This work was supported by the University of Georgia's Center for Undergraduate Research Opportunities program. Thank you to all the food relief organizations in the Athens-Clarke County, Georgia area for being interviewed. Thank you also to Dr. Jennifer Jo Thompson for providing her expertise on the subject.

REFERENCES

1. Economic Research Service (ERS), U.S. Department of Agriculture (USDA). Food Access Research Atlas, *https://www.ers.usda.gov/data-products/food-access-research-atlas/* (accessed February 2024)
2. Honório, O. S., Pessoa, M. C., Gratão, L. H. A., Rocha, L. L., de Castro, I. R. R., Canella, D. S., Horta, P. M., & Mendes, L. L. (2021) Social inequalities in the surrounding areas of food deserts and food swamps in a Brazilian metropolis. *International Journal for Equity in Health*, 20(1), 168. *https://doi.org/10.1186/s12939-021-01501-7*
3. Walker, J. (2023) 'Food desert' vs. 'food apartheid': Which term best describes disparities in food access? University of Michigan School for Environment and Sustainability. *https://seas.umich.edu/news/food-desert-vs-food-apartheid-which-term-best-describes-disparities-food-access* (accessed April 2024)
4. Andersen, E. C. (2009) Talking about hunger : mediating between purpose and practice : a case study of food provision in Athens, Georgia.
5. Freeman, M. (2007) Food Not Waste: A Spatial Analysis of Athen's Food Gleaning Network.
6. Howerton, G. (2013) Coding of place, racialization, and social barriers in small-scale neighborhood groceries : a case study in Athens, Georgia.
7. Wilson, S. B. (2011) Perceptions of the local food environment among low-income residents of Athens, Georgia.
8. Map the meal gap. Overall (all ages) Hunger & Poverty in the United States. (n.d.) *https://map.feedingamerica.org/* (accessed February 2024)
9. Kevin M. Fitzpatrick, Casey Harris, Grant Drawve & Don E. Willis (2020) Assessing Food Insecurity among US Adults during the COVID-19 Pandemic, *Journal of Hunger & Environmental Nutrition*, 16:1, 1-18, *https://doi.org/10.1080/19320248.2020.1830221*
10. Economic Research Service (ERS), U.S. Department of Agriculture (USDA). Key Statistics and Graphics, *https://www.ers.usda.gov/topics/food-nutrition-assistance/food-security-in-the-u-s/key-statistics-graphics/* (accessed August 2024)
11. Ashby, S., Kleve, S., McKechnie, R., & Palermo, C. (2016) Measurement of the dimensions of food insecurity in developed countries: a systematic literature review. *Public Health Nutrition*, 19(16), 2887–2896. *https://doi.org/10.1017/S1368980016001166*
12. Marques, E. S., Reichenheim, M. E., de Moraes, C. L., Antunes, M. M. L., & Salles-Costa, R. (2015) Household food insecurity: a systematic review of the measuring instruments used in epidemiological studies. *Public Health Nutrition,* 18(5), 877–892. *https://doi.org/10.1017/S1368980014001050*
13. Jung, N. M., Bairros, F. S. de, Pattussi, M. P., Pauli, S., & Neutzling, M. B. (2016) Gender differences in the prevalence of household food insecurity: a systematic review and meta-analysis. *Public Health Nutrition*, 20(5), 902–916. *https://doi.org/10.1017/S1368980016002925*
14. Kakaei, H., Nourmoradi, H., Bakhtiyari, S., Jalilian, M., & Mirzaei, A. (2022) Effect of COVID-19 on food security, hunger, and food crisis. *COVID-19 and the Sustainable Development Goals*, 3–29. https://doi.org/10.1016/B978-0-323-91307-2.00005-5
15. Mark Nord & Kathleen Romig (2007) Hunger in the Summer, *Journal of Children and Poverty,* 12:2, 141-158, *https://doi.org/10.1080/10796120600879582*
16. Milovanska-Farrington, S. (2023) Job loss and food insecurity during the Covid-19 pandemic. *Journal of Economic Studies,* 50(2), 300-323. *https://doi.org/10.1108/JES-08-2021-0400*
17. Braun, V., & Clarke, V. (2006) Using thematic analysis in psychology. *Qualitative research in psychology*, 3(2), 77-101. *http://doi.org/10.1191/1478088706qp063oa*
18. Esin, C., Fathi, M., & Squire, C. (2014) Narrative analysis: The constructionist approach. *The SAGE handbook of qualitative data analysis,* 203-216.
19. Lokot, M. (2021) Whose voices? Whose knowledge? A feminist analysis of the value of key informant interviews. *International Journal of Qualitative Methods*, 20, *https://doi.org/10.1177/1609406920948775*
20. Wolfson, J. A., Lahne, J., Raj, M., Insolera, N., Lavelle, F., Dean, M. (2020) Food Agency in the United States: Associations with Cooking Behavior and Dietary Intake. *Nutrients* 12(3):877. https://doi.org/10.3390/nu12030877
21. USFSA. (n.d.) US Food Sovereignty Alliance. *https://usfoodsovereigntyalliance.org/what-is-food-sovereignty/* (accessed April 2024)

22. Economic Research Service (ERS), U.S. Department of Agriculture (USDA). Food Prices and Spending, *https://www.ers.usda.gov/data-products/food-access-research-atlas/* (accessed August 2024)
23. ACC Government (2019) Pathways to Prosperity Athens-Clarke County, Georgia a member community in the Network for Southern Economic Mobility, *https://data.census.gov/table/ACSDP5Y2022.DP05?q=Athens-Clarke%20County,%20Georgia* (accessed February 2024)
24. CCSD Resources - CCSD Food Service. (n.d.) Google Sites. *https://sites.google.com/nv.ccsd.net/distanceeducation/ccsd-resources/food-distribution-information/ccsd-food-service* (accessed April 2024)

ABOUT THE STUDENT AUTHOR

Natalie Wong is expected to graduate in the Spring of 2026 with a Bachelor of Science in Environmental Health. She plans on furthering her education by attending medical school to become a doctor.

PRESS SUMMARY

Athens is considered a food desert or low-income low-access area, which refers to limited access to nutritious, affordable foods in a given area. During the COVID-19 pandemic, several studies suggested that food insecurity rates increased. Our study focuses on 6 local organizations in Athens, Georgia to examine how they handled food insecurity relief during 2020. Through key informant interviews conducted on Zoom, we were able to create several emergent themes, such as emergency preparedness and response, food justice and sovereignty, low-income and low-access, barriers and solutions to food access, disparate impacts, and food relief networks. Overall, our findings show the need for targeted public policy interventions, which include increasing accessibility, increasing affordability, and addressing disparities among race, income, and gender.

APPENDIX A

1. Who are you and what is your role within your organization? How long have you been working here?
2. Based on what you've experienced, what are the demographics of individuals affected by food insecurity, and have these demographics changed since the COVID-19 pandemic?
3. Did you observe an increase in the number of children receiving food assistance when schools shifted to online learning?
4. Food insecurity was on the rise, which the COVID-19 exacerbated. Did your organization have a plan to meet this increasing demand? Did your organization have an emergency management plan before the lockdown began in March 2020 to handle increased relief efforts? Has your organization partnered with other organizations to adjust for demand?
5. How does your organization receive funding? Did funding increase or decrease during the COVID-19 lockdown in 2020?
6. Before the COVID-19 pandemic, what was your organization's monthly or annual output (i.e., number of meals served)? Is there any way you might be willing to share your annual report or records with me?
7. Based on these questions, is there anything else you'd like to share with me?

APPENDIX B

Organization	Description
A	Affiliated with the University of Georgia; sustainable solutions to hunger.
B	Affiliated with the University of Georgia; student-led community farm.
C	Senior citizens focused; the primary food relief program during the pandemic.
D	Food bank; one of the few sources for families facing emergencies prior to the pandemic.
E	Faith-based organization; community kitchen and dining with resource tables.
F	Small nonprofit pantry for those experiencing homelessness.

Inadvertent User Outcomes of Wearable Health Technology

Jeremy Cafritz

Department of Science, Technology, and Society, Colby College, Waterville, ME

https://doi.org/10.33697/ajur.2024.120

Student: jeremycafritz@gmail.com
Mentor: christopher.soto@colby.edu

ABSTRACT
Wearable health technologies are designed to improve a user's self-awareness of their state of health and increase motivation and physical activity, but there is limited understanding of the psychological and behavioral impact these devices have. The present research attempts to further clarify the influence of individual characteristics on the cognitive, affective, and behavioral outcomes of activity tracker usage, including the development of dependency. A cross-sectional study of 212 college students who used activity trackers was conducted to evaluate the psychological and behavioral impact of activity tracker usage and users' affective response to their device. Participants expressed more positive affect while wearing their device as opposed to when they were unable to wear it. Female participants exhibited more positive affect than male participants while wearing their device but less when unable to wear it. Only 9% of the sample reported a dependency effect. The dependency effect was negatively associated with intrinsic motivation to be physically active, motivation by the idea of success, and the personality traits of agreeableness and conscientiousness. The dependency effect was positively associated with extrinsic motivation for physical activity and tracker usage, as well as need for cognitive closure. This research elucidates the unintended outcomes of activity tracker usage along with the individual characteristics that present as predictors of these outcomes.

KEYWORDS
Health Wearables; Activity Trackers; Physical Activity; Motivation; Dependency; Gamification; Personality

INTRODUCTION

From tracking vital signs to continuous monitoring of blood levels of a specific substrate related to a disease of concern, individuals appear to be aiming to maximize awareness of their body state and enhance their ability to manage their own health.[1] The Apple Watch, Fitbit, Whoop, and other wearable lifestyle devices have taken the world by storm as hundreds of millions of active users across the globe have integrated the technology into their health and fitness regimen.[2]

The present study attempts to clarify the overall impact of health wearable usage on physical activity and subjective well-being through a replication and extension of Ryan et al. (2019) and Attig and Franke (2019).[8,11] These studies suggested user outcomes may be associated with individual traits and that users can develop a dependency on their devices. The present research will investigate whether users experience differing levels of positive affect during use vs. when they are unable to wear their device. The prevalence of physical and emotional dependency on one's device will also be assessed, along with its association with user variables, such as personality traits and sources of motivation.

Use and effects of activity trackers

Wrist-mounted devices, the main focus of the present research, have become one of the most popular forms of biosensors.[1] Physical activity is commonly tracked, including steps taken or distance walked, and an estimate of calories burned throughout the day. Many of these devices are also capable of non-invasively monitoring heart rate and blood pressure, along with glucose and sodium levels through sweat contents.[1] The data tracked can be used to interpret sleep quality, exercise, hydration, nutrition, and whatever other parameters are deemed relevant to the user. Many health wearables are programmed to use this data and, in turn, send both reactive and proactive messages acting as small cognitive punishments or rewards to motivate the user.[3]

While little research has been shown to support the positive impact of these wearable technologies on long-term behavioral change, research has exhibited their ability to act as early detectors of certain diseases by tracking vital signs and their role in providing ill users with valuable information on their current state of health.[4] Li et al. (2017), for example, explored the utility and accuracy of portable biosensors for 43 participants and found that the wearable devices were capable of uncovering early signs of Lyme disease and could differentiate between insulin-sensitive and -resistant people when measuring their blood glucose level.[4] Some research also suggests that health wearables can have a positive psychological impact on ill users. Lynch et al. (2022)

compiled data from three case studies investigating different wearable assistive technologies and discovered a positive association between the usage of these devices and feelings of reassurance. Many users felt comforted by the idea of their device continuously monitoring and validating their state of health.[5]

Researchers have recently begun to take an interest in the motivational impact of the gamification of physical activity via activity trackers.[6, 7] Gamification is defined as "the use of game design elements in non-game contexts," a mechanism used to increase the motivation of users.[6] The data tracked by these devices–distance traveled, steps, heart rate, sleep, etc.--are not innately game-like, but the tracker gamifies this data by presenting the self as quantified, and many devices also incorporate rewards, often intangible in the form of rankings on community leaderboards and competitions among users. A meta-analysis of empirical studies of gamification suggests that it appears to be a viable method to promote motivation, but the outcomes can be influenced by situational and individual factors.[7] Gamification appears to play into a user's extrinsic motivation, and depending on several variables, can enhance or hinder the intrinsic motivation of the user. If the means of gamification contribute to basic psychological needs, such as autonomy and competence, then intrinsic motivation is generally shown to be sustained or increased. Tangible rewards, competitive aspects, and a sense of being controlled by the gamification of the activity appear to work in the opposite manner and can compromise the individual's intrinsic motivation. These effects are moderated, however, by user characteristics and past experiences, such as age, personality traits, and familiarity with games.[7]

Consumers and healthcare professionals must be aware of the holistic influence these technologies have in order to make an informed decision on integrating them into their lives and potential treatment plans. There are conflicting findings on the impact of wearable health technology, specifically regarding its association with motivation, affect, and other psychological and behavioral constructs. Some studies have shown that the devices better the mental and physical health of their users,[5, 8] while others have identified a negative impact of health wearables on mental health, often leading to decreased motivation and life satisfaction.[9, 10] A dependency effect has also been uncovered.[11] Some users appear to become dependent on their activity tracker over time and their engagement in the desired behavior becomes externally motivated (i.e. driven by rewards) by positive feedback from their device. Thus, when a situation arises when the device can no longer be used or the user stops using their device, their activity level often regresses.[11]

One study elucidated the consequences of wearable fitness devices on the well-being of users in a sample of employees from a financial institution in the southern United States.[9] The company had noted high rates of diabetes and heart disease, among other chronic illnesses, within their employee population and began a workplace wellness program that included a free Fitbit for each employee. Participants were interviewed on their reasoning for participation and the extent to which they used Fitbit, and they responded to open-ended questions to express their perceptions of the pros and cons of the device in their daily lives. Results suggested that the implementation of health wearables in a corporate wellness program negatively impacted the job satisfaction and overall well-being of employee participants.[9] A similar study with adolescents in physical education classes was conducted and uncovered a significant decrease in psychological need satisfaction and autonomous motivation as well as short-term increases in motivation due to feelings of competition, guilt, and internal pressure.[10]

Affective response, dependency, and user characteristics

Psychological and physical outcomes of health wearable usage have been shown to be largely dependent on the characteristics of the individual user. Personality traits and sociodemographic identifiers, for example, are two predictors of these outcomes. People who measure high levels of neuroticism, a trait associated with negative emotionality, and low levels of openness, a trait associated with creativity and broad-mindedness, have been shown to be at greater risk of having their mental health negatively affected by a health wearable.[8] The source of motivation (i.e. intrinsic vs extrinsic motivation) to improve or maintain health has been associated with the dependency effect resulting from wearable usage.[11] Skin color can also impact the effectiveness of certain devices, as data recorded for people of darker skin tones has been shown to be less accurate.[12] Finally, socioeconomic status (SES) can play a role in how these devices impact behavioral changes, with people of higher SES experiencing a more substantial increase in physical activity upon usage,[13] further exacerbating already apparent health disparities.

Two recent studies have examined the cognitive and behavioral impact of health wearables and the possible development of dependency. Ryan et al. (2019) examined the affective response to health wearable usage and how it can potentially be explained by individual characteristics and personality traits.[8] This study sampled Australian residents above the age of 18 years old who were current users of "smart" wearable activity monitors. The participants completed a questionnaire that consisted of socio-demographic questions asking for the participant's sex, age, and education level along with the approximate frequency with which they checked the data tracked by their device. Participants' affective responses relating to their wearable technology were measured, specifically describing their affect while wearing their device and when they were unable to wear their device. The participants' Big Five personality traits (i.e. extraversion, agreeableness, conscientiousness, neuroticism, and openness to experience) were also assessed to see if individual differences in personality moderate any effect of wearing condition (i.e. during use vs. when unable to wear) on affective response. Results suggested that wearable activity trackers can have a positive

psychological influence on their users' psychological state, specifically regarding motivation and sense of accountability. Participants with low degrees of conscientiousness or openness to experience, however, were more prone to an increase in negative affect, including feelings of anxiety, guilt, and self-consciousness.[8] This study's findings appear to endorse the use of activity trackers but note personality traits may play a role in how positive or negative a certain individual's experience with them will be.

Attig and Franke (2019) examined the possible dependency effect associated with tracker usage.[11] On average, users expressed that their physical activity would decrease if they did not have their wearable device on them or if they were unable to use it to track their activity for whatever reason. Not all users, however, encountered this dependency effect to the same degree. People who exercised and used their activity trackers due to extrinsic motivation, such as for external rewards, and those who felt a stronger need for cognitive closure were more susceptible to experiencing a strong dependency effect and would more likely reduce their activity levels if they were not being tracked. Conversely, people who exercised for more intrinsic reasons of motivation, such as inherent enjoyment of the activity, were more likely to avoid acquiring a dependency or would exhibit it to a lesser extent.[11] These findings put into question the habit-forming capabilities of health wearables.

The Present Research

Fitness- and health-focused wearables are designed to support their users in reaching their health goals, but their holistic impact on individual well-being and the future of healthcare disparities is overlooked. As recent research has suggested the possibility that health wearables can have a negative inadvertent impact on individual outcomes,[9, 10, 12] people must be more aware of their consumption. A greater understanding of the effects of these devices is necessary for current and prospective users to make informed decisions on integrating them into their daily practice. The current literature on health wearables mostly focuses on the basic relationship between health wearable usage and users' mental responses without providing substantial evidence describing how other variables may explain the differing impacts of the devices on users' mental states. More evidence is needed to clarify why certain people have more or less positive relationships with their wearable health devices, and what individual characteristics present as risk factors for experiencing these negative outcomes.

Thus, the aim of the present research is to further the understanding of how health wearables impact a user's psychological state as well as how certain individual characteristics may impact psychological and behavioral outcomes. This study will replicate portions of both Ryan et al. (2019) and Attig and Franke (2019) to further investigate the dependency effect and the cognitive and behavioral impact of health wearables, as well as clarify specific personality traits and other individual characteristics that may act as risk or protective factors for their usage.[8, 11] Specifically, this study will assess Q1) whether users' affective response to their activity tracker differs when measured during use vs. when unable to wear it; Q2) how many participants exhibit a dependency effect relating to their activity tracker; Q3) what user variables are associated with dependency; and Q4) how relative intrinsic and extrinsic motivation for both physical activity and tracker usage is associated with dependency.

I expect to find evidence of both beneficial and detrimental effects of health wearables on motivation, physical activity levels, and well-being. I also expect to find that certain user characteristics–personality traits, source of motivation, and need for cognitive closure–moderate these effects as well as the degree of dependency experienced. See **Table 1** for more specific research questions and hypotheses. These expectations are grounded in the past empirical findings reviewed above, as well as an understanding of the mechanisms underlying how tracker devices work to motivate their users.

	Research Question	**Hypothesis**	
Q1	Do users' affective responses to their activity tracker differ during and when unable to wear it? Are there gender differences?	**H1a**	Participants will exhibit greater positive affect while wearing their activity tracker than when unable to wear it
		H1b	There will be no gender differences in the affective response to their activity tracker
Q2	How many participants exhibit a dependency effect relating to their activity tracker?	**H2a**	The majority of participants will not exhibit a dependency effect
Q3	What user variables are associated with dependency?	**H3a**	Positive affect when unable to wear a tracker is negatively associated with the dependency effect

		H3b	Intrinsic motivation for tracker usage is negatively associated with the dependency effect
		H3c	Extrinsic motivation for tracker usage is positively associated with the dependency effect
		H3d	Intrinsic motivation for physical activity is negatively associated with the dependency effect.
		H3e	Extrinsic motivation for physical activity is positively associated with the dependency effect.
		H3f	Need for cognitive closure is positively associated with the dependency effect.
		H3g	Achievement motivation through fear of failure is positively associated with the dependency effect
		H3h	Neuroticism is positively associated with the dependency effect
Q4	How are relative intrinsic and extrinsic motivation for both physical activity and tracker usage associated with dependency?	**H4a**	Participants who are more extrinsically than intrinsically motivated to use the tracker will exhibit a greater dependency effect than participants who are more intrinsically motivated to use the tracker.
		H4b	Participants who are more extrinsically than intrinsically motivated to be physically active will exhibit a greater dependency effect than participants who are more intrinsically motivated to be physically active.

Table 1. Research questions and hypotheses of the present study.

METHODS AND PROCEDURES

Participants

Study participants were recruited from Colby College, a small liberal arts college in Waterville, Maine. A study questionnaire was approved by the school's Institutional Review Board (IRB; 2023-001). An all-school email was sent to students with a link to the survey included, and they were each compensated $2 upon completion of the survey. Two hundred and twelve students responded and were included in the analysis. The participants ranged from 18 to 23 years old (M = 19.74, SD = 1.28) with the majority being female (n=144; 67.6%), 29.6% male (n=62), and 2.82% non-binary (n=6). Similar to the makeup of the Colby College student population, most participants described themselves as White or Caucasian (71.8%), with Asian (17.8%) being the next most common racial or ethnic identity.

Of the 212 study participants, 71.8% had been using an activity tracker for at least 12 months (M = 30.36, SD = 26.32) and 69.0% reported using their tracker 7 days per week during a typical week (M = 6.34, SD = 1.21). One hundred and forty-four participants (68.0%) reported using their device between 12 and 23 hours and 18.8% wore it for all 24 hours in a typical day (M = 16.62, SD = 5.52). The most popular brand of activity tracker among participants was Apple (66.7%), then Garmin (11.3%), Fitbit (8.9%), and Whoop (7.0%), with the remaining 6.1% using activity trackers from other brands (e.g. Amazon, Samsung). Participants also described the specific data that they regularly track and monitor: heart rate (82.2%), step count (77.0%), active minutes (71.4%), distance traveled (69.5%), type and amount of sporting activities/exercise (68.1%), sleep activity (49.3%), stairs (35.25%), and calories consumed/burned (30.5%).

Measures

The participants' affective responses to their health wearables were assessed according to a ten-item scale constructed by Ryan et al. (2019).[8] This measure is based on the Positive and Negative Affect Schedule[14] but narrows its focus to affect in relation to wearable usage. A total of ten items split into two subscales asked the participants to state their degree of agreement to experiencing a specific affect or emotion during a designated time frame. Six items evaluated the user's affect while wearing their device: "When I am using my wearable it makes me feel [empowered, motivated, accountable, guilty, self-conscious, anxious]." Four items focused on the users' affect when not wearing their device: "When I'm not using/forget/can't use my wearable it

makes me feel [liberated, guilty, frustrated, anxious]." Responses were recorded using a 5-point Likert scale ranging from 1 (*disagree strongly*) to 5 (*agree strongly*). All scores describing the users' agreement to feeling negative affect, like guilt and anxiety, were reverse coded. The scores for each subscale were averaged, with higher scores exhibiting a more positive affective state. Internal consistency was modest for both the "affect during wear" subscale (Cronbach's $\alpha = .55$) and "affect when unable to wear" subscale (Cronbach's $\alpha = .44$). However, all items exhibited positive corrected item-total correlations (mean $r = .30$) and were therefore retained for analysis.

The dependency effect caused by wearable usage was assessed using two novel measures constructed by Attig and Franke (2019).[11] The first outlines four situations that wearable users may or may not have experienced which could produce a reduction in physical activity due to the absence of the device on their person. For example, one scenario describes the participant arriving at work/university needing to go to the fourth floor, but they forgot their tracker at home. Another involves the participant's activity tracker being broken, and that it will take five days to fix it. As explained by Attig and Franke (2019), these scenarios were developed based on experimental observations of the undermining effect: losing motivation upon the removal of the external reward.[15, 16] Participants were asked to envision themselves in each of the four scenarios or remember how they responded to the same or a similar scenario if they had previously experienced it. Participants then stated their agreement to two alternative statements regarding their theoretical behavioral reaction to each scenario in order to measure their degree of activity continuity ("I will very likely maintain my activity level as if the tracker was available") or reduction ("I will very likely reduce my activity level"). Answers were provided on a 6-point Likert scale ranging from 1 (*completely disagree*) to 6 (*completely agree*). The statement describing activity continuity was reverse coded and the mean of the two scores for the statements for each scenario was calculated with higher scores depicting a greater dependency effect. Following the methods of Attig and Franke (2019), a score greater than 3.5, the midpoint on the scale, was interpreted as indicating some degree of dependency.[11] Internal consistency was acceptable for this scale (Cronbach's $\alpha = .79$) and all items showed positive corrected item-total correlations (mean $r = .48$).

The second measure took the form of a 13-item questionnaire that assessed the dependency effect through five dimensions: shift to external attribution (i.e. becoming more externally motivated), behavioral outcomes of not wearing the tracker (i.e. experiencing a maintenance or reduction in activity levels), activity evaluation (i.e. perceiving activity as more valuable when it is measured by a tracker), affective outcomes of intrinsic motivation loss (i.e. only feeling successful when the tracker validates adequate activity levels), and cognitive occupancy (i.e. thinking about the tracker). Answers were provided on 6-point Likert scales ranging from 1 (completely disagree) to 6 (completely agree) with higher scores representing a stronger dependency effect. As mentioned previously, a score greater than 3.5 indicated some degree of dependency.[11] Internal consistency for this scale was good (Cronbach's $\alpha = .89$).

A measure constructed by Attig and Franke (2019) based on self-determination theory was used to assess motivation for tracker usage.[11] The 6-item measure was composed of two subscales, in which the first three items appraised intrinsic motivation to use their wearable device (e.g. "I use my activity tracker because I want to learn more about my physical activity"), and the following three appraised extrinsic motivation to use their device (e.g. "I use my activity tracker because reaching my step or activity goals encourages me"). Answers were provided on a 6-point Likert scale ranging from 1 (*completely disagree*) to 6 (*completely agree*). Internal consistency was good for intrinsic motivation (Cronbach's $\alpha = .82$) and acceptable for extrinsic motivation for tracker usage (Cronbach's $\alpha = .71$).

To more explicitly describe each participant's reason for using their device, participants were able to express whether they primarily use their tracker for enjoyment ("In case of doubt, my slogan is 'The fun I have through using my tracker comes before the gain!'") or for health benefits ("In case of doubt, my slogan is 'The gain I have through using my tracker comes before the fun!'") through two additional items taken and modified from the Incentive-Focus Scale.[11, 17] Participants provided their answers on a 6-point Likert scale ranging from 1 (*completely disagree*) to 6 (*completely agree*). The second of these two additional items was reverse coded and the mean of these two scores was calculated with higher scores denoting using the tracker more for reasons of enjoyment. The correlation between these two items was $r = .35$, yielding Cronbach's α of .51.

A measure developed by Attig and Franke (2019)[11] based on the Situational Motivation Scale[18] assessed the users' motivation for physical activity. The 8-item scale was composed of two subscales with the first four items measuring intrinsic motivation for physical activity (e.g. "I am physically active/exercise because this activity is fun") and the next four items measuring extrinsic motivation (e.g. "I am physically active/exercise because I feel that I have to do it"). Answers were provided on a 6-point Likert scale ranging from 1 (completely disagree) to 6 (completely agree). Similar to Attig and Franke (2019), the participants were asked to respond to the items thinking of their motivation for physical activity before they first started using their wearable device. Internal consistency was excellent for intrinsic motivation (Cronbach's $\alpha = .90$) and good for explicit motivation for physical activity (Cronbach's $\alpha = .83$).

The 15-item need for closure scale (NFCS) short version was used to measure the degree to which a person has the desire for certainty.[19, 20] An example item is "I dislike it when a person's statement could mean many different things." Answers were provided on a 6-point Likert scale from 1 (*completely disagree*) to 6 (*completely agree*). Internal consistency was good (Cronbach's α = .87).

The users' affinity for technology was assessed using the 9-item ATI scale given on a 6-point Likert scale from 1 (*completely disagree*) to 6 (*completely agree*).[21] An example item is "I try to make full use of the capabilities of a technical system." Internal consistency was good (Cronbach's α = .81).

Achievement motivation was measured with an adapted version of the 10-item Achievement Motives Scale (AMS-R).[22] This measure is composed of two subscales scored on a 5-point Likert scale ranging from 1 (*completely disagree*) to 5 (*completely agree*) with the first five items measuring hope of success (approach tendency, e.g. " I like situations in which I can find out how capable I am") and the next five measuring fear of failure (avoidance tendency, e.g. "I feel uneasy to do something if I am not sure of succeeding"). Internal consistency was good (Cronbach's α = .81).

The Big Five personality traits (openness to experience, conscientiousness, extraversion, agreeableness, and neuroticism) were evaluated using the 10-item BFI-10 measure.[23] Answers were provided on a 5-point Likert scale ranging from 1 (completely disagree) to 5 (completely agree). The inter-item correlations were .33 for openness, .34 for conscientiousness, .46 for extraversion, .18 for agreeableness, and .48 for neuroticism, yielding Cronbach's α values ranging from .31 to .64. Despite these relatively low internal consistency values, which reflect the brevity of the BFI-10, previous research has shown that this instrument shows high test-retest reliability and large associations with more comprehensive Big Five measures.[23]

Data analysis

Several steps were taken to replicate the data analysis conducted by Ryan et al. (2019) and Attig and Franke (2019).[8, 11] Data from survey responses were downloaded and analyzed using IBM SPSS Statistics (Version 27), and all variables were screened for outliers. The responses of one participant were identified as an outlier as the responses provided were the minimum value for all items, and it was excluded from data analysis. After examining the distribution of participant demographic characteristics, Pearson correlations between all variables included in the questionnaire were calculated in order to clarify which user variables were associated with the dependency effect. For all analyses, statistical significance is interpreted using the conventional $p < .05$ criterion. However, due to the large number of associations examined, exact p-values are also provided to indicate whether the key results would also be significant under more stringent criteria (e.g., $p < .01$, $p < .001$).

Next, independent t-tests were conducted to test mean differences between participants' affect scores in the two wearing conditions (wearing and not wearing), as well as between affect scores and participant gender. A repeated measures ANOVA was then conducted to analyze the joint effects of gender and wearing condition on affect.

Next, a one-sample t-test was conducted for each of the three dependency scales–including the calculated composite score–to determine the degree of the dependency effect observed in the sample. Following Attig and Franke (2019),[11] difference values between intrinsic and extrinsic motivation for both physical activity and tracker usage were first calculated in order to determine how relative intrinsic and extrinsic motivation is associated with dependency. Individuals who did not differ in their scores of intrinsic and extrinsic motivation for physical activity or tracker usage were excluded from the respective analyses. After being grouped, independent t-tests were performed to investigate differences in the dependency effect between them. Following this, an independent samples t-test was conducted to investigate a possible gender difference in the dependency effect.

RESULTS

Q1: Affective response to their activity tracker differs by wearing or not wearing

In order to investigate whether users' affective response to their activity differs during vs. when unable to wear their tracker, an independent samples t-test compared positive affect scores between wearing conditions. Participants exhibited significantly greater positive affect during wear ($M = 3.77$, $SD = .57$) than when unable to wear their device ($M = 3.17$, $SD = .74$), $F(1, 211) = 90.89$, $p<.001$, thus aligning with previous research.[8] Independent samples t-tests were then conducted to investigate the relationship between gender and affect during each wearing condition. Female participants ($M = 3.84$, $SD = .54$) showed significantly greater positive affect while wearing their activity tracker than males ($M = 3.65$, $SD = .63$), $F(1, 204) = 4.74$, $p = .031$. Interestingly, the opposite gender difference was observed when unable to wear their device. In these conditions, males ($M = 3.43$, $SD = 0.58$) showed significantly greater positive affect than females ($M = 3.07$, $SD = 0.78$), $F(1, 204) = 10.15$, $p = .002$. This result led me to conduct an exploratory analysis via a repeated measures ANOVA, which showed there was a significant interaction between gender and positive affect during wearing conditions, $F(1, 204) = 15.63$, $p < .001$ (**Figure 1**). These results indicate that females experience more positive affect than males while wearing their device but less positive affect than males

when they are unable to wear their device. This finding goes beyond previous studies, as no gender differences in affect during different wearing conditions nor an interaction between gender and wearing conditions have been found previously.

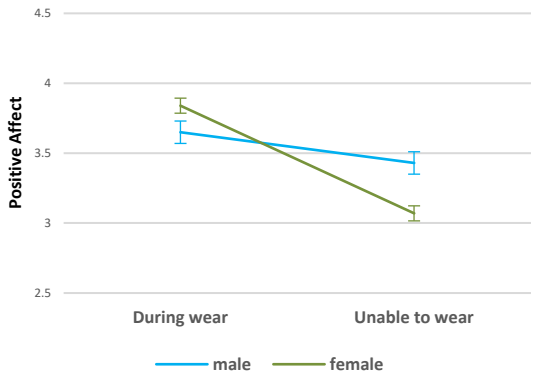

Figure 1. Line graph depicting a *gender* x *wearing conditions* interaction via a repeated measures ANOVA including error bars denoting standard error. *Note.* Participants who did not identify as male or female were not included in this analysis due to the small sample size.

Q2 : Dependency effect of activity tracker

In order to investigate whether participants exhibit a dependency effect relating to their activity tracker, one-sample t-tests were conducted comparing the mean scores of each dependency effect scale to the center of the response scale, 3.5. Regarding the scenario scale for the dependency effect, the mean score was M = 2.30 (SD = 0.86) and was significantly less than the center of the response scale at 3.5, t (211) = -20.38, p < .001, d = 0.86. This result shows that participants tended to choose the more active option in each scenario (e.g. "I will very likely maintain my activity level as if the tracker was available"). Regarding the questionnaire scale for the dependency effect, the mean score was M = 2.57 (SD = 0.93) and was significantly less than 3.5, t (211) = -14.61, p < .001, d = 0.93. This result similarly suggests that participants generally did not feel dependent on their device. The composite dependency score incorporating both the scenario and questionnaire scales found a mean score of M=2.43 (SD=0.78) and was significantly less than 3.5, t (211) = -19.89, p < .001, d = 0.78. Only 9% of participants scored above 3.5 (**Figure 2**). Following Attig and Franke (2019), we interpret a dependency score greater than 3.5 as exhibiting dependency on their device. These results suggest that most participants do not experience such an effect, but there is a notable number of participants who do exhibit dependency. These results align with past research.[11]

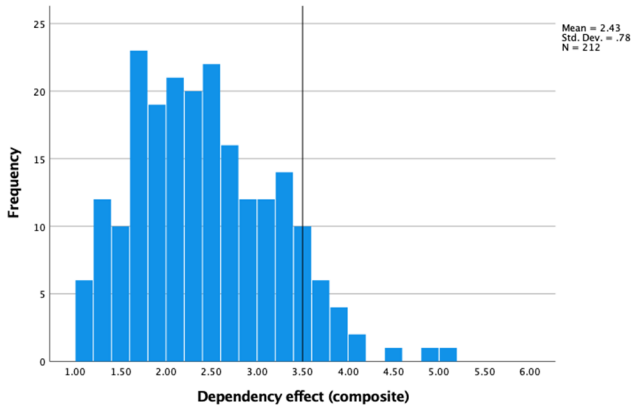

Figure 2. Histogram depicting frequency distribution of composite dependency effect scores with a vertical line denoting the center of the response scale

Due to the observed interaction between gender and wearing condition concerning affect scores noted above, an exploratory analysis was conducted in order to further investigate possible gender differences in dependency. While female participants (n = 144) had slightly higher composite dependency effect scores (M = 2.47, SD 0.79) than male participants (n = 62, M = 2.33, SD = 0.73), this gender difference was not significant, t (204) = 1.17, p = .245. According to the composite dependency effect scores, these results indicate that males and females experience a similar degree of dependency on their activity trackers.

Q3: User Variables Associated with Dependency

In order to investigate which user variables were associated with dependency, correlations were calculated and presented in a correlation matrix (**Table 3**). Many significant relationships were found, thus aligning with previous research suggesting users with

	Variable	1	2	3	4	5	6	7	8	9	10	11	12	13	14	15	16	17	18
(1)	**Positive affect during wear**																		
(2)	**Positive affect when unable to wear**	.03																	
(3)	**Dependency effect - Scenarios**	-.15^{+}	-.31***																
(4)	**Dependency effect - Questionnaire**	-.19**	-.44***	.53***															
(5)	**Dependency effect - Composite**	-.20**	-.43***	.86***	.88***														
(6)	**Intrinsic motivation for tracker usage**	.23***	-.15^{+}	-.07	.02	.03													
(7)	**Extrinsic motivation for tracker usage**	.09	-.30***	.26***	.42***	.39***	.39***												
(8)	**Incentive focus regarding tracker usage**	-.04	-.18**	.18**	.33***	.30***	.03	.34***											
(9)	**Intrinsic motivation for physical activity**	.13	.05	-.32***	-.22**	-.31***	.36***	.05	-.07										
(10)	**Extrinsic motivation for physical activity**	-.17^{+}	-.25***	.06	.24***	.18**	.10	.23***	.22**	-.05									
(11)	**Need for cognitive closure**	-.06	-.16^{+}	.23***	.32***	.32***	.15^{+}	.23***	.16^{+}	-.07	.22**								
(12)	**Affinity for technology interaction**	-.09	-.09	.05	.10	.09	.18**	.09	.12	-.08	.12	.06							
(13)	**Achievement motivation – hope of success**	.09	-.03	-.20**	-.12	-.19**	.44***	.14^{+}	-.11	.36***	.20**	.06	.15*						
(14)	**Achievement motivation – fear of failure**	-.08	-.18**	.18**	.31***	.28***	.11	.26***	.13	.01	.26***	.62***	-.01	.03					
(15)	**Extraversion**	.06	-.05	-.06	.01	.03	-.10	-.04	.01	.12	.08	-.27***	-.05	.16^{+}	-.32***				
(16)	**Agreeableness**	.07	.06	-.21**	-.14^{+}	-.20**	.01	-.05	.04	.19**	-.16^{+}	-.14^{+}	.04	.06	-.09	.10			
(17)	**Conscientiousness**	.13	-.01	-.19**	-.11	-.17^{+}	.17^{+}	-.02	-.23***	.31***	-.13	.03	-.06	.35***	-.03	.07	-.03		
(18)	**Neuroticism**	.10	-.17^{+}	.08	.23***	.18**	-.09	.14	.01	-.01	.21**	.42***	-.07	-.08	.52***	-.21**	-.18**	-.07	
(19)	**Openness**	.08	-.02	-.12	.07	-.03	-.01	.01	.08	.09	-.02	.04	-.15^{+}	.08	.07	.04	.00	.09	.06

Table 3. Pearson correlation coefficients for all variables. *Note.* * p < .05; ** p < .01; *** p < .001; all p-values refer to two-sided significance

certain characteristics tend to also depict greater levels of dependency. For example, significant correlations were found between dependency and multiple personality traits. The correlations between composite dependency effect scores and agreeableness, conscientiousness, and neuroticism were r = -.20, r = -.17, and r = .18, respectively. Several other user variables, especially those that describe sources of motivation, were found to have significant correlations with the composite dependency score. The strongest of the correlations include but are not limited to extrinsic motivation for tracker usage (r = .39), need for cognitive closure (r = .32), intrinsic motivation for physical activity (r = -.31), and fear of failure (r = .28). These results suggest that user characteristics are associated with differing degrees of dependency. Specifically, individuals who are disagreeable, unconscientious, prone to negative emotions, intolerant of uncertainty and ambiguity, and motivated by extrinsic factors and a fear of failure are most likely to become emotionally dependent on their activity trackers.

Q4: Relative Intrinsic and Extrinsic Motivation for physical and tracker usage associated with dependency

Participants were split into groups depending on their relative degrees of intrinsic and extrinsic motivation for physical activity and tracker usage, thus following the methods of Attig and Franke (2019).[11] Descriptive statistics of all four possible groups are depicted in **Table 4**. An independent samples t-test found that participants with greater extrinsic than intrinsic motivation for physical activity (n = 52) felt a greater dependency effect (M = 2.81, SD = 0.87) than those with greater intrinsic motivation for physical activity (n = 140, M = 2.27, SD = 0.68), t (190) = 4.53, p < .001. The difference represented a medium-to-large effect size (d = 0.74). Similarly, participants with greater extrinsic than intrinsic motivation for tracker usage (n = 40) felt a greater dependency effect (M = 2.87, SD = 0.75) than those with greater intrinsic motivation for tracker usage (n = 146, M = 2.27, SD = 0.71), t (184) = 4.72, p < .001. The difference represented a medium-to-large effect size (d = 0.72). A two-way ANOVA was conducted to shed light on any possible interaction effect involving groupings determined by relative levels of intrinsic and extrinsic motivation for both physical activity and tracker usage, but no interaction was found, F (1) = 0.047, p = 0.829. Aligning with previous research, these results indicate that when extrinsic motivation is greater than intrinsic motivation for physical activity or tracker usage, the user is likely to experience a greater degree of dependency on their device.[11]

Group	n	M	SD
1. Extrinsic physical activity & extrinsic tracker usage	16	3.01	0.82
2. Intrinsic physical activity & extrinsic tracker usage	22	2.66	0.66
3. Extrinsic Physical activity & intrinsic tracker usage	29	2.63	0.87
4. Intrinsic physical activity & intrinsic tracker usage	105	2.17	0.64

Table 4. Means and standard deviations of the composite dependency effect for the four groups composed of possible combinations of relative extrinsic and intrinsic motivation for physical activity and tracker usage. (n= 172). *Note.* To directly replicate the analyses conducted by Attig and Franke (2019), n = 40 users were excluded because there was no difference in their scores for extrinsic and intrinsic motivation for physical activity and/or tracker usage. However, we note that this exclusion criterion may affect some results. Intrinsic = intrinsic > extrinsic; extrinsic = intrinsic < extrinsic.

DISCUSSION

Summary of results

The present study aimed to further clarify the influence of certain individual characteristics on the cognitive, affective, and behavioral outcomes of activity tracker usage. Participants expressed that they had more positive affect while wearing their device as opposed to when they were unable to wear it, thus aligning with past findings.[8] A gender difference was also found, as female participants exhibited more positive affect than male participants while wearing their device but less when unable to wear their device, suggesting greater affective dependency among women. While participants generally exhibited no decline in physical activity when they were unable to use their device, a portion of the sample did. Specifically, this decline in physical activity when the device is not on their person appears to be more salient when people use their device for external goals or rewards as motivation for physical activity, have a large need for closure, are motivated by a fear of failure, and are neurotic. Conversely, dependency appears to be less of a problem for individuals who are innately motivated to be physically active, are motivated by the idea of success, and are agreeable and conscientious. These findings align with past research in suggesting that the dependency effect does not manifest universally and that only some people experience decreases in motivation and physical activity when not wearing their activity tracker.[11]

Implications

The present study enhances our understanding of how an individual's behavior and psychological state can be influenced by the usage of an activity tracker. While these devices are designed to increase motivation, comfortability, and confidence in reaching health goals, a portion of users experience negative affect (i.e. anxiety, guilt, and self-consciousness) and experience a regression in their physical activity in response to the absence of their device. These findings urge consumers to better understand their relationship with their activity trackers to ensure that usage is not detrimental to their overall mental or physical health.

Beginning with the positive psychological effects of activity tracker usage, the present study supports past findings that many users associate a sense of comfort with their device. Similar to Lynch et al. (2022) who examined the role of multiple types of wearable health technology and ultimately discovered an association between wearing the device and feelings of reassurance, study participants generally felt greater positive affect (i.e. empowered, motivated) while wearing their device in comparison to when they were not able to.[5] Activity trackers thus appear to serve an important role in supporting the affective needs of the user.

However, while many people feel a sense of comfort by having their activity tracker on person, the present study confirms the finding that users' psychological states can be negatively impacted when they are not wearing their tracker.[8] Specifically, the finding that people with a high degree of neuroticism are more likely to exhibit less positive affect when unable to wear their tracker was replicated. Among other user variables, greater extrinsic motivation for both tracker usage and physical activity was found to be associated with less positive affect when unable to wear their device. Furthermore, personality traits, including low agreeableness, low conscientiousness, and high neuroticism, along with extrinsic rather than intrinsic motivation, predicted relative participant dependency on their device. These correlations imply that psychological characteristics can predict how positive or negative the health wearable user experience will be, at least in terms of affective response and development of dependency. Practically, these results raise the question: should people with certain psychological characteristics use activity trackers if these characteristics are deemed risk factors for an unhealthier user-tracker relationship?

One notable novel finding in the present study is a gender difference in the affective response to wearable health technology. Female participants were found to feel greater levels of positive affect than male participants while wearing their activity tracker, but they felt less positive affect than male participants when unable to wear their tracker. These results go beyond past findings,[11] as no gender differences in the affective response to health wearables have been previously published, and they may suggest greater affective dependency among women. This interaction may be explained by the difference in how men and women tend to value feedback. Women have been shown to perceive informational feedback on achievement as more telling of their accomplishments or abilities than men.[24] Men thus depend more on their own self-perceptions than informative feedback and are less likely to feel a large affective difference based on the presence or absence of a device providing them with such feedback. This gender difference may explain why female participants exhibited a greater difference in affect scores between wearing conditions when compared to male participants.

The effects of gamification can be seen in the results associating sources of motivation with the dependency effect. Individuals motivated to exercise or use their activity tracker by external rewards (i.e. extrinsic motivation) were shown to experience a greater dependency effect than those who are more motivated by inherent enjoyment or desire (i.e. intrinsic motivation). Past research suggests that gamification takes advantage of a user's extrinsic motivation, and depending on other individual characteristics, can hinder the intrinsic motivation of the user.[7] Thus, the integration of an activity tracker can exacerbate the extrinsic motivation of the user and diminish their intrinsic motivation. Upon the loss of the device or when the device cannot be worn, the user's intrinsic motivation has already been reduced and the extrinsic motivation provided by the feedback of the activity tracker is no longer in play, ultimately resulting in the manifestation of the dependency effect.

Limitations and Future Research

The present study had some notable strengths, including its sample size, breadth of variables measured, and its ability to be compared with previous studies. However, there remain several important limitations to our understanding of the role of individual characteristics on the behavioral, cognitive, and affective outcomes of health wearable usage.

Does the current literature suggest individuals become overly dependent on their wearable health devices? Or do the research methods used leave this up to question? The present study and Ryan et al.'s cross-sectional approaches analyzed users' affect during wear and when unable to wear their devices which allowed us to determine which personality traits and socio-demographic identifiers were associated with the affective response of the user to their device; nonetheless, they were not able to compare individuals' affective experiences before vs. after integrating their device into their lifestyle. Users were shown to have more positive affect during wear as opposed to when unable to wear their device. Does this tell us the devices have positive psychological effects? Or is it possible that the users have developed an unhealthy dependence on their devices, in which they rely on their devices to alleviate their health anxiety? Or could their more positive affect while wearing their device be connected to their anticipation of the gratification associated with reaching their activity goals? Furthermore, without comparing their affect

scores to those of a true control group or pretest, it is impossible to discern if their measured positive affect is greater than the affect of individuals who do not use activity trackers. While Ryan et al. (2019) did compare the affective experiences of current device users vs. previous users,[8] the previous users' lower affect scores during wear may have contributed to their decision to stop wearing their devices. Other studies, such as Giddens et al. (2019) and Kerner and Goodyear (2017) studied the impact of health wearables on the users' psychological states over time. These longitudinal studies found that health wearables i) negatively impacted the job satisfaction and overall employee well-being of employees participating in a workplace wellness program[9] and ii) decreased levels of psychological need satisfaction and autonomous motivation and increased short-term motivation due to feelings of competition, guilt, and internal pressure in adolescents in physical education classes.[10]

The results of the present study suggest that activity trackers induce some positive psychological response, but we cannot know this for sure without taking a longitudinal approach or comparing them to a true control group. The longitudinal approach could tell us much more about the psychological power of a health wearable over time. The difference between initial and subsequent levels of mental health would thus be able to be compared, using the initial measurements as controls. The present study utilizes a cross-sectional study design due to time and funding constraints, and thus cannot paint the entire picture. A longitudinal multivariate design involving the periodic administration of the measures used in the present study would better clarify the long-term and gradual development of dependency and change in affect due to health wearable usage.

Another limitation of the study is the general lack of diversity among the sample. Though relatively representative of the Colby College student population, the sample was not very diverse and its cross-cultural replicability is questionable. Furthermore, the sample is largely composed of female participants, with male participants comprising under a third of the sample. This discrepancy may have contributed to the gender difference in affective response to activity trackers found in the present study. Future research involving a larger and more diverse sample would better clarify replicable relationships concerning the affective response to activity trackers and dependency. This would also provide the researchers with a better opportunity to uncover any possible racial, ethnic, or cultural differences in dependency.

CONCLUSIONS

Activity trackers have been successfully designed to promote physical activity for most people, but some users have a negative relationship with their device. The present findings show that individual variables, such as personality traits and sources of motivation, contribute to the disparate efficacy of health wearables and the degree of dependency users are at risk of developing. This research elucidates the unintended consequences of activity trackers and predictors of these outcomes.

ACKNOWLEDGEMENTS

I thank the Colby College Department of Science, Technology, and Society for funding the present study. I also thank Prof. Christopher Soto, Prof. Ashton Wesner, and Prof. Erin Sheets for assisting with various aspects of this project, including data analysis and manuscript review.

REFERENCES

1. Guk, K., Han, G., Lim, J., Jeong, K., Kang, T., Lim, E.-K., & Jung, J. (2019) Evolution of Wearable Devices with Real-Time Disease Monitoring for Personalized Healthcare. *Nanomaterials*, *9*(6), 813. *https://doi.org/10.3390/nano9060813*
2. Phaneuf, A. (2022) Latest *trends in medical monitoring devices and wearable health technology*. Insider Intelligence. https://www.insiderintelligence.com/insights/wearable-technology-healthcare-medical-devices/
3. Qu, Q., Sum, K., & Nathan-Roberts, D. (2016) *How Fitness Trackers Facilitate Health Behavior Change. https://journals.sagepub.com/doi/abs/10.1177/1541931213601247*
4. Li, X., Dunn, J., Salins, D., Zhou, G., Zhou, W., Schüssler-Fiorenza Rose, S. M., Perelman, D., Colbert, E., Runge, R., Rego, S., Sonecha, R., Datta, S., McLaughlin, T., & Snyder, M. P. (2017) Digital Health: Tracking Physiomes and Activity Using Wearable Biosensors Reveals Useful Health-Related Information. *PLOS Biology*, *15*(1), e2001402. *https://doi.org/10.1371/journal.pbio.2001402*
5. Lynch, J., Hughes, G., Papoutsi, C., Wherton, J., & A'Court, C. (2022) "It's no good but at least I've always got it round my neck": A postphenomenological analysis of reassurance in assistive technology use by older people. *Social Science & Medicine*, *292*, 114553. *https://doi.org/10.1016/j.socscimed.2021.114553*
6. Deterding, S., Dixon, D., Khaled, R., & Nacke, L. (2011) *From Game Design Elements to Gamefulness: Defining Gamification. 11*, 9–15. *https://doi.org/10.1145/2181037.2181040*
7. Hamari, J., Koivisto, J., & Sarsa, H. (2014, January 1) *Does Gamification Work? — A Literature Review of Empirical Studies on Gamification*. Proceedings of the Annual Hawaii International Conference on System Sciences. *https://doi.org/10.1109/HICSS.2014.377*
8. Ryan, J., Edney, S., & Maher, C. (2019) Anxious or empowered? A cross-sectional study exploring how wearable activity trackers make their owners feel. *BMC Psychology*, *7*(1), 42. *https://doi.org/10.1186/s40359-019-0315-y*

9. Giddens, L., Gonzalez, E., & Leidner, D. (2019) Unintended *Consequences of Wearable Fitness Devices in Corporate Wellness Programs*. 4–4. *https://doi.org/10.1145/3322385.3322416*

10. Kerner, C., & Goodyear, V. A. (2017) The Motivational Impact of Wearable Healthy Lifestyle Technologies: A Self-determination Perspective on Fitbits With Adolescents. *American Journal of Health Education*, *48*(5), 287–297. *https://doi.org/10.1080/19325037.2017.1343161*

11. Attig, C., & Franke, T. (2019) I track, therefore I walk – Exploring the motivational costs of wearing activity trackers in actual users. *International Journal of Human-Computer Studies*, *127*, 211–224. *https://doi.org/10.1016/j.ijhcs.2018.04.007*

12. Colvonen, P. J., DeYoung, P. N., Bosompra, N.-O. A., & Owens, R. L. (2020) Limiting racial disparities and bias for wearable devices in health science research. *Sleep*, *43*(10), 159. *https://doi.org/10.1093/sleep/zsaa159*

13. Western, M. J., Armstrong, M. E. G., Islam, I., Morgan, K., Jones, U. F., & Kelson, M. J. (2021) The effectiveness of digital interventions for increasing physical activity in individuals of low socioeconomic status: A systematic review and meta-analysis. *International Journal of Behavioral Nutrition and Physical Activity*, *18*(1), 148. *https://doi.org/10.1186/s12966-021-01218-4*

14. Watson, D., Clark, L. A., & Tellegen, A. (1988) Development and validation of brief measures of positive and negative affect: The PANAS scales. *Journal of Personality and Social Psychology*, *54*(6), 1063. *https://doi.org/10.1037/0022-3514.54.6.1063*

15. Deci, E. L. (1971) Effects of externally mediated rewards on intrinsic motivation. *Journal of Personality and Social Psychology*, *18*, 105–115. *https://doi.org/10.1037/h0030644*

16. Lepper, M. R., Greene, D., & Nisbett, R. E. (1973) Undermining children's intrinsic interest with extrinsic reward: A test of the "overjustification" hypothesis. *Journal of Personality and Social Psychology*, *28*, 129–137. *https://doi.org/10.1037/h0035519*

17. Rheinberg, F., Iser, I., & Pfauser, S. (1997) *Doing something for fun and/or for gain? Transsituational consistency and convergent validity of the Incentive-Focus Scale. 43*.

18. Guay, F., Vallerand, R. J., & Blanchard, C. (2000) On the Assessment of Situational Intrinsic and Extrinsic Motivation: The Situational Motivation Scale (SIMS) *Motivation and Emotion*.

19. Roets, A., & Van Hiel, A. (2011) Item selection and validation of a brief, 15-item version of the Need for Closure Scale. *Personality and Individual Differences*, *50*(1), 90–94. *https://doi.org/10.1016/j.paid.2010.09.004*

20. Webster, D. M., & Kruglanski, A. W. (1994) Individual differences in need for cognitive closure. *Journal of Personality and Social Psychology*, *67*(6), 1049. *https://doi.org/10.1037/0022-3514.67.6.1049*

21. Franke, T., Attig, C., & Wessel, D. (2018) A Personal Resource for Technology Interaction: Development and Validation of the Affinity for Technology Interaction (ATI) Scale. *International Journal of Human–Computer Interaction*, *35*(6), 456–467. *https://doi.org/10.1080/10447318.2018.1456150*

22. Lang, J., & Fries, S. (2006) *(PDF) A revised 10-item version of the Achievement Motives Scale: Psychometric properties in German-speaking samples. https://www.researchgate.net/publication/232492141_A_revised_10-item_version_of_the_Achievement_Motives_Scale_Psychometric_properties_in_German-speaking_samples*

23. Rammstedt, B., & John, O. P. (2007) Measuring personality in one minute or less: A 10-item short version of the Big Five Inventory in English and German. *Journal of Research in Personality*, *41*(1), 203–212. *https://doi.org/10.1016/j.jrp.2006.02.001*

24. Roberts, T.-A. (1991) Gender and the influence of evaluations on self-assessments in achievement settings. *Psychological Bulletin*, *109*, 297–308. *https://doi.org/10.1037/0033-2909.109.2.297*

ABOUT THE STUDENT AUTHOR

Jeremy Cafritz graduated in May 2023 from Colby College, in Waterville, ME, where he was a double major in Psychology and Science, Technology, and Society (Honors). Jeremy is currently working as a surgical technician at a skin cancer surgery clinic and hopes to begin medical school in Fall 2025.

PRESS SUMMARY

The present research attempted to clarify the relationship between individual characteristics, such as personality and sources of motivation, on the cognitive, affective, and behavioral outcomes of activity tracker usage, including the development of dependency. Participants expressed more positive affect while wearing their device as opposed to when they were unable. Female participants exhibited more positive affect than male participants while wearing their device but less when unable to wear their device. Only 9% of the sample exhibited a dependency effect. People who were more intrinsically motivated to be physically active, more motivated by the idea of success, more agreeable and conscientious, less extrinsically motivated for physical activity and tracker usage, and had less of a need for cognitive closure were less likely to be dependent on their device.

Print Edition ISSN 1536-4585
Online Edition ISSN 2375-8732